EVALUATION OF POSTPROCESSING DUAL ENERGY

QUANTITATIVE COMPUTED TOMOGRAPHY

(Evaluatie van postprocessing methoden voor kwantitatieve

computer tomografie met twee energieën)

PROEFSCHRIFT

Ter verkrijging van de graad van doctor

aan de Erasmus Universiteit Rotterdam

op gezag van de rector magnificus

Prof.Dr. C.J. Rijnvos

en volgens besluit van het College van Dekanen

De openbare verdediging zal plaatsvinden op

woensdag 5 juni 1991 om 13.45 uur

door

CORNELIS VAN KUIJK

geboren te DORDRECHT

PROMOTIECOMMISSIE

Promotor　　　　　　　:Prof.Dr. H.E. Schütte

Overige leden　　　　:Prof.Dr.Ir. J.H. van Bemmel

　　　　　　　　　　　　　Prof.Dr. J.C. Birkenhäger

　　　　　　　　　　　　　Prof.Dr.Ir. C.J. Snijders

"If the wise man listens, he will increase his learning,

and the man of understanding will acquire skill

to understand proverbs and parables,

the sayings of wise men and their riddles"

Proverbs 1,5-6.

"De wijze hore en vermeerdere inzicht

en wie verstandig is, verwerve overleg,

om te verstaan spreuk en beeldspraak,

woorden en raadselen van wijzen"

Spreuken 1,5-6.

Voor Elly en Elsemiek.

Contents.

CHAPTER 1

GENERAL INTRODUCTION

1.1 INTRODUCTION

In 1895 Wilhelm Conrad Röntgen discovered a new form of radiation that he named X-rays. The prospects for X-ray diagnosis in medicine were immediately recognized. Since then, the use of X-ray has become wide-spread and abundant. In 1972, nearly eighty years later, an X-ray computed tomography (CT) apparatus for medical use was announced by Godfrey Newbold Hounsfield. This announcement is considered to be the next major step in radiology after the discovery of X-rays. Before the introduction of CT, soft-tissue could only be visualized indirectly using contrast media. CT enabled to visualize soft-tissue directly and because of its tomographic nature, to visualize the human anatomy in section, providing depth information.

Hounsfield, who received the Nobel prize in 1979, did not invent the CT concept but he was the first to implement the ideas in a machine suitable for clinical practice. The CT concept itself was tested experimentally in the 1950's and 1960's in different institutions throughout the world (1). Now, at the end of the 20th century, CT scanners are present in many departments of radiology.

CT scanners are used primarily for imaging the human body. They can also be used to provide information on tissue composition, called quantitative computed tomography (QCT) (1,2). When applied to parts of the skeleton, this information can be used to give a measure of bone mineral content within the skeleton (3-5).

Apart from bone mineral content analysis, quantitative CT methods are also proposed for quantification of calcification of pulmonary nodules (6-8), of liver iron content (9-11), for determination of the composition of urinary calculi (12) and of gallstones (13,14), for assessment of lung damage due to bleomycin (15), for assessment of the success of radiotherapy of vertebral metastases (16) and for assessing the density distribution of subchondral bone, representing the long-term loading history of individual joints (17).

Furthermore, the quantitative information of CT is used for isodose computations in treatment planning in radiotherapy (18,19) and for xenon enhanced CT scanning for the measurement of cerebral blood flow (20-22).

Outside the field of medicine, QCT is used to study density gradients in structural ceramics (23).

The application of QCT for bone mineral analysis has become a clinically established method for non-invasive bone mineral assessment (24-26). The vertebral body is the part of the skeleton most commonly used as site of investigation (27-33); the forearm and femur also being sites of interest (34-36). The application of QCT for bone mineral assessment can be divided into single- and dual-energy quantitative computed tomography. Because QCT for bone mineral assessment is usually applied to the vertebral body, both single- and dual-energy QCT will be discussed with respect to that specific skeletal site.

1.2 SINGLE ENERGY QUANTITATIVE COMPUTED TOMOGRAPHY

Single-energy quantitative computed tomography (SEQCT) means that a CT slice is made at one specific X-ray tube potential. In QCT for bone mineral content assessment of the vertebral body, a mid-vertebral CT slice is made perpendicular to the axis of the vertebra. Usually, slices are made of three or four consecutive vertebrae (L1-L3 or T12-L3). A specific region of interest (ROI) is chosen within the trabecular part of the vertebral body. Within this ROI the mean CT number, which is a measure of the X-ray attenuation is determined. This mean CT number is converted to a bone mineral equivalent value which is achieved by scanning a reference device that contains materials with known concentrations of bone-mimicking substances. A more detailed description of the technique will be given in chapters 2 and 3.

The accuracy and precision of bone mineral assessment with SEQCT is influenced by a number of factors. The following error sources require consideration: unknown fat content in the vertebral body (37-42), beam-hardening (43-47), scattered radiation (47-49), selection of CT slice (5,37,50-53), selection of ROI (52,54-57), and apparatus instability (37). Some of these problems can be alleviated by scanning a reference device simultaneously with the patient (5,36,58). Others can be minimized by automation of scanning and measurement procedures (53-54,56-57). Error due to the variable fat content of the vertebral body, however, remains. This is due to the fact that in SEQCT the multi-component trabecular region of the vertebral body is described as a two-compartment model. Estimates of the fat-error on bone mineral content

2

assessment vary from 10-30% (37-42). This is the largest source of error in SEQCT, the error increasing with increasing fat content in the vertebral body (25). Fat content increases with age, while the trabecular bone volume decreases. The increasing fat-error in aging is particularly important as the main topic of interest within the field of non-invasive bone mineral assessment is osteoporosis. This syndrome of diminishing bone content and subsequent fracturing of skeletal parts is a major health problem in Western society with its increasingly aging population.

Dual-energy methods have been proposed to solve the fat-error problem (59-61). Greater accuracy of bone mineral content determination is predicted with dual-energy methods, but at the cost of precision.

1.3 DUAL ENERGY QUANTITATIVE COMPUTED TOMOGRAPHY

In dual-energy quantitative computed tomography (DEQCT) attenuation data are gathered at two different X-ray tube potentials. The X-ray attenuation information obtained can be processed to determine an estimate of the bone mineral content. Two different methods of processing are described in the literature.

First, a method called preprocessing dual-energy QCT. The attenuation data obtained at two different X-ray tube potentials are combined to a special projection data set that is used to reconstruct CT images. The projection data set can be decomposed into an incoherent scattering medium image and a photo-electric absorbing medium image (60,62-63) or into images representing two natural substances (64-65). As specific hardware and software is required to perform this technique, it cannot be used on standard CT systems.

Second, postprocessing methods are described (59,66-68). The CT images at both scanning energies are reconstructed as in SEQCT. These methods are much easier to use and more accessible in clinical practice. The mean CT number of the ROI within the vertebral body is determined in both images. Then they are combined using specific algorithms to give a bone mineral estimate. Various postprocessing DEQCT methods have been proposed to increase the accuracy of bone mineral content estimation.

It is suggested that a more accurate estimation could be important for the prediction of vertebral strength (69,70). As already indicated, this is important

for research and clinical decision making in osteoporosis. The distinct values of the various postprocessing DEQCT methods for bone mineral content analysis have not been evaluated. It is not clear to what extent these methods correct the fat-error. Further, it is not established which of these methods is the method of choice.

Apart from a solution to the fat-error in bone mineral content determination, DEQCT can provide additional information about the anatomic composition of the vertebral body. It has been used experimentally to estimate fat content within the vertebral body of patients with different clinical syndromes, such as Cushing's disease and anorexia nervosa (71-73). Again, the value of the methods used for this purpose has not been evaluated. Determination of the fat content could be of importance for prediction of positive and negative results in treatment of osteoporosis or for unravelling different types of osteoporosis (with or without an increase in intravertebral marrow fat content), as it is suggested that bone formation is deficient adjacent to fatty marrow as a result of diminished vascularity or due to the fact that the adipocytes (cells containing fat) and the osteoblasts (the "bone-makers") share a common pole of stem cells (74).

1.4 AIM OF THE STUDY

Neither the distinct value of the different postprocessing DEQCT methods for bone mineral analysis, nor the value of these methods for providing additional information about the anatomic composition of the vertebral body have been evaluated. Therefore, a study was performed to evaluate the different postprocessing DEQCT methods for bone mineral content determination within the trabecular region of the vertebral body. In addition, acquisition of a more fundamental insight to the possibilities of postprocessing DEQCT methods could be advantageous for application of these methods outside the field of bone mineral analysis.

Ideally, the questions to be answered by the evaluation are:

1.   What are the differences and similarities between the various postprocessing DEQCT methods?

2.   Are some methods better than others?

3.   Do they really improve the accuracy of bone mineral measurements compared with single-energy QCT?

4

4. Can these methods give a reliable estimate of the intravertebral fat content?

5. What are the practical problems when these methods are used in clinical practice?

6. Is there a place for DEQCT in clinical practice at this moment?

7. What area's of future research could improve the performance of postprocessing DEQCT methods?

1.5 OUTLINE OF THE STUDY

After this general introduction, a brief introduction to the physics of X-ray interactions, CT imaging and QCT is given in chapter 2. The postprocessing DEQCT methods are then discussed in chapter 3.

Evaluation of the postprocessing DEQCT methods is made in several steps:

1. Theoretical analysis of the algorithms used in the different methods (chapter 3).

2. Analysis of the methods by applying dual-energy methods in a phantom study on a standard CT scanner (chapter 4).

3. Analysis of the problems encountered in the phantom study by transferring these to a patient simulation set-up. This set-up allows the modelling of a range of physiologic and pathologic conditions within the trabecular region of the vertebral body, as well as the modelling (separately or combined) of error sources inherent to the method or to the use of a CT scanner (chapters 5 and 6).

4. Analysis of the precision of the postprocessing methods using the patient simulation set-up and an in vitro study with a human cadaver specimen of the lumbar spine (chapter 7).

5. Exploration of the use and practical problems of postprocessing DEQCT in a patient case study (chapter 8).

A conclusion is formulated about the use and prospects of DEQCT in radiological practice in chapter 9 and areas of future research are indicated.

1.6 REFERENCES.

1. Swindell W, Webb S. X-ray transmission computed tomography. In: Webb S, ed. The physics of medical imaging. Bristol and Philadelphia. Adam Hilger. 1988:98-127.

2. Huddleston AL. Quantitative computed tomography. In: Quantitative methods in bone densitometry. Boston. Kluwer Academic Publishers. 1988:85-112.

3. Reich NE, Seidelmann FE, Tubbs RR, MacIntyre WJ, Meaney TF, Alfidi RJ, Pepe RG. Determination of bone mineral content using CT scanning. Am J Roentgenol 1976;127:593-594.

4. Bradley JG, Huang HK, Ledley RS. Evaluation of calcium concentrations in bones from CT scans. Radiology 1978;128:103-107.

5. Cann CE, Genant HK. Precise measurement of vertebral mineral content using computed tomography. J Comput Assist Tomogr 1980;4:493-500.

6. Cann CE, Gamsu G, Birnberg FA, Webb WR. Quantification of calcium in solitary pulmonary nodules using single- and dual-energy CT. Radiology 1982;145:493-496.

7. Zerhouni EA, Boukadoum M, Siddiky MA, Newbold JM, Stone DC, Spivey MP, Hesselman CW, Leo FP, Stitik FP, Siegelman SS. A standard phantom for quantitative CT analysis of pulmonary nodules. Radiology 1983;149:767-773.

8. Huston III J, Muhm JR. Solitary pulmonary nodules: evaluation with a CT reference phantom. Radiology 1989;170:653-656.

9. Goldberg HI, Cann CE, Moss AA, Ohto M, Brito A, Federle M. Noninvasive quantitation of liver iron on dogs with hemochromatosis using dual-energy CT scanning. Invest Radiol 1982;17:375-380.

10. Sephton RG. The potential accuracy of dual energy computed tomography for the determination of hepatic iron. Brit J Radiol 1986;59:351-353.

11. Leighton DM, De Campo JF, Matthews R, Sephton RG. Dual energy CT estimation of liver iron content in thalassaemic children. Australas Radiol 1988;32:214-219.

12. Mitcheson HD, Zamenhof RG, Bankoff MS, Prien EL. Determination of the chemical composition of urinary calculi by computerized tomography. J Urol 1983;130:814-819.

13. Baron RL, Rohrmann Jr CA, Lee SP, Shuman WP, Teefey SA. CT evaluation of gallstones in vitro: correlation with chemical analysis. AJR 1988;151:1123-1128.

14. Brakel K, Laméris JS, Nijs HGT, Terpstra OT, Steen G, Blijenberg BC. Predicting gallstone composition with CT: in vivo and in vitro analysis. Radiology 1990;174:337-341.

15. Bellamy EA, Nicholas D, Husband JE. Quantitative assessment of lung damage due to bleomycin using computed tomography. Brit J Radiol 1987;60:1205-1209.

16. Reinbold WD, Wannenmacher M, Hodapp N, Adler CP. Osteodensitometry of vertebral metastases after radiotherapy using quantitative computed tomography. Skeletal Radiol 1989;18:517-521.

17.   Müller-Gerbl M, Putz R, Hodapp N, Schulte E, Wimmer B. Computed tomography-osteodensitometry for assessing the density distribution of subchondral bone as a measure of long-term mechanical adaptation in individual joints. Skeletal Radiol 1989;18:507-512.

18.   McCullough EC. Factors effecting the use of quantitative information from a CT-scanner. Radiology 1977;124:99-107.

19.   van Panthaleon van Eck RB. Three dimensional teletherapy treatment planning. PhD Thesis. University of Eindhoven, 1986.

20.   Gur D, Yonas H, Good WF. Local cerebral blood flow by Xenon-enhanced CT: current status, potential improvements, and future directions. Cerebrovasc Brain Mtab Rev 1989;1:68-86.

21.   Lee TY, Elis RJ, Dunscombe PB, McClarty B, Hodson DI, Kroeker MA, Bews J. Quantitative computed tomography of the brain with xenon enhancement: a phantom study with the GE9800 scanner. Phys Med Biol 1990;35:925-935.

22.   Bews J, Dunscombe PB, Lee TY, McClarty B, Kroeker MA. The role of noise in the measurement of cerebral blood flow and partition coefficient using xenon enhanced computed tomography. Phys Med Biol 1990;35:937-945.

23.   Ellingson LA, Vannier MW. Applications of dual-energy X-ray computed tomography to structural ceramics. In: Advances in X-ray analysis, Vol 32. Barrett CS, et al. eds. Plenum Publishing Corp. 1989:629-639.

24.   Genant HK. Quantitative computed tomography: update 1987. Calcif Tissue Int 1987;41:179-186.

25.   Tothill P. Methods of bone mineral measurement. Phys Med Biol 1989;34:543-572.

26.   Genant HK, Block JE, Steiger P, Glueer CC, Ettinger B, Harris ST. Appropriate use of bone densitometry. Radiology 1989;170:817-822.

27.   Block JE, Smith R, Steiger P, Glüer CC, Ettinger B, Genant HK. Models of spinal trabecular bone loss as determined by quantitative computed tomography. Bone 1989;4:249-257.

28.   Cann CE, Genant HK, Kolb FO, Ettinger B. Quantitative CT for prediction of vertebral fracture risk. Bone 1985;6:1-7.

29.   Ettinger B, Genant HK, Cann CE. Postmenopausal bone loss is prevented by treatment with low dosage estrogen with calcium. Ann Int Med 1987;106:40-45.

30.   Montag M, Dören M, Meyer-Galander HM, Montag Th, Peters PE. Computertomographisch bestimmter Mineralgehalt in der LWS-Spongiosa. Radiologe 1988;161-165.

31.   Compston JE, Evans WD, Crawley EO, Evans C. Bone mineral content in normal UK subjects. Brit Med J 1988;61:631-636.

32.   Fujii Y, Tsutsumui M, Tsunennari T, Fukase M, Yoshimoto Y, Fujita T, Genant HK. Quantitative computed tomography of lumbar vertebrae in Japanese patients with osteoporosis. Bone Mineral 1989;6:87-94.

33. Kalender WA, Felsenberg D, Louis O, Lopez P, Klotz E, Osteaux M, Fraga J. Reference values for trabecular and cortical vertebral bone density in single and dual-energy quantitative computed tomography. Eur J Radiol 1989;9:75-80.

34. Müller A, Rüegsegger E, Rüegsegger P. Peripheral QCT: a low risk procedure to identify women predisposed to osteoporosis. Phys Med Biol 1989;34:741-749.

35. Sartoris DJ, Andre M, Resnick C, Resnick D. Trabecular bone density in the proximal femur: quantitative CT assessment. Radiology 1986;160:707-712.

36. Sakurai K, Marumo F, Iwanami S, Uchida H, Matsubayashi T. Quantitative computed tomographic evaluation of femoral bone mineral content in renal osteodystrophy compared with radial photon absorptiometry. Invest Radiol 1989;24:375-382.

37. Kalender WA, Klotz E, Suess C. Vertebral bone mineral analysis: an integrated approach with CT. Radiology 1987;164:419-423.

38. Mazess RB. Errors in measuring trabecular bone by computed tomography due to marrow and bone composition. Calcif Tissue Int 1983;35:148-152.

39. Mazess RB, Vetter J. The influence of marrow on measurement of trabecular bone using computed tomography. Bone 1985;6:349-351.

40. Rohloff R, Hitzler H, Arndt W, Frey KW. Experimentelle Untersuchungen zur Genauigkeit der Mineralsalzgehaltsbestimmung spongiöser Knochen mit Hilfe der quantitativen CT (Einenergiemessung). Fortschr Röntgenstr 1985;143:693-697.

41. Laval-Jeantet AM, Roger B, Bouysse S, Bergot C, Mazess RB. Influence of vertebral fat on quantitative CT density. Radiology 1986;159:463-466.

42. Webber CE. The effect of fat on bone mineral measurements in normal subjects with recommended values of bone, muscle and fat attenuation coefficients. Clin Phys Physiol Meas 1987;8:143-158.

43. Brooks RA, Di Chiro G. Beam-hardening in X-ray reconstructive Tomography. Phys Med Biol 1976;21:390-398.

44. Weissberger MA, Zamenhof RG, Aronow S, Neer RM. Computed tomography scanning for the measurement of bone mineral in the human spine. J Comput Assist Tomogr 1978;2:253-262.

45. Imamura K, Fujii M. Empirical beam hardening correction in the measurement of vertebral bone mineral content by computed tomography. Radiology 1981;138:223-226.

46. Rao PS, Alfidi RJ. The environmental density artifact: a beam-hardening effect in computed tomography. Radiology 1981;141:223-227.

47. Moström U, Ytterbergh C. Reliability of attenuation measurements in CT of the lumbar spine: evaluation with an anthropomorphic phantom. J Comput Assist Tomogr 1988;12:474-481.

48. Johns PC, Yaffe M. Scattered radiation in fan beam imaging systems. Med Phys 1982;9:231-238.

49. Joseph PM, Spital RD. The effects of scatter in X-ray computed tomography. Med Phys 1982;9:464-472.

50. Breatnach E, Robinson PJ. Repositioning errors in measurement of vertebral attenuation values by computed tomography. Brit J Radiol 1983;56:299-305.

51. Rosenthal DI, Ganott MA, Wyshak G, Slovik DM, Doppelt SH, Neer RM. Quantitative computed tomography for spinal density measurement: Factors affecting precision. Invest Radiol 1985;20:306-310.

52. Felsenberg D, Kalender WA, Banzer D, Schmilinsky G, Heyse M, Fischer E, Schneider U. Quantitative computertomographischen Knochenmineralgehaltsbestimmung. Fortschr Röntgenstr 1988;148:431-436.

53. Kalender WA, Brestowsky H, Felsenberg D. Bone mineral measurement: automated determination of midvertebral CT section. Radiology 1988;168:219-221.

54. Sandor T, Kalender WA, Hanlon WB, Weissman BN, Rumbaugh C. Spinal bone mineral determination using automated contour detection: application to single and dual energy CT. SPIE 1985;555:188-194.

55. Banks LM, Stevenson JC. Modified method of spinal computed tomography for trabecular bone mineral measurements. J Comput Assist Tomogr 1986;10:463-467.

56. Louis O, Luypaert R, Kalender W, Osteaux M. Reproducibility of CT bone densitometry: operator versus automated ROI definition. Eur J Radiol 1988;8:82-84.

57. Steiger P, Block JE, Steiger S, Heuck AF, Friedlander A, Ettinger B, Harris ST, Glüer CC, Genant HK. Spinal bone mineral density measured with quantitative CT: Effect of region of interest, vertebral level, and technique. Radiology 1990;175:537-543.

58. Kalender WA, Suess C. A new calibration phantom for quantitative computed tomography. Med Phys 1987;14:863-866.

59. Genant HK, Boyd D. Quantitative bone mineral analysis using dual energy computed tomography. Invest Radiol 1977;12:545-551.

60. Brooks RA. A quantitative theory of the Hounsfield unit and its application to dual energy scanning. J Comput Assist Tomogr 1977;1:487-493.

61. Adams JE, Chen SZ, Adams PH, Isherwood I. Measurement of trabecular bone mineral by dual energy computed tomography. J Comput Assist Tomogr 1982;6:601-607.

62. Alvarez RE, Macovski A. Energy-selective reconstructions in X-ray computerized tomography. Phys Med Biol 1976;21:733-744.

63. Rutherford RA, Pullan BR, Isherwood I. Measurement of effective atomic number and electron density using an EMI scanner. Neuroradiology 1976;11:15-21.

64. Hemmingson A, Jung B, Ytterbergh C. Dual energy computed tomography: Simulated monoenergetic and material-selective imaging. J Comput Assist Tomogr 1986;10:490-499.

65. Kalender W, Felsenberg D. Suess C. Materialselektive Bildgebung und Dichtemessung mit der Zwei-Spektren-Methode III: Knochenmineralbestimmung mit CT an der Wirbelsaüle. Digit Bilddiagn 1987;7:170-176.

66. Laval-Jeantet AM, Cann CE, Roger B, Dallant P. A postprocessing dual energy technique for vertebral CT densitometry. J Comput Assist Tomogr 1984;8:1161-1167.

67. Nickoloff EL, Feldman F. Bone mineral assessment with dual energy computerized tomography (CT) imaging. SPIE 1985;555:178-187.

68. Goodsitt MM, Rosenthal DI, Reinus WR, Coumas J. Two postprocessing CT techniques for determining the composition of trabecular bone. Invest Radiol. 1987;22:209-215.

69. Eriksson SAV, Isberg BO, Lindgren JU. Prediction of vertebral strength by dual photon absorptiometry and quantitative computed tomography. Calcif Tissue Int 1989;44:243-250.

70. Mosekilde L, Bentzen SM, Ortoft G, Jorgensen J. The predictive value of quantitative computed tomography for vertebral body compressive strength and ash density. Bone 1989;10:465-470.

71. Rosenthal DI, Mayo-Smith W, Goodsitt MM, Doppelt S, Mankin HJ. Bone and bone marrow changes in Gaucher disease: evaluation with quantitative CT. Radiology 1989;170:143-146.

72. Mayo-Smith W, Rosenthal DI, Goodsitt MM, Klibanski A. Intravertebral fat measurement with quantitative CT in patients with Cushing disease and anorexia nervosa. Radiology 1989;170:835-838.

73. Rosenthal DI, Hayes CW, Rosen B, Mayo-Smith W, Goodsitt MM. Fatty replacement of spinal bone marrow by dual energy quantitative CT and MR imaging. J Comput Assist Tomogr 1989;13:463-465.

74. Martin RB, Chow BD, Lucas PA. Bone marrow fat content in relation to bone remodelling and serum chemistry in intact and ovariectomized dogs. Calcif Tissue Int 1990;46:186-194.

CHAPTER 2
BASIC PRINCIPLES OF CT AND QCT

2.1 INTRODUCTION

In this chapter some basic principles of X-ray diagnostic radiology and in particular the basic principles of CT (Computed Tomography) and quantitative CT are discussed. It is not the intention to give a full description of X-ray (and CT) physics and mathematics in this chapter. The reader is referred to: "The Physics of Medical Imaging" S. Webb ed. 1988, Adam Hilger, Bristol Philadelphia (1). For an introduction to CT the reader is referred to: "Computed Tomography. Principles and Practice" 1990, Philips Medical Systems, Eindhoven (2).

2.2 BASIC PRINCIPLES OF X-RAY INTERACTIONS

X-rays are electromagnetic waves which are produced when electrons strike a solid target. These electromagnetic waves consist of photons, which are packets of energy. In X-ray imaging, photons are emitted from an X-ray tube, enter the object of interest (the patient) and can interact in different ways with the matter they encounter. Photons are absorbed or scattered, or just pass the object without any interaction. The photons which have transversed the object can be visualized using an X-ray film or fluoroscopic screen, or can be detected by radiation detectors. Detection or visualization of the photons transversing an object gives a "photon attenuation map" of the object.

In more detail: in the energy range used for diagnostic purposes, photon attenuation can be divided in terms of three different photon interactions; namely, photo-electrical effect, coherent scattering and incoherent scattering. Generally, photon interactions are described using two parameters, that are much easier to understand; namely, absorption and scatter. Both parameters will decrease the intensity of the radiation. Absorption decreases as the voltage used to generate the X-ray beam is increased. At low voltages (i.e. soft radiation), absorption is the prime interaction, whereas at higher voltages (i.e. hard radiation) scatter becomes the prime interaction.

The degree of attenuation depends on the composition and thickness of the material. For a homogeneous material:

$$I_t = I_o e^{-\mu d} \tag{1},$$

where, I_t is the transmitted intensity; I_o is the incident intensity; μ is the linear attenuation coefficient (in cm^{-1}) and d is the thickness of the material (in cm).

The linear attenuation coefficient is in fact a measure for the probability that an X-ray photon will be attenuated in the material per unit length. The linear attenuation coefficient is, as indicated above, energy (E) and material dependent; $\mu(E,Z,r)$, where, Z indicates the anatomic composition and r the physical density. For a compound or mixture the mass attenuation coefficient μ/r can be approximated from the coefficients of the constituent elements by (3):

$$\mu / r = \Sigma \, m_i \, \mu_i / r_i \tag{2},$$

where, m_i is the mass fraction of element i.

2.3 BASIC PRINCIPLES OF COMPUTED TOMOGRAPHY

In CT, an X-ray source is rotated around an object of interest. Photon attenuation is measured along several lines from the focal spot of the X-ray source to the detectors which are opposite to the focal spot (figure 2.1). These measurements are used to reconstruct a two-dimensional map of photon attenuation of the object of interest (1,2). This map is composed of so-called picture elements or "pixels". The volume of the scanned object which is represented by a pixel is called a volume element or "voxel".

In CT the attenuation values are expressed as Hounsfield Units (HU), according to equation 3:

$$CT\# = 1000 * (\mu_o - \mu_w) / \mu_w \tag{3},$$

where CT# is the CT number in Hounsfield Units; μ_o is the energy dependent attenuation coefficient of the object of interest; μ_w is the energy dependent attenuation coefficient of water.

The Hounsfield scale relates the photon attenuation of an object to the photon
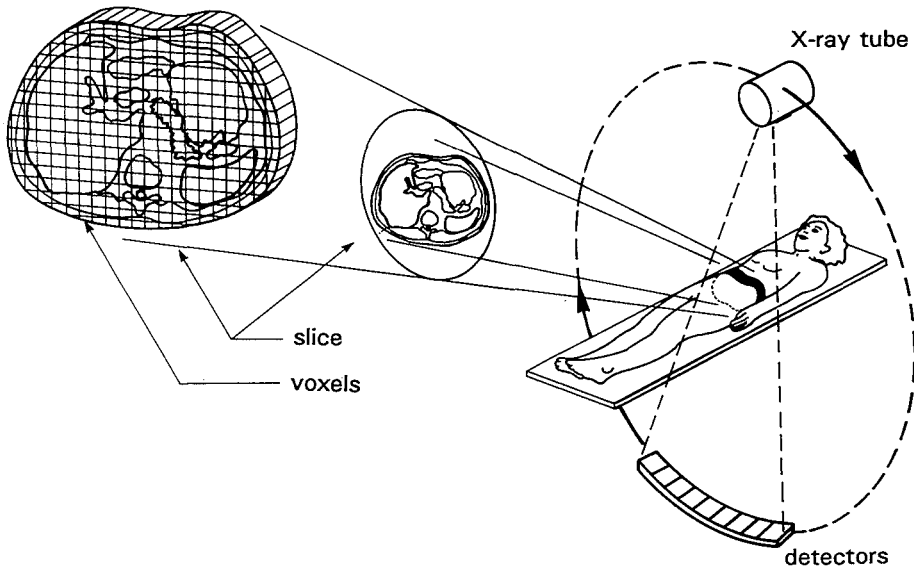
Figure 2.1. Principles of CT scanning. *(Courtesy of Philips Medical Systems).*

attenuation of water. Matter which attenuates the photon beam more than water gets a positive CT number, while matter which attenuates the photon beam less than water gets a negative CT number.

One important feature of attenuation and CT numbers should be addressed: beam hardening. As the X-ray beam is polychromatic, the energy spectrum changes as the X-rays pass through an object. The lower energies in the X-ray spectrum are attenuated more than the higher energies. Consequently, the effective energy, defined as the equivalent monochromatic energy, increases as more tissue is transversed. Therefore, the CT number of a compound or tissue will not be equal when located at different positions in an object, and will vary in time if the object itself changes in size or composition. The reader is referred to the literature for more details (1-9).

2.4 BASIC PRINCIPLES OF QUANTITATIVE COMPUTED TOMOGRAPHY

The CT image is a two-dimensional display of a map of attenuation values. This map can be used to determine the average attenuation value (expressed in CT

numbers) of the object or of a specific region of interest (ROI) within the object. One of the first studies which used the probabilities of the specific features of CT scanning for quantitative assessment of bone mineral content was published by Reich et al in 1976 (10). From a numerical printout of scans made of bone specimens from tibias and fibulas of ten cadavers with a Delta CT scanner they determined the average CT number. This number correlated well with calcium determinations of the specimens. A similar study by Bradley et al was published in 1978 (11). They made scans of lumbar vertebrae with an ACTA CT scanner and calculated the average CT number of the cancellous part of the lumbar vertebral bodies. A good correlation was found between the average CT number and the calcium content of the lumbar vertebral bodies.

As indicated in paragraph 2.3, CT numbers should not be considered as absolute values. Although the CT scale is defined clearly, the beam hardening phenomenon will cause the CT scale to drift within the scan field (9). The CT numbers show dependency on the object size, object shape, and the spectrum of the X-ray source. Several correction schemes have been developed to solve the beam hardening problem. There are preprocessing corrections like prefiltering and linearization (8), and postprocessing corrections (12-16). Significant differences in CT numbers between scanners have been reported (17-19), as well as differences within one scanner due to scanner instabilities, like changes in X-ray spectral quality (20). Therefore, reference devices were introduced in QCT for bone mineral analysis, which are scanned together with the patient (also called "simultaneous calibration") (21,22) or separate from the patient ("non-simultaneous calibration") (23). The reference devices contain a bone-mimicking material [usually dipotassium hydrogenphosphate (K_2HPO_4) or calcium hydroxyapatite] in different concentrations within a "soft-tissue environment" (usually water or a water-equivalent plastic). Using the reference device, the average CT number of the object of interest is converted to a bone equivalent value. See chapter 3 for more details.

The trabecular region of the vertebral bodies in the spine is the region of interest used most frequently in QCT studies. As the turn-over rate of trabecular bone is thought to be eight times that of cortical bone, pathologic changes will become apparent more readily in this part of the skeleton. Further, some types of osteoporosis (postmenopausal and corticosteroid-induced osteoporosis) have a predilection for the spine (24). Therefore, we will confine this discussion to QCT

14

of the trabecular region of the vertebral body.

As indicated in chapter 1, the accuracy of the single-energy QCT technique is impaired by the presence of intravertebral fat. The linear attenuation coefficient of fat is lower than that of water. Therefore, the CT number of fat is negative according to equation 3. The trabecular region of the vertebral body consists of trabecular bone substance (a collagen matrix with mineral deposits), hematopoietic tissue (red marrow) and adipose tissue (yellow marrow). Trabecular bone, and more particular bone mineral (primarily calcium hydroxyapatite) has a high attenuation resulting in a positive CT number. Hematopoietic tissue has an attenuation that is similar to that of water, resulting in a CT number close to zero. In SEQCT the trabecular region of the vertebral body is described as a two-compartment model, namely bone mineral within a watery environment. As indicated, the different components have their own characteristic quantitative behaviour, which is partly neglected when performing SEQCT. Especially, the influence of the fat content is neglected. Therefore, accuracy of the bone mineral content estimation with SEQCT will be limited.

Furthermore, as intravertebral fat content varies interindividually as well as with age and disease, this results in an accuracy error of unknown magnitude and difficulties in interpretation of longitudinal studies of bone mineral content changes as measured with SEQCT.

Dual-energy QCT (DEQCT) may be a solution to this problem. By adding an extra measurement at a different energy, the trabecular region is described as a three-compartment model. Fat tissue can be treated as a separate compartment with DEQCT, ruling out its negative influence. DEQCT is based on the difference of the energy dependency of the attenuation characteristics of the various constituents of the vertebral body. Figure 2.2 shows the mass attenuation coefficients (μ/r) of bone, water and fat as a function of energy (data derived from reference 25).

Several techniques of DEQCT have been proposed: postprocessing techniques and preprocessing techniques. The postprocessing methods will be discussed extensively in chapters 3 and 4; their evaluation being the main aim of this study. The other techniques will be discussed briefly here.

One of the first studies concerning tissue description with DEQCT was published by Rutherford et al in 1976 (26). In their paper a preprocessing technique was described which used a decomposition of the attenuation data in terms of the
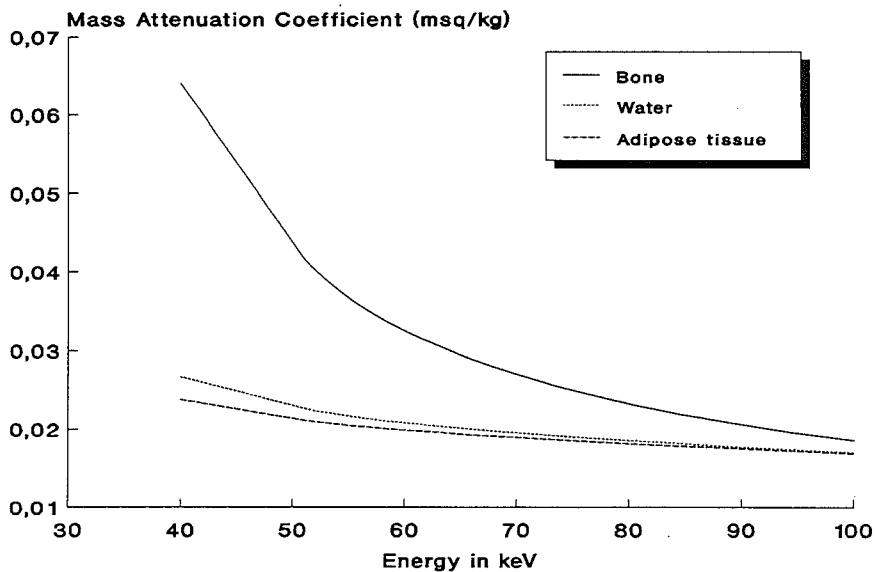
Mass Attenuation Coefficient (msq/kg)

Energy in keV

Figure 2.2. Mass attenuation coefficients (m²/kg) of different tissues versus energy (keV).

photo-electric part and the coherent scatter part of the X-ray interaction with matter. The outcome is an estimation of the effective atomic number and the effective electron density of the material under investigation. A similar approach was chosen by Brooks (27). Both approaches have been criticised (5,28-30) and are seldom applied in practice (29,31,32). Another decomposition technique was introduced by Marshall and coworkers (33,34). The projection data acquired with CT were used along with calibration data obtained with aluminium and plastic to reconstruct aluminium and plastic equivalent images. The initial clinical use was for tissue characterization of brain lesions. A similar approach was chosen by Kalender et al (35,36). It was applied to bone mineral content determination in the trabecular region in the vertebral body. In the aluminium equivalent images, the average pixel value of the ROI was converted to a mineral equivalent value, using a calibration curve generated by scanning $CaCl_2$ solutions of different concentrations. It was also tested for skull examinations and liver studies (37). This dual-energy concept was implemented in commercially available CT scanners by Siemens AG. Changes to calcium / lucite decomposition were made and evaluated (38). In addition, water / calcium decomposition is described (39,40). Research continues to find more efficient decomposition methods (41,42).

16

2.5 REFERENCES

1. Webb S, ed. The Physics of Medical Imaging. 1988, Adam Hilger, Bristol Philadelphia.

2. Computed Tomography Principles and Practice. 1990, Philips Medical Systems, Eindhoven.

3. McCullough EC. Photon attenuation in computed tomography. Med Phys 1975;2:307-320.

4. Phelps ME, Gado MH, Hoffman EJ. Correlation of effective atomic number and electron density with attenuation coefficients measured with polychromatic X rays. Radiology 1975;117:585-588.

5. Hawkes DJ, Jackson DF. An accurate parametrisation of the X-ray attenuation coefficient. Phys Med Biol 1980;25:1167-1171.

6. Brooks RA, Mitchell LG, O'Connor CM, Di Chiro G. On the relationship between computed tomography numbers and specific gravity. Phys Med Biol 1981;26:141-147.

7. Rao PS, Gregg EC. Attenuation of monoenergetic gamma rays in tissues. Amer J Roentgenol 1975;123:631-637.

8. Brooks RA, Di Chiro G. Beam hardening in X-ray reconstructive tomography. Phys Med Biol 1976;21:390-398.

9. Zatz LM, Alvarez RE. An inaccuracy in computed tomography: the energy dependence of CT values. Radiology 1977;124:91-97.

10. Reich NE, Seidelmann FE, Tubbs RR, MacIntyre WJ, Meaney TF, Alfidi RJ, Pepe RG. Determination of bone mineral content using CT scanning. Amer J Roentgenol 1976;127:593-594.

11. Bradley JG, Huang HK, Ledley RS. Evaluation of calcium concentration on bones from CT scans. Radiology 1978;128:103-107.

12. Joseph PM, Spital RD. A method for correcting bone induced artifacts in computed tomography scanners. J Comput Assist Tomogr 1978;2:100-108.

13. Rüegsegger P, Hangartner Th. Keller HU, Hinderling Th. Standardization of computed tomography images by means of a material-selective beam hardening correction. J Comput Assist Tomogr 1978;2:184-188.

14. Nalcioglu O, Lou RY. Post-reconstruction method for beam hardening in computerised tomography. Phys Med Biol 1979;24:330-340.

15. Imamura K, Fujii M. Empirical beam hardening correction in the measurement of vertebral bone mineral content by computed tomography. Radiology 1981;138:223-226.

16. Robertson Jr DD, Huang HK. Quantitative bone measurements using X-ray computed tomography with second-order correction. Med Phys 1986;13:474-479.

17. Levi C, Gray JE, McCullough EC, Hattery RR. The unreliability of CT numbers as absolute values. AJR 1982;139:443-447.

18. Moström U, Ytterbergh C. Reliability of attenuation measurements in CT of the lumbar spine: evaluation with an anthropomorphic phantom. J Comput Assist Tomogr 1988;12:474-481.

19. Cann CE. Quantitative CT applications: comparison between scanners. Radiology 1987;162:257-261

20. Kalender WA, Klotz E, Suess C. Vertebral bone mineral analysis: an integrated approach with CT. Radiology 1987;164:419-423.

21. Cann CE, Genant HK. Precise measurement of vertebral mineral content using computed tomography. J Comput Assist Tomogr 1980;4:493-500.

22. Kalendar WA, Suess C. A new calibration phantom for quantitative computed tomography. Med Phys 1987;14:863-866.

23. Goodsitt MM, Rosenthal DI. Quantitative computed tomography scanning for measurement of bone and bone marrow fat content. A comparison of single- and dual-energy techniques using a solid synthetic phantom. Invest Radiol 1987;22:799-810.

24. Wright CDP, Crawley EO, Evans WD, Garrahan NJ, Mellish RWE, Croucher PI, Compston JE. The relationship between spinal trabecular bone mineral content and iliac crest trabecular bone volume. Calcif Tissue Int 1990;46:162-165.

25. Hubbell JH. Photon mass attenuation and energy-absorption coefficients from 1 keV to 20 MeV. Int J Appl Radiat Isot 1982;33:1269-1290.

26. Rutherford RA, Pullan BR, Isherwood I. Measurement of effective atomic number and electron density using an EMI scanner. Neuroradiology 1976;11:15-21.

27. Brooks RA. A quantitative theory of the Hounsfield unit and its application to dual energy scanning. J Comput Assist Tomogr 1977;1:487-493.

28. Jackson DF, Hawkes DJ. Energy dependence in the spectral factor approach to computed tomography. Phys Med Biol 1983;28:289-293.

29. Dunscombe PB, Katz DE, Stacey AJ. Some practical aspects of dual energy CT scanning. Brit J Radiol 1984;57:82-87.

30. Hawkes DJ, Jackson DF, Parker RP. Tissue analysis by dual-energy computed tomography. Brit J Radiol 1986;59:537-542.

31. Adams JE, Chen SZ, Adams PH, Isherwood I. Measurement of trabecular bone mineral by dual energy computed tomography. J Comput Assist Tomogr 1982;6:601-607.

32. Eriksson S, Isberg B, Lindgren U. Vertebral bone mineral measurement using dual photon absorptiometry and computed tomography. Acta Radiol 1988;29:89-94.

33. Marshall WH, Alvarez RE, Macovski A. Initial results with prereconstruction dual-energy computed tomography (PREDECT). Radiology 1981;140:421-430.

34. Marshall W, Hall E, Doost-Hoseini A, Alvarez R, Macovski A, Cassel D. An implementation of dual energy CT scanning. J Comput Assist Tomogr 1984;8:745-749.

35. Kalender WA, Perman WH, Vetter JR, Klotz E. Evaluation of a prototype dual-energy computed tomographic apparatus. I. Phantom studies. Med Phys 1986;13:334-339.

36. Vetter JR, Perman WH, Kalendar WA, Mazess RB, Holden JE. Evaluation of a prototype dual-energy computed tomographic apparatus. II. Determination of vertebral bone mineral content. Med Phys 1986;13:340-343.

37. Hemmingson A, Jung B, Ytterbergh C. Dual energy computed tomography: simulated monoenergetic and material-selective imaging. J Comput Assist Tomogr 1986;10:490-499.

38. Montner SM, Lehr JL, Oravez WT. Quantitative evaluation of a dual energy CT system. J Comput Assist Tomogr 1987;11:144-150.

39. Kalender W, Felsenberg D, Suess C. Materialselektive Bildgebung und Dichtemessung mit der Zwei-Spektren-Methode III. Knochenmineralbestimmung mit CT an der Wirbelsäule. Digit Bilddiagn 1987:7:170-176.

40. Felsenberg D. Quantitative Knochenmineralgehalts-bestimmung mit der Zwei-Spektren-Computertomographie. Radiologe 1988;28:166-172.

41. Chuang KS, Huang HK. Comparison of four dual energy image decomposition methods. Phys Med Biol 1988;33:455-466.

42. Cardinal HN, Fenster A. An accurate method for direct dual-energy calibration and decomposition. Med Phys 1990;17:327-341.

CHAPTER 3
THEORETICAL CONSIDERATIONS [1]

3.1 INTRODUCTION

The accuracy of bone mineral measurements of the vertebral body with single-energy quantitative computed tomography (SEQCT) is influenced by the occurrence of intravertebral fat. Dual-energy quantitative computed tomography (DEQCT) has been proposed to improve the accuracy of bone mineral content determination (1-11) and to give additional information regarding the composition of the trabecular region of the vertebral body (10,12-14).

DEQCT can be done using preprocessing (11) or postprocessing methods (5-10). For preprocessing, special DEQCT hardware and software is required. However, postprocessing methods can be done easily on CT systems that allow a variable kVp selection. Various methods for postprocessing DEQCT have been proposed (5-10); the aim of this study was to evaluate these methods and to establish their distinct value. In this chapter, the methods are reported theoretically. In the next chapter, the practical aspects of using these methods are discussed.

3.2 THEORY

All quantitative CT methods in principle are based on the relation between the linear attenuation coefficient of a mixture of materials and the attenuation coefficients and concentrations of each of the materials (Equation 1):

$$\mu\{E\} = \sum_{i=1}^{n} (\mu_i\{E\}/r_i)c_i \qquad [1]$$

where, μ is the energy $\{E\}$ dependent linear attenuation coefficient of the mixture and μ_i that of the materials; r_i is the mass densities and c_i the concentrations. A list of abbreviations used for variables and subscripts is given in Appendix C.

The concentrations of the materials can be expressed in terms of their volumes

---

and mass densities:

$$c_i = r_i V_i \qquad\qquad [2]$$

where, V_i is the fractional volumes of the materials. In computed tomography the CT number (CT) is related to the attenuation coefficient by:

$$CT\{E\} = 1000 \ (\mu\{E\} - \mu_w\{E\}) \ / \ \mu_w\{E\} \qquad\qquad [3]$$

where, μ_w is the linear attenuation coefficient of water at energy E.
Equations 1 through 3 can be combined and rearranged to:

$$CT\{E\} = \Sigma(CT_i V_i\{E\}) \qquad\qquad [4]$$

where

$$1 = \Sigma V_i \qquad\qquad [5]$$

See Appendix A, for more details. Equation 4 states that the energy-dependent CT number of a mixture of materials (CT{E}) is the sum of the CT numbers of the pure materials (CT_i) multiplied by the fractions of volume (V_i) of the materials. The sum of the fractions of volume is 1 (Equation 5).

For understanding QCT of the trabecular region of the vertebral body, this region should be described in terms of Equation 4. The trabecular volume is composed of trabecular bone substance, water, red marrow and fat. The trabecular bone substance itself is a mixture of the collagen matrix and bone mineral (calcium hydroxyapatite). Translating this anatomic description to Equation 4 yields:

$$CT_v\{E\} = CT_{bm}\{E\}V_{bm} + CT_c\{E\}V_c + CT_{rm}\{E\}V_{rm} + CT_f\{E\}V_f + CT_w\{E\}V_w \quad [6]$$

The subscripts v, bm, c, rm, f and w, indicate the trabecular region of the vertebral body, bone mineral, collagen, red marrow, fat and water, respectively.
To understand the distinct features of the different postprocessing dual-energy QCT methods, these methods can be translated to Equation 6, which will be called the "basic formula".

3.3 DESCRIPTION OF METHODS

Postprocessing DEQCT methods were proposed initially by Rutherford et al (1), Genant and Boyd (2) and Brooks (3). Their suggestions were followed by Cann et al (5), who reported a method that is an extension of the single-energy method.

In SEQCT, a calibration device that contains different solutions of a material that mimicks bone (usually K_2HPO_4 in water, or calcium hydroxyapatite in a water-equivalent plastic) is scanned simultaneously with the patient. The calibration device is used to generate a bone equivalent calibration line that relates the mean CT number ($CT\#_{bc}$) of the different solutions to g/cm^3 K_2HPO_4 (or calcium hydroxyapatite):

$$CT\#_{bc} = a * Beq + b \qquad\qquad [7]$$

in which, "a" is the slope and "b" is the intercept of the calibration line; "Beq" is the bone mineral equivalent value (usually called bone mineral content) in g/cm^3 ; and subscript bc stands for bone equivalent calibration. Throughout this chapter the "#" after "CT" indicates mean CT numbers of objects that are measured.

The mean CT number ($CT\#_v$) of the vertebral body is converted to g/cm^3 Beq with the help of the calibration line:

$$Beq = (CT\#_v - b) / a \qquad\qquad [8]$$

The single-energy method describes the anatomic multi-component reality of the vertebral body in terms of a two-component model, e.g. bone mineral in water. Translating this description (see Appendix B for more details) to the basic formula (Equation 6) means that slope "a" represents $(CT_{bm}\{E\} - CT_x\{E\}) / r_{bm}$ and intercept "b" represents $CT_x\{E\}$ where CT_x is the CT number of the mixture of the non-mineral components of the trabecular body (collagen, red marrow, water and fat). This results in: $CT_xV_x = CT_cV_c + CT_{rm}V_{rm} + CT_fV_f + CT_wV_w$. The assumption that this mixture has the attenuation characteristics of water leads to the limited accuracy of bone mineral measurements with single-energy. It is assumed that $CT_{bm}\{E\}$ can be approximated by $CT\#_{bc}\{E\}$. Currently, dipotassium hydrogenphosphate (K_2HPO_4) is the most widely used bone-mimicking material for calibration purposes. It has attenuation characteristics similar to those of calcium hydroxyapatite.

Cann et al (5) assume for their postprocessing dual-energy method that the difference in the mean CT number of the trabecular portion of the vertebral body, determined at two different energies, is due to the mineral content only. This means that the influence of the fat content on the CT number should be the same at both energies. However, this is not the case. A bone equivalent calibration line is generated for both the scanning energies. The bone mineral equivalent value is computed subsequently using the equation:

$$Beq = \frac{(CT\#_v\{E1\} - CT\#_v\{E2\}) - (b\{E1\} - b\{E2\})}{(a\{E1\} - a\{E2\})} \qquad [9]$$

{E1} and {E2} indicate the two different scanning energies. In terms of the basic formula (Equation 6), this means that slope "a" represents $(CT_{bm}\{E\} - CT_y\{E\}) / r_{bm}$ and intercept "b" represents $(1 - V_f)CT_y\{E\}$. CT_y is the CT number of the mixture of the non-mineral and non-fat components of the vertebral body. This is: $CT_yV_y = CT_cV_c + CT_{rm}V_{rm} + CT_wV_w$. Using the calibration technique $b\{E\} \approx CT\#_w\{E\}$, where the subscript w indicates water-equivalent, it follows that $CT\#_w\{E\}$ should be equal to $(1 - V_f) CT_y\{E\}$. CT_w is zero according to Equation 3. On one hand the condition can be fulfilled if $V_f = 1$, which means that the trabecular region contains fat only; this is not an anatomic reality. However, the condition can be fulfilled if $CT_y\{E\}$ is zero, which is impossible for the two scanning energies. Therefore, this method will not give optimal results in bone mineral content determination.

In 1984 another dual-energy approach was reported by Laval-Jeantet et al (6). This approach takes into account the energy dependency of the fat influence. Apart from bone equivalent calibration lines, which yield slope a{E} and intercept b{E}, fat equivalent calibration lines are generated for each energy using the CT number of 0 g/cm³ bone equivalent (0% fat) and the CT number ($CT\#_f$) of a fat equivalent material (100% fat). The slopes ($\alpha\{E\}$) and intercepts ($\beta\{E\}$) of these fat equivalent calibration lines are used in the following equations:

$$CT\#\{E1\} = a\{E1\} * Beq + b\{E1\} + \alpha\{E1\} * F + \beta\{E1\} \qquad [10]$$

$$CT\#\{E2\} = a\{E2\} * Beq + b\{E2\} + \alpha\{E2\} * F + \beta\{E2\} \qquad [11]$$

in which F is the percentage of fat by volume in the vertebral body. These equations are solved to obtain the bone mineral equivalent value and the percentage of fat by volume.

Transforming these equations to the basic formula (Equation 6) shows that slope "a" of the bone-equivalent calibration line represents $(CT_{bm}\{E\} - CT_y\{E\}) / r_{bm}$. The slope "$\alpha$" of the fat equivalent calibration line represents $(CT_f\{E\} - CT_y\{E\}) / 100$. This method assumes that $CT\#_f\{E\} = CT_f\{E\}$; this is only true if the fat equivalent material used for calibration purposes has exactly the same attenuation characteristics as the intravertebral fat tissue. The sum of the intercepts "b + ß" should represent $CT_y\{E\}$. However, when using the calibration technique b and ß are both determined by the 0 g/cm³ sample, which simulates $CT_y\{E\}$. So b + ß is in fact two times $CT_y\{E\}$. Therefore, this method will cause inaccuracies in determination of both the bone mineral content and fat content.

In 1987, Goodsitt et al (8) proposed two new dual-energy methods. The first approach uses the same bone equivalent calibration lines as the approaches of Laval-Jeantet et al and Cann et al. In addition, the CT numbers of fat equivalent $(CT\#_f\{E\})$ and soft tissue equivalent $(CT\#_s\{E\})$ materials are used. This leads to the following equations:

$$CT\{E1\}N = a\{E1\} * Beq + b\{E1\} \tag{12}$$

$$CT\{E2\}N = a\{E2\} * Beq + b\{E2\} \tag{13}$$

$$CT\#\{E1\} = CT\{E1\}N + V_f * (CT\#_f\{E1\} - CT\#_s\{E1\}) \tag{14}$$

$$CT\#\{E2\} = CT\{E2\}N + V_f * (CT\#_f\{E2\} - CT\#_s\{E2\}) \tag{15}$$

$CT\#_s$ is the CT number of the 0 g/cm₃ sample in the calibration device. $CT\{E\}N$ is the calculated estimate of what the mean CT number of trabecular bone would be if the spongiosa contained no fat. These equations are solved for the bone mineral equivalent value and the volume fraction of fat.

Transforming these equations to the basic formula (Equation 6) shows that slope "a" represents $(CT_{bm}\{E\} - CT_y\{E\}) / r_{bm}$; intercept "b" represents $CT_y\{E\}$; and $(CT\#_f\{E\} - CT\#_s\{E\})$ should be equal to $(CT_f\{E\} - CT_y\{E\})$. As with the method of Laval-Jeantet et al, it is assumed that $CT\#_f\{E\}$ is equal to $CT_f\{E\}$. Therefore, a

fat-equivalent material used for calibration purposes should have exactly the same attenuation characteristics of the intravertebral fat. Furthermore, this method assumes that $CT\#_s\{E\}$ equals $CT_y\{E\}$. Because CT_y is the CT number of a mixture of materials (collagen and red marrow and water) for which the fractions of volume will vary interindividually, this condition cannot be fulfilled. However, this problem could be avoided partly, if calibration materials were available that simulate trabecular bone substance (calcium hydroxyapatite within a collagen matrix) diluted in a red marrow environment. Then, the assumption should be made that there is a fixed mineralization of the collagen matrix. If such calibration materials were available, slope "a" would represent $(CT_{bs}\{E\} - CT_{rm}\{E\}) / r_{bs}$; intercept "b" would represent $CT_{rm}\{E\}$; $(CT\#_f\{E\} - CT\#_s\{E\})$ should then be equal to $(CT_f\{E\} - CT_{rm}\{E\})$. The subscript bs indicates <u>b</u>one <u>s</u>ubstance. The water compartment of the trabecular region should then be combined with the red marrow compartment.

The only difference between the approaches of Goodsitt et al and Laval-Jeantet et al is the intercept ß used by the latter. The difference (D) between the bone mineral equivalent value calculated according to Laval-Jeantet et al and the value calculated according to Goodsitt et al can be derived easily:

$$D = \frac{(ß\{E1\} * \alpha\{E2\}) - (ß\{E2\} * \alpha\{E1\})}{(\alpha\{E1\} * a\{E2\}) - (\alpha\{E2\} * a\{E1\})} \qquad [16]$$

A similar relation for the fat content can be derived.

The second approach of Goodsitt et al (8) is a direct derivation of the basic formula (Equation 6):

$$CT\#\{E1\} = V_{bs} * CT\#_{bs}\{E1\} + V_f * CT\#_f\{E1\} + V_s * CT\#_s\{E1\} \qquad [17]$$

$$CT\#\{E2\} = V_{bs} * CT\#_{bs}\{E2\} + V_f * CT\#_f\{E2\} + V_s * CT\#_s\{E2\} \qquad [18]$$

$$1 = V_{bs} + V_f + V_s \qquad [19]$$

$CT\#_{bs}\{E\}$ is the CT-number of pure bone substance (bone mineral in collagen matrix); V_{bs} is the fraction of volume of bone substance. This method will be called "the basic approach" hereafter, to avoid confusion with the approach of Goodsitt et al discussed earlier.

In the original study by Goodsitt et al, $CT\#_{bs}\{E\}$ was estimated by scanning a sample of femoral cortex at the two energies separately from the patient, and determining the maximum CT number in the cortical region of the midshaft. This sample was scanned separately to avoid imaging artifacts. Ethylalcohol 100% was used to determine $CT\#_f\{E\}$; $CT\#_a\{E\}$ was defined as 0.

$CT\#_{bs}\{E\}$ represents the CT number of the mixture of bone mineral ($CT_{bm}\{E\}$) and collagen ($CT_c\{E\}$). The combination of these two materials is justified by assuming a constant mineralization of the collagen matrix. The basic approach should give good results if $CT\#_f\{E\}$ is equal to $CT_f\{E\}$ and $CT\#_a\{E\}V_a$ is equal to $CT_{rm}\{E\}V_{rm} + CT_w\{E\}V_w$, and if $CT\#_{bs}\{E\} * V_{bs}$ equals $CT_{bm}\{E\} * V_{bm} + CT_c\{E\} * V_c$.

The last method reported in this chapter is an approach reported by Nickoloff and Feldman in 1985 (7) and presented in more detail in 1988 (10). Their approach is a direct derivation of the basic formula:

$$CT\#\{E1\} = \Omega\{E1\}*c_b + \Theta\{E1\}*c_f + \sigma\{E1\}*c_s + \delta + \pi\{E1\} \qquad [20]$$

$$CT\#\{E2\} = \Omega\{E2\}*c_b + \Theta\{E2\}*c_f + \sigma\{E2\}*c_s + \delta + \pi\{E2\} \qquad [21]$$

$\Omega\{E\}$, $\Theta\{E\}$ and $\sigma\{E\}$ are the energy-dependent and material-specific coefficients calculated from the linear attenuation coefficients of the different materials. c_b, c_f, and c_s are the concentrations of bone substance, adipose tissue and soft tissue, respectively. δ is -1000. $\pi\{E\}$ is the offset value for water. The coefficient can be described in terms of the CT number of the pure materials: $(CT_i\{E\} + 1000) / r_i$. Combining this with Equation 2, this approach can be rewritten to the basic approach of Goodsitt et al discussed earlier in this chapter. Only one difference between the two methods remains; the water offset value used by Nickoloff. This water offset does not originate from the basic formula (Equation 6), because the soft tissue compartment incorporates water and red marrow (10). Therefore the water offset value is an empirical correction factor for CT number scale drift.

To use this method, a determination of the effective energy is required. To achieve this, a device with compartments containing different concentrations of calcium hydroxyapatite is scanned simultaneously with the patient and the effective energy is computed from the slope of the linear regression fit of the measured CT numbers of the compartments versus the concentrations. This

effective energy estimation may be in error because the effective energies at the site of the calibration device are different from those at the vertebral body.

The material-specific coefficients are calculated using knowledge of the elemental composition and the mass density of bone substance (again, it is assumed that there is a constant mineralization of the collagen matrix), intravertebral fat and red marrow, including the water compartment. Instead of finding suitable materials that mimick tissue for calibrating purposes, as required in the methods reported previously, this method requires an exact knowledge of the chemical and physical properties of the anatomic components of the vertebral body.

3.4 DISCUSSION

Four of the five methods discussed in this chapter use materials that mimick tissue for calibration purposes. It is assumed that CT_{bm} can be simulated by $CT\#_{bc}$. This is only true if the material that mimicks bone has the same attenuation characteristics as the real bone mineral. For instance, when dipotassium hydrogenphosphate (K_2HPO_4) is chosen as calibration material, an error in bone mineral estimation will occur, due to the (slight) difference in attenuation characteristics between K_2HPO_4 and calcium hydroxyapatite. This error was discussed by Glüer et al (15) and a correction factor was calculated. Furthermore, when using K_2HPO_4 solutions for calibration, additional errors can occur due to the so-called displacement effect. The errors arising from the use of K_2HPO_4 are discussed extensively by Rao et al (16) and Crawley et al (17).

For the postprocessing method of Cann et al, it is first assumed that CT_f is independent of energy. Secondly, the collagen compartment is combined with the red marrow and water compartments. It is assumed that this "soft tissue" compartment has the same attenuation characteristics as water (-equivalent). Both assumptions will lead to errors; as reported by Rao et al (16).

For the method of Laval-Jeantet et al, CT_f is approximated by $CT\#_f$. This means that the fat equivalent material should have the same attenuation characteristics as the intravertebral fat for a correct determination of the bone mineral content and the fat content. However, this method shows a methodologic problem due to the double intercept, which will lead to inaccuracies. Apart from the intercept problem, the calibration method of Goodsitt et al (8) is essentially the same as that of Laval-Jeantet et al (6). The same can be said about fat calibration. The

combination of the collagen compartment, red marrow compartment and water compartment to one soft tissue compartment can be a source of error. This combination of compartments is used by Cann et al and by Laval-Jeantet et al. Authors justify this combination by assuming that the attenuation characteristics of "soft tissue" are the same as those of water.

This "soft tissue problem" could be avoided partly by rearranging the compartments. Then, the assumption should be made that there is a fixed mineralization of the collagen matrix. The collagen and mineral compartments can be combined to a bone substance compartment. In that case, the "soft tissue" compartment contains red marrow and water only. However, calibration materials that mimick bone substance within a red marrow environment are not available currently. The assumption that red marrow could be mimicked by water for all energies is an approximation with limited value. The CT numbers for red marrow, calculated for the elemental composition as specified by Woodard and White (18), would vary from -34 HU (Hounsfield Units) at 40 keV to +13 HU at 80 keV. The CT number of water is 0 for all energies, due to the Hounsfield scale definition (Equation 3).

Ignoring the collagen matrix as an attenuating component when using materials that mimick bone mineral in a water-equivalent environment, inevitably will cause inaccuracies. This was shown in an experimental set-up by Goodsitt et al (19).

The basic approach of Goodsitt et al avoids, as well as possible, the "soft tissue problem". The collagen and bone mineral compartments are combined to a bone substance compartment. Therefore, the calibration materials used for this method should have the same attenuation characteristics as trabecular bone substance, intravertebral fat and red marrow/water. If so, this method will give good results. However, an accurate determination of $CT_{bs}\{E\}$ will be difficult due to beam hardening.

The method of Nickoloff et al (10) does not use calibration materials, so uncertainties due to the choice of calibration materials can be avoided. Instead, it uses material-specific coefficients that can be derived, if the physical and chemical properties of the various constituents are known, and if a reliable estimation can be made of the effective scanning energy at the place of the vertebral body. If so, this method will produce good results.

In this chapter it was intended to evaluate theoretically five postprocessing dual-energy methods for quantitative CT. Sources of error were indicated. In the next

chapter, the practical aspects of these methods will be discussed, and will focus on the following items: 1) choice of the DEQCT method; 2) influence of the choice of tissue-equivalent materials for calibration purposes; 3) the difference between simultaneous peripheral calibration and non-simultaneous central calibration for those methods using tissue-equivalent calibration lines; 4) the difference between effective energy estimation at the place of the calibration device and at the place of the vertebral body, for the method of Nickoloff et al (10).

In summary: five postprocessing methods for dual-energy quantitative computed tomography of the vertebral body were evaluated theoretically. The methods were compared by transforming the original sets of equations to a standard set. Only two of these methods produced optimal results, namely the basic approach of Goodsitt et al (8) and the method of Nickoloff et al (10). The calibration approach of Goodsitt et al will produce optimal results only if calibration materials are available that mimick the anatomic constituents of the vertebral body better than those available currently. Theoretically, the methods of Cann et al (5) and of Laval-Jeantet et al (6) will not produce optimal results.

APPENDIX A

Derivation of Equation (4): Equation (2) substituted in Equation 1 gives:

$$\mu\{E\} = \sum_{i=1}^{n} (\mu_i\{E\} V_i) \qquad \text{[AA.1]}$$

According to Equation (3):

$$\mu\{E\} = \mu_w (1 + CT\{E\} / 1000) \qquad \text{[AA.2]}$$

Substitution of [AA.2] in [AA.1] gives:

$$\mu_w (1 + CT\{E\} / 1000) = \sum_{i=1}^{n} (V_i \, \mu_w (1 + CT_i\{E\} / 1000)) \qquad \text{[AA.3]}$$

After division by μ_w and after cancelling the left side 1, by the sum of the fractions of volume (= 1 according to Equation [5]) on the right side, and after multiplication by 1000, [AA.3] can be reduced to Equation (4).

APPENDIX B

Translation of Equation (8) into the basic formula (Equation [6]). Theoretically, Beq is the concentration of bone mineral: c_{bm}. Then, Equation 8 can be rewritten to:

$$CT\#_v = (a * c_{bm}) + b \qquad [AB.1]$$

Equation (6) can be rewritten to:

$$CT_v = CT_{bm} * V_{bm} + CT_x * V_x \qquad [AB.2]$$

with,

$$CT_x * V_x = CT_c * V_c + CT_{rm} * V_{rm} + CT_f * V_f + CT_w * V_w$$

Using Equation (2) in [AB.2] gives:

$$CT_v = CT_{bm} * c_{bm} / r_{bm} + CT_x * V_x \qquad [AB.3]$$

$$V_x = 1 - V_{bm} = 1 - c_{bm} / r_{bm} \qquad [AB.4]$$

[AB.4] substituted in [AB.3] gives:

$$CT_v = c_{bm} / r_{bm} (CT_{bm} - CT_x) + CT_x \qquad [AB.5]$$

Comparing [AB.1] to [AB.5], gives:

$$a = (CT_{bm} - CT_x) / r_{bm},$$

and

$$b = CT_x$$

APPENDIX C

Legend of variables and subscripts used in this paper:

Variables
μ: linear attenuation coefficient (cm^{-1})
E: energy (keV)
r: mass density (g/cm^3)
c: concentration (g/cm^3)
V: volume fraction
CT: CT number
CT#: mean CT number measured on objects
a: slope of bone equivalent calibration line
b: intercept of bone equivalent calibration line
Beq: bone equivalent value (g/cm^3)
α: slope of fat equivalent calibration line
ß: intercept of fat equivalent calibration line
F: percentage of fat by volume
Ω: material-specific coefficient for bone substance
Θ: material-specific coefficient for fat
σ: material-specific coefficient for soft tissue
δ: -1000
π: water offset value

Subscripts
i: any material.
w: water
v: trabecular region of vertebral body
bm: bone mineral
c: collagen
rm: red marrow
f: fat
bc: bone equivalent calibration
s: soft tissue
x: combination of collagen, red marrow, fat and water
y: combination of collagen, red marrow and water
bs: bone substance: combination of bone mineral and collagen

3.5 REFERENCES

1. Rutherford RA, Pullan BR, Isherwood I. Measurement of effective atomic number and electron density using an EMI scanner. Neuroradiology 1976;11:15-21.

2. Genant HK, Boyd D. Quantitative bone mineral analysis using dual-energy computed tomography. Invest Radiol 1977;12:545-551.

3. Brooks RA. A quantitative theory of the Hounsfield unit and its application to dual-energy scanning. J Comput assist Tomogr 1977;1:487-493.

4. Adams JE, Chen SZ, Adams PH, Isherwood I. Measurement of trabecular bone mineral by dual-energy computed tomography. J Comput Assist Tomogr 1982;6:601-607.

5. Cann CE, Gamsu G, Birnberg FA, Webb WR. Quantification of calcium in solitary pulmonary nodules using single- and dual-energy CT. Radiology 1982;145:493-496.

6. Laval-Jeantet AM, Cann CE, Roger B, Dallant P. A postprocessing dual-energy technique for vertebral CT densitometry. J Comput Assist Tomogr 1984;8:1164-1167.

7. Nickoloff EL, Feldman F. Bone mineral assessment with dual-energy computerized tomography (CT) imaging. SPIE 1985;555:178-187.

8. Goodsitt MM, Rosenthal DI, Reinus WR, Coumas J. Two postprocessing CT techniques for determining the composition of trabecular bone. Invest Radiol 1987;22:209-215.

9. Goodsitt MM, Rosenthal DI. Quantitative computed tomography scanning for measurement of bone and bone marrow fat content. A comparison of single- and dual-energy techniques using a solid synthetic phantom. Invest Radiol 1987;22:799-810.

10. Nickoloff EL, Feldman F, Atherton JV. Bone mineral assessment: new dual-energy CT approach. Radiology 1988;168:223-228.

11. Kalender WA, Perman WH, Vetter JR, Klotz E. Evaluation of a prototype dual-energy computed tomographic apparatus. I. Phantom studies. Med Phys 1986;13:334-339.

12. Rosenthal DI, Mayo-Smith W, Goodsitt MM, Doppelt S, Mankin HJ. Bone and bone marrow changes in Gaucher disease: evaluation with quantitative CT. Radiology 1989;170:143-146.

13. Mayo-Smith W, Rosenthal DI, Goodsitt MM, Klibanski A. Intravertebral fat measurement with quantitative CT in patients with Cushing disease and anorexia nervosa. Radiology 1989;170:835-838.

14. Rosenthal DI, Hayes CW, Rosen B, Mayo-Smith W, Goodsitt MM. Fatty replacement of spinal bone marrow by dual-energy quantitative CT and MR imaging. J Comput Assist Tomogr 1989;13:463-465.

15. Glüer C, Reiser UJ, Davis CA, Rutt BK, Genant HK. Vertebral mineral determination by quantitative computed tomography (QCT): accuracy of single and dual-energy measurements. J Comput Assist Tomogr 1988;12:242-258.

16. Rao GU, Yaghmai I, Wist AO, Arora G. Systematic errors in bone mineral measurements by quantitative computed tomography. Med Phys 1987;14:62-69.

17. Crawley EO, Evans WD, Owen GM. A theoretical analysis of the accuracy of single-energy CT bone-mineral measurements. Phys Med Biol 1988;33:1113-1127.

18. Woodard HQ, White DR. Bone models for use in radiotherapy dosimetry. Brit J Radiol 1982;55:277-282.

19. Goodsitt MM, Kilcoyne RF, Gutcheck RA, Richardson ML, Rosenthal DI. Effect of collagen on bone mineral analysis with CT. Radiology 1988;167:787-791.

CHAPTER 4
PRACTICAL ASPECTS [2]

4.1 INTRODUCTION

Single-energy quantitative computed tomography (SEQCT) is a well-established method for determining the bone mineral content in the vertebral body (1-3). The accuracy of SEQCT is, however, limited due to the occurrence of other constituents of the vertebral body, such as fat (3-8) and collagen (9). Dual-energy quantitative computed tomography (DEQCT) has been proposed to improve the accuracy of bone mineral measurements (4,10-18) and to provide additional information about the composition of the trabecular region of the vertebral body (17-21). DEQCT can be done using preprocessing methods (14,15) or postprocessing methods (10-13,16-18). Preprocessing methods require access to the raw projection data at the two scanning energies together with sophisticated software that is not available for all commercial CT scanners. In the past decade, several postprocessing methods have been proposed that can be divided into two different approaches. The first approach uses materials that mimick tissue for calibration purposes, as in the single-energy method (11,12,16); the second uses material-specific coefficients, calculated for the effective scanning energies (13,18).

In the previous chapter, the various postprocessing methods were evaluated theoretically, by transforming the original sets of equations to a standard set. A detailed description of the various DEQCT methods and the similarities and differences between these methods was reported (22).

In this chapter, the practical aspects of using these methods are discussed, as evaluated in a phantom study. The study design allowed control of the composition of the vertebral body, which is not possible with in vivo studies. The following items were assessed: 1) influence of the choice of DEQCT method; 2) influence of the choice of the tissue-equivalent materials for calibration purposes; 3) the difference between peripheral and central calibration.

The aim was to establish the distinct value of these methods and, if possible, to appoint a method of choice.

4.2 MATERIALS AND METHODS

An anthropomorphic phantom was used (Computerized Imaging Reference Systems, [CIRS], Norfolk, VA) as "the patient" allowing to change the vertebral body composition by using "trabecular bone" inserts. A range of different concentrations of bone, red marrow and fat simulating inserts was available. An extra set of CIRS trabecular inserts that contained 0, 50, 100 and 150 mg/cm^3 of calcium hydroxyapatite in a red marrow-equivalent solid plastic and 100% fat-equivalent material was used as a reference device.

To study the influence of tissue-equivalent materials in the reference device on the estimation of bone mineral content and fat content, a homemade reference device was used (Erasmus University Rotterdam [EUR] device, The Netherlands). This device contains freshly made solutions (0, 50, 100, 200 mg/cm^3) of dry K_2 HPO_4 (Baker Chemicals BV, Deventer, The Netherlands) in water as bone mineral-equivalent, within tubes provided with an air-lock to entrap air bubbles. Furthermore, it contains liquid paraffin, polyethylene and 70% ethanol as fat-equivalent materials. These devices were placed under the anthropomorphic phantom for the performance of simultaneous peripheral calibration. Figure 4.1 shows a CT image of the CIRS anthropomorphic phantom with the extra set of CIRS inserts as reference device.

Non-simultaneous central calibration was performed using either the CIRS inserts without fat and with 100% fat, or the materials of the EUR device placed in the trabecular slot of the phantom. Figure 4.2 shows the anthropomorphic phantom with a tube containing dipotassium hydrogenphosphate within the trabecular slot of the phantom. Scanning was done with a Philips Tomoscan 350 (Philips Medical Systems, Best, The Netherlands). Two separate scans were made through every insert; one at 70 kVp, the other at 120 kVp, (the lowest and highest kVp setting possible on the Tomoscan 350), with a standard slice thickness of 6 mm. A circular region of interest was used to determine the mean CT number (CT#) of the trabecular insert and of the materials in the calibration device.

Calculations were done for the postprocessing methods of Cann et al (11), Laval-
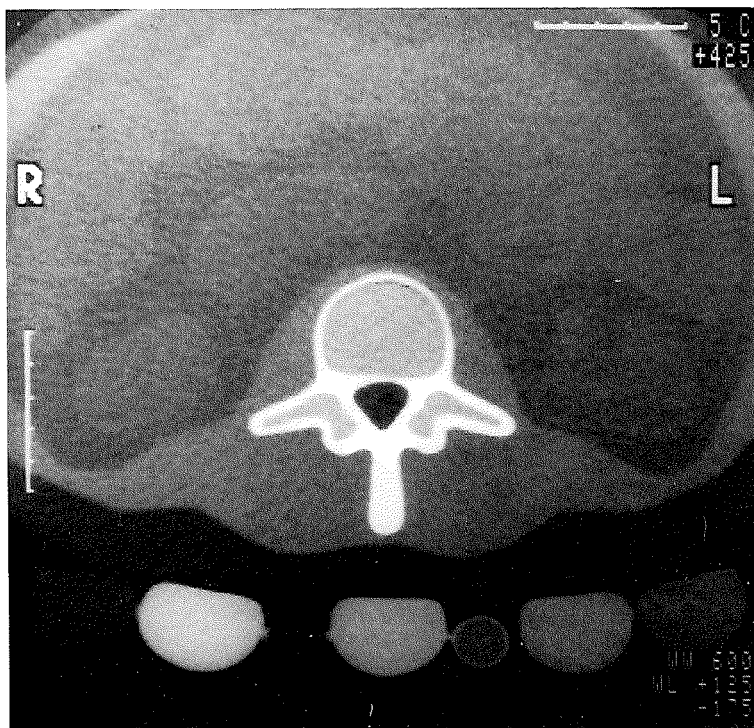
Figure 4.1. CT image of CIRS anthropomorphic phantom with CIRS reference device.

Jeantet et al (12), the calibration approach of Goodsitt et al (16), the basic approach of Goodsitt et al (16), and the method of Nickoloff et al (18). These methods were outlined in detail in chapter 3 (22). In addition, for comparison the single-energy results are given. For the basic approach of Goodsitt et al (16), the CT numbers of the pure materials were not found by scanning these materials, because it is not possible to scan 100% calcium hydroxyapatite without imaging artifacts. Therefore, these CT numbers were calculated from the linear attenuation coefficients of these materials for the effective scanning energies. This approach will be called "the modified method".

For the last method and for the method of Nickoloff et al (18), the slope of the calibration equations was used to estimate the effective scanning energies. The water offset value used by Nickoloff et al is a red marrow offset value when using the CIRS inserts as calibration device. It is determined by the difference between the measured CT number for the insert, consisting of 100% red

37
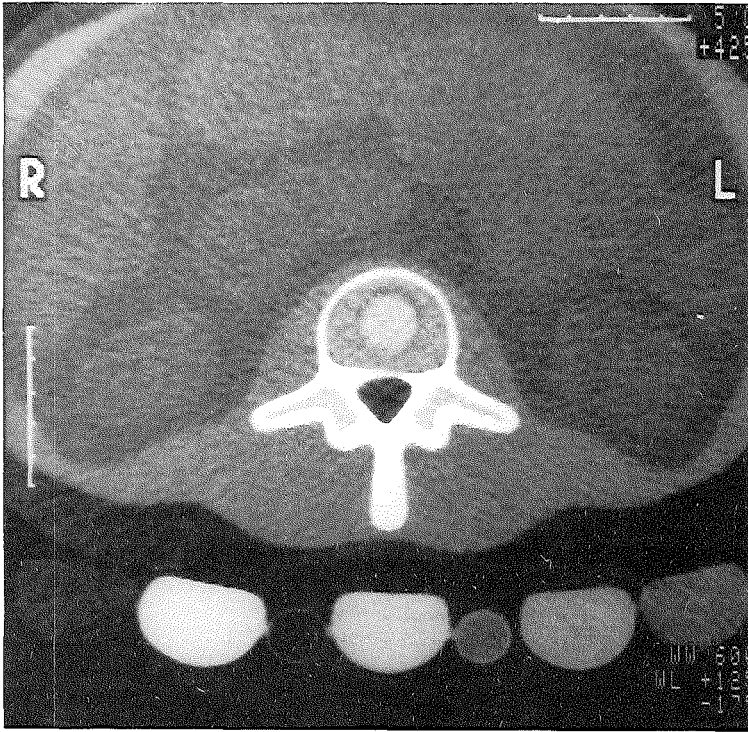
Figure 4.2. CIRS phantom with tube containing K_2HPO_4 in the trabecular slot.

marrow-equivalent material and the "ideal" CT number calculated for this insert at the effective scanning energy. The "ideal" CT numbers were calculated using knowledge of the elemental composition and mass densities for the different materials used by CIRS. Furthermore, the effective scanning energies were determined independently for the two calibration devices.

All measurements were corrected for drifts in the CT number scale. Because the water offset value used in the method of Nickoloff et al is an empirical correction for scale drift (22), this correction was applied to all other DEQCT methods; thus a uniform correction was made for all methods.

The precision was assessed by scanning the samples six times and by calculating the standard deviation of these measurements. In some cases, for illustration purposes, differences in estimates between the different postprocessing DEQCT methods have been evaluated statistically with a paired Student's t test.

4.3 RESULTS

4.3.1 Single-energy results

The single-energy results for the different calibration devices and techniques (peripheral vs central) are shown in Table 4.1. The influence of the fat content on the estimates of bone mineral content is shown.

TABLE 4.1. Single-energy results for different reference devices and calibration techniques.

True content of CIRS insert[1]. mg/cm³[3(2)]	%fat[3]	Reference Device: 1		2		3		4	
		70kV	120kV	70kV	120kV	70kV	120kV	70kV	120kV
0	0	19.4	17.5	19.8	18.8	-1.8	-1.2	-0.7	0.2
50	0	59.1	57.3	63.9	61.8	44.0	43.2	51.0	49.9
100	0	98.9	98.3	106.0	104.7	87.2	88.0	100.2	99.7
150	0	139.9	138.7	148.1	148.4	131.4	132.4	149.5	150.3
0	100	-53.7	-72.2	-59.9	-78.2	-83.8	-101.6	-93.9	-112.2
50	15	46.6	40.2	48.7	43.3	28.1	24.1	33.1	28.5
100	15	87.5	83.1	93.8	87.7	74.7	70.4	86.0	79.9
150	15	127.1	123.9	135.9	132.1	117.4	116.2	135.3	131.4
50	30	34.9	26.4	35.5	27.0	14.4	7.0	17.7	9.6
100	30	77.6	70.5	81.7	75.1	61.7	57.1	71.7	65.4

Reference device:
1. EUR Reference Device (peripheral)
2. EUR Reference Device (central)
3. CIRS Reference Device (peripheral)
4. CIRS Reference Device (central)

Values in mg/cm³ K_2HPO_4 for 1 and 2; in mg/cm³ calcium hydroxyapatite for 3 and 4. All CT measurements are corrected for CT number scale drift.

[1] According to the manufacturer.
[2] Calcium hydroxyapatite.
[3] Percent fat by volume.

For the EUR reference device decreases of 8 mg/cm³ K_2HPO_4 at 70 kVp and 10 mg/cm³ at 120 kVp for the peripheral calibration technique are observed for an increase of 10% fat by volume. For the central calibration technique the decreases are 9 mg/cm³ and 11 mg/cm³ at 70 kVp and 120 kVp, respectively. For the CIRS reference device decreases of 9 mg/cm³ calcium hydroxyapatite at 70 kVp and 11 mg/cm³ at 120 kVp for the peripheral calibration technique are

seen. For the central calibration technique the decreases are 10 mg/cm^3 and 12 mg/cm^3 at 70 kVp and 120 kVp, respectively.

4.3.2 Dual-energy results

Dual-energy results for bone mineral content and fat content determination are shown in Tables 4.2 through 4.5. The results vary depending on the post-processing method used.

4.3.2.1 Dual-energy results for central calibration technique with CIRS reference device.

Table 4.2 shows the estimates for the CIRS reference device and the central calibration technique. This technique can be considered the ideal calibration set-up in the current phantom study because the same materials are used in the reference device as in the trabecular inserts. Furthermore, calibration is done at the same place as the trabecular inserts. The estimated effective energies were 59.0 kV at 70 kVp and 75.3 kV at 120 kVp.

Cann's method decreases the fat-induced error, as seen with SEQCT, by a factor of approximately two. For the other methods, the fat-induced error is suppressed completely. All the estimates of bone mineral for the method of Laval-Jeantet et al are 3.1 mg/cm^3 lower than for the method of Goodsitt et al. In comparison with the method of Nickoloff et al, the estimates for the method of Laval-Jeantet et al are 1.8 mg/cm^3 (average; standard deviation [SD] 1.3 mg/cm^3; P-value 0.0014; t=4.52) lower. Consequently, the estimates for the method of Goodsitt et al are 1.3 mg/cm^3 (average; SD 1.3 mg/cm^3; P-value 0.01; t=3.22) higher than the estimates for Nickoloff's method.

All estimates of the fat content are 16.3% higher for the method of Laval-Jeantet et al compared with the method of Goodsitt et al. The estimates of fat content with the method of Laval-Jeantet et al are systematically too high, compared with the true fat content. Compared with the method of Nickoloff et al, the estimates of fat content for the method of Laval-Jeantet et al are 19.2% higher (average; SD 3%; P-value <0.0001; t=20.4).

The results for the modified method of Goodsitt et al and for the method of Nickoloff et al are identical; this is due to the fact that all CT measurements are corrected for CT number scale drift. Therefore, the offset value used in the

TABLE 4.2. Bone mineral estimates (in mg/cm³ calcium hydroxyapatite) and fat content estimates (in percentage of volume) for the postprocessing dual-energy methods.

True content of CIRS inserts[1]		Method				
C[2]	F[3]	Cann	Laval-J.	Goodsitt	Modified	Nickoloff
0		-2.7	-8.1	-5.0	-4.8	-4.8
	0		12%	-5%	-4%	-4%
50		53.3	52.9	56.0	55.6	55.6
	0		22%	5%	5%	5%
100		101.5	100.0	103.1	102.7	102.7
	0		19%	3%	2%	2%
150		147.9	142.9	146.0	145.8	145.8
	0		13%	-4%	-4%	-4%
0		-52.9	-8.1	-5.0	-9.2	-9.2
	100		112%	95%	86%	86%
50		43.6	52.8	55.9	54.7	54.7
	15		41%	24%	22%	22%
100		99.6	112.4	115.5	113.8	113.8
	15		48%	32%	28%	28%
150		144.0	151.1	154.2	153.0	153.0
	15		37%	20%	18%	18%
50		35.9	54.0	57.1	55.1	55.1
	30		59%	42%	38%	38%
100		86.1	99.8	102.9	101.1	101.1
	30		50%	33%	30%	30%

Calibration is performed centrally with the CIRS reference device. The effective energy is determined centrally. All CT measurements are corrected for CT number scale drift.

[1] According to the manufacturer.
[2] mg/cm³ calcium hydroxyapatite.
[3] Percent fat by volume.

approach of Nickoloff et al is zero, leading to the identical results (22). The results for the modified method, therefore, will be omitted in the remainder of this study.

4.3.2.2 Dual-energy results for peripheral calibration technique with CIRS reference device.

The results for the peripheral calibration technique with the CIRS reference device are shown in Table 4.3. The estimated effective energies are 54.8 kV at 70 kVp and 69.4 kV for 120 kVp. The bone mineral content determination becomes less accurate by this calibration technique. There is an underestimation of the bone mineral estimates for the inserts with a higher true bone mineral content (> 50 mg/cm^3). Compared with the central calibration technique (Table 4.2), the estimates of bone mineral for all DEQCT methods are significantly lower: for Cann's method 10.2 mg/cm^3 (average; SD 9.3 mg/cm^3; P-value 0.0073; t=3.45); for the method of Laval-Jeantet et al, 13.2 mg/cm^3 (average; SD 13.6 mg/cm^3; P-value 0.0136; t=3.06); for the method of Goodsitt et al, 12.0 mg/cm^3 (average; SD 11.8 mg/cm^3; P-value 0.0105; t=3.22) and for the method of Nickoloff et al, 11.7 mg/cm^3 (average; SD 11.6 mg/cm^3; P-value 0.011; t=3.19). The estimates of fat content are not significantly changed.

With the peripheral calibration technique, the estimates of bone mineral for the method of Laval-Jeantet et al are 4.3 mg/cm^3 lower than for the method of Goodsitt et al (average; SD 3.1 mg/cm^3; P-value 0.0015; t=4.48) and 3.3 mg/cm^3 lower than for the method of Nickoloff et al (average; SD 4.6 mg/cm^3; P-value 0.0496; t=2.27). There is no significant difference between the estimates of bone mineral for the methods of Goodsitt et al and Nickoloff et al. The estimates of fat content for the method of Laval-Jeantet et al are 14.3% higher than for the method of Goodsitt et al (average; SD 2.7%; P-value < 0.0001; t=16.5), and 19.4% higher than for the method of Nickoloff et al (average; SD 7.9%; P-value < 0.0001; t=7.75). The estimates of fat content for the method of Goodsitt et al are 5.2% higher (not significant) than for the method of Nickoloff et al (average; SD 7.5%; P-value 0.0583; t=2.17).

True content of CIRS inserts[1]		Method			
C[2]	F[3]	Cann	Laval-J.	Goodsitt	Nickoloff
0		-3.3	-9.2	-5.6	-5.1
	0		12%	-5%	-4%
50		45.8	43.0	48.3	47.7
	0		20%	5%	4%
100		85.5	76.5	82.9	83.2
	0		8%	-5%	-4%
150		129.3	119.1	125.4	126.4
	0		6%	-7%	-6%
0		-46.0	-3.4	-5.3	-0.3
	100		120%	109%	90%
50		36.8	43.9	51.0	47.0
	15		40%	27%	20%
100		83.8	93.4	94.6	94.5
	15		43%	24%	21%
150		120.0	116.2	123.6	122.9
	15		20%	8%	6%
50		31.4	60.3	62.2	51.6
	30		76%	57%	40%
100		71.4	77.8	83.9	83.0
	30		41%	27%	23%

Calibration is performed peripherally with the CIRS reference device. The effective energy is determined peripherally. All CT measurements are corrected for CT number scale drift. The ROI measurements are corrected for their central place and the reference device measurements are corrected for their peripheral place.

[1] According to the manufacturer.
[2] mg/cm³ calcium hydroxyapatite.
[3] Percent fat by volume.

4.3.2.3 Dual-energy results for central calibration technique with EUR reference device.

To study the influence of choosing other tissue-equivalent materials in the calibration device, the EUR reference device was used.

If the bone-equivalent calibration is changed to K_2HPO_4 solutions in water, without changing the fat equivalent calibration, the bone mineral content and fat content estimates are changed (Table 4.4).

Compared with the central calibration technique, using the CIRS reference device (Table 4.2), the bone mineral estimates for the method of Cann, Laval-Jeantet et al, and Goodsitt et al are higher for the insert with a lower true bone mineral content (<150 mg/cm^3). However, for the method of Nickoloff et al, the estimates are lower for the inserts with a higher true bone mineral content (>50 mg/cm^3). For the central calibration technique with dipotassium hydrogenphosphate, the estimated effective energies are 54 kV at 70 kVp and 70 kV at 120 kVp. This differs from the effective energies estimated with the CIRS reference device. The bone mineral estimates and fat content estimates for the methods of Laval-Jeantet et al and Goodsitt et al have a fixed difference, although the estimates are nearly the same. There is a difference of 1.8 mg/cm^3 (average; SD 0.1 mg/cm^3; P-value <0.0001; t$=49.3$) for the bone mineral estimates, and a difference of 3.8% (average; SD 0.05%; P-value 0; t$=250$).

4.3.2.4 Dual-energy results for central calibration technique with different fat equivalent materials.

In Table 4.5, the bone mineral content estimates and fat content estimates are given for the insert that contains 100 mg/cm^3 of calcium hydroxyapatite and 30% fat. The estimates are obtained with various fat equivalent calibration materials. As bone mineral equivalent, either the CIRS inserts without fat or the K_2HPO_4 solutions are used. The uncorrected CT numbers of the fat equivalent materials are for CIRS fat equivalent, -135 Hounsfield Units (HU) at 70 kVp and -115 HU at 120 kVp; for paraffin -195 HU and -165 HU, respectively; for 70% ethanol -140 HU and -130 HU, respectively; and for polyethylene -102 HU and -71 HU respectively. Thus, a proper choice of fat equivalent material and of bone equivalent material is important, especially for the fat content determination.

TABLE 4.4. *Bone mineral estimates (in mg/cm³ dipotassium hydrogenphosphate) and fat content estimates (in percentage of volume) for the postprocessing dual-energy methods.*

True content of CIRS inserts[1]		Method			
C[2]	F[3]	Cann	Laval-J.	Goodsitt	Nickoloff
0		21.9	21.3	23.4	13.5
	0		2%	5%	13%
50		68.6	69.4	71.1	55.7
	0		8%	12%	10%
100		108.8	108.6	110.4	87.2
	0		4%	7%	-2%
150		147.5	145.3	147.1	115.2
	0		-6%	-2%	-18%
0		-20.0	0.0	1.8	25.3
	100		100%	104%	112%
50		60.5	65.2	67.0	57.9
	15		27%	31%	29%
100		107.2	112.7	114.5	98.9
	15		31%	35%	24%
150		144.3	147.0	148.8	123.6
	15		18%	22%	5%
50		54.1	62.5	64.2	60.9
	30		45%	48%	47%
100		96.0	102.0	103.7	90.6
	30		33%	37%	28%

Calibration is performed centrally with the EUR reference device and CIRS fat-equivalent. The effective energy is determined with the EUR reference device. All CT measurements are corrected for CT number scale drift.

[1] According to the manufacturer.
[2] mg/cm³ calcium hydroxyapatite.
[3] Percent fat by volume.

4.3.3 Precision

The precision for the bone mineral estimates, expressed as standard deviation, is 0.5 mg/cm^3 for SEQCT at 120 kVp; 0.8 mg/cm^3 for SEQCT at 70 kVp; 3 mg/cm^3 for the DEQCT method of Cann; and 5 mg/cm^3 for all other postprocessing DEQCT methods. The precision for the estimates of fat content was 5% (by volume) of fat. All data in this study should be interpreted with the precision figures in mind.

TABLE 4.5. Bone mineral estimates (in mg/cm^3 calcium hydroxyapatite or dipotassium hydrogenphosphate) and fat content estimates (in percentage of volume) for the insert with 100 mg/cm^3 and 30% fat[1].

Reference Device:	Method			
	Cann	Laval-J.	Goodsitt	Nickoloff
BEQ CIRS	86.1	99.8	102.9	101.1
FEQ CIRS		50%	33%	30%
BEQ CIRS	86.1	99.9	102.9	101.1
FEQ Paraffin		36%	24%	30%
BEQ CIRS	86.1	84.9	92.9	101.1
FEQ 70% Ethanol		33%	22%	30%
BEQ CIRS	86.1	767.8	551.4	101.1
FEQ Polyethylene		970%	651%	30%
BEQ K$_2$HPO$_4$	96.0	102.0	103.7	90.6
FEQ CIRS		33%	37%	28%
BEQ K$_2$HPO$_4$	96.0	104.0	106.0	90.6
FEQ Paraffin		24%	27%	28%
BEQ K$_2$HPO$_4$	96.0	96.1	97.2	90.6
FEQ 70% Ethanol		23%	25%	28%
BEQ K$_2$HPO$_4$	96.0	219.7	235.0	90.6
FEQ Polyethylene		323%	360%	28%

Calibration is performed centrally with the EUR reference device or the CIRS reference device. All CT measurements are corrected for CT number scale drift.

[1] According to the manufacturer.
BEQ: Bone Equivalent calibration
FEQ: Fat Equivalent calibration

4.4 DISCUSSION

4.4.1 Single-energy

Underestimation of the bone mineral content by SEQCT due to the fat content is comparable with data reported in the literature (4,6,7) (Table 4.1). Bone mineral content estimates for the CIRS reference device are lower than for the EUR reference device. The difference is too large to be explained by the differences in attenuation characteristics between calcium hydroxyapatite and dipotassium hydrogenphosphate alone. Mainly, it is due to the red marrow equivalent within the CIRS inserts. The attenuation characteristics of this material are dissimilar from those of water. The estimates for the inserts without fat show that bone mineral determination is improved by performing a central calibration technique. With this technique, differences in scanner-related error sources, such as beam hardening and scatter, between the centrally located vertebra and the peripherally located reference device are avoided.

4.4.2 Dual-energy

The method suggested by Cann et al (11), assumes that the influence of constituents other than bone mineral on the mean CT number of the vertebral body is approximately the same at every energy. Then, the difference in mean CT number is due only to the bone mineral component in the vertebral body; therefore, this method uses only calibration equations of bone equivalent materials. As shown, this method reduces the fat-induced error by a factor of two, but it does not provide an estimation of fat content.

The methods suggested by Laval-Jeantet et al and by Goodsitt et al use calibration of bone mineral-equivalent and fat-equivalent materials. These methods take into account the energy-dependence of the fat influence. Furthermore, these methods allow estimation of the fat content of the vertebral body, thus offering potentially useful clinical information.

The method of Laval-Jeantet et al does not provide accurate estimates of fat content; even when the most ideal calibration is done, e.g. central calibration with the same materials, the estimates are disappointing. The cause is the use of a double intercept (22). Apart from this intercept problem, the methods of Laval-Jeantet et al and Goodsitt et al are essentially the same, and there is a fixed relationship between the estimates obtained with these methods (22). These

estimates, however, will show larger variations, dependent on the calibration materials chosen.

The differences noted between the estimates obtained with the two reference devices for the methods of Laval-Jeantet et al and of Goodsitt et al (Tables 4.2 and 4.4) are caused by the assumptions made when K_2HPO_4 solutions in water are used for bone equivalent calibration. First, it is assumed that K_2HPO_4 has the same attenuation characteristics as calcium hydroxyapatite; this, however, is not true (6). Second, it is assumed that red marrow is water-equivalent; for the CIRS inserts this is not the case. The 100% red marrow-equivalent has a CT number of 40 HU - 25 HU in the energy range of 50 - 75 keV.

With the EUR reference device and the central calibration technique the estimates for the methods of Laval-Jeantet et al and Goodsitt et al are approximately the same. They would be exactly the same if both the intercepts of the bone-equivalent and fat-equivalent calibration lines were zero (22). Although the CT number correction sets the CT number of water at zero, the intercepts will not be zero because they are the results of a linear regression fit between the CT numbers and the actual concentrations of the K_2HPO_4 solutions.

Furthermore, these methods give accurate results only if a central calibration technique is done, avoiding differences in effective energy between the central place of the vertebral body and the peripheral place of the calibration device.

The method of Nickoloff et al (18) provides accurate results if the effective energy is estimated centrally with materials that have exactly the same attenuation characteristics as the materials in the region of interest. Furthermore, it requires an offset value that is a correction for CT number scale drift. This value should be determined centrally.

Goodsitt and Rosenthal (17) compared the methods of Cann, Laval-Jeantet et al, and their own calibration approach in a phantom study. A non-simultaneous central calibration technique was used with the CIRS reference device, and a simultaneous peripheral calibration technique was used with the UCSF phantom that contained K_2HPO_4 solutions. The fat equivalent used for calibration purposes was not specified. Furthermore, it is not clear if an attempt was made to correct their measurements for CT number scale drift. The results in their study cannot be used to compare the results obtained with both reference devices or to compare the peripheral calibration technique with the central one, because both parameters were changed simultaneously. Nevertheless, the study of Goodsitt

and Rosenthal was important because it discussed the variance in bone mineral and fat content estimates with DEQCT methods, due to the choice of the reconstruction circle size, which can be varied on the CT scanner that was used in their study (Model 9800, General Electric, Milwaukee, WI).

In summary, the results obtained in this study indicate that application of the DEQCT methods are hampered by several restrictions: 1) The calibration or effective energy determination should be done centrally. If it is done peripherally, a conversion should be made to the central place of the vertebral body. 2) The CT number scale drift should be corrected for the central focus of the vertebral body. 3) The calibration materials should mimick exactly the attenuation properties of the anatomic constituents of the vertebral body for the scanning energies used, or the composition of these constituents should be known exactly so that the material-specific coefficients can be calculated.

If these conditions can be fulfilled, only the methods of Goodsitt et al and Nickoloff et al will give accurate results. However, the postprocessing methods reported in this study assume that the vertebral body can be described as a three-component entity. In the current phantom study, the composition of the trabecular inserts could also be described perfectly as a three-component model. The consequences of this simplification should be studied first, before a definite judgment can be given about the proper use of methods for postprocessing dual-energy quantitative computed tomography in medicine.

4.5 REFERENCES

1. Cann CE. Quantitative CT for determination of bone mineral density: a review. Radiology 1988;166:509-522.

2. Genant HK. Quantitative computed tomography: update 1987. Calcif Tissue Int 1987;41:179-186.

3. Tothill P. Methods of bone mineral measurement. Phys Med Biol 1989;34:543-572.

4. Laval-Jeantet AM, Roger B, Bouysee S, Bergot C. Mazess RB. Influence of vertebral fat content on quantitative CT-density. Radiology 1986;159:463-466.

5. Mazess RB. Errors in measuring trabecular bone by computed tomography due to marrow and bone composition. Calc Tissue Int 1983;35:148-152.

6. Glüer C, Reiser UJ, Davis CA, Rutt BK, Genant HK. Vertebral mineral determination by quantitative computed tomography (QCT): Accuracy of single and dual-energy measurements. J Comput Assist Tomogr 1988;12:242-258.

7. Burgess AE, Colborne B, Zoffmann E. Vertebral trabecular bone: comparison of single and dual-energy CT measurements with chemical analysis. J Comput Assist Tomogr 1987;11:506-515.

8. Webber CE. The effect of fat on bone mineral measurements in normal subjects with recommended values of bone, muscle and fat attenuation coefficients. Clin Phys Physiol Meas 1987;8:143-158.

9. Goodsitt MM, Kilcoyne RF, Gutchek RA, Richardson ML, Rosenthal DI. Effect of collagen on bone mineral analysis with CT. Radiology 1988;167:787-791.

10. Genant HK, Boyd D. Quantitative bone mineral analysis using dual-energy computed tomography. Invest Radiol 1977;12:545-551.

11. Cann CE, Gamsu G, Birnberg FA, Webb WR. Quantification of calcium in solitary pulmonary nodules using single and dual-energy CT. Radiology 1982;145:493-496.

12. Laval-Jeantet AM, Cann CE, Roger B, Dallant P. A post-processing dual-energy technique for vertebral CT densitometry. J Comput Assist Tomogr 1984;8:1164-1167.

13. Nickoloff EL. Feldman F. Bone mineral assessment with dual-energy computed tomography (CT) imaging. SPIE 1985;555:178-187.

14. Kalender WA, Perman WH, Vetter JR, Klotz E. Evaluation of a prototype dual-energy computed tomographic apparatus. I Phantom studies. Med Phys 1986;13:334-339.

15. Vetter JR, Perman WH, Kalender WA, Mazess RB, Holden JE. Evaluation of a prototype dual-energy computed tomographic apparatus. II Determination of vertebral bone mineral content. Med Phys 1986;13:340-343.

16. Goodsitt MM, Rosenthal DI, Reinius WR, Coumas J. Two post-processing CT techniques for determining the composition of trabecular bone. Invest Radiol 1987;22:209-215.

17. Goodsitt MM, Rosenthal DI. Quantitative computed tomography scanning for measurement of bone and bone marrow fat content. A comparison of single and dual-energy techniques using a solid synthetic phantom. Invest Radiol 1987;22:799-810.

18. Nickoloff EL, Feldman F, Atherton JV. Bone mineral assessment: new dual-energy approach. Radiology 1988;168:223-228.

19. Rosenthal DI, Mayo-Smith W, Goodsitt MM, Doppelt S, Mankin HJ. Bone and bone marrow changes in Gaucher disease: evaluation with quantitative CT. Radiology 1989;170:143-146.

20. Mayo-Smith W, Rosenthal DI, Goodsitt MM, Klibanski A. Intravertebral fat measurement with quantitative CT in patients with Cushing disease and anorexia nervosa. Radiology 1989;170:835-838.

21. Rosenthal DI, Hayes CW, Rosen B, Mayo-Smith W, Goodsitt MM. Fatty replacement of spinal bone marrow by dual-energy quantitative CT and MR imaging. J Comput Assist Tomogr 1989;13:463-465.

22. van Kuijk C, Grashuis JL, Steenbeek JCM, Schütte HE, Trouerbach WTh. Evaluation of postprocessing dual-energy methods in QCT. Part 1: Theoretical considerations. Invest Radiol 1990;25:876-881.

CHAPTER 5

PATIENT SIMULATION STUDIES: SKELETAL AGING

5.1 INTRODUCTION

In previous chapters five different postprocessing DEQCT methods were evaluated theoretically (chapter 3) and in practice with phantom studies (chapter 4) (1,2). The postprocessing methods evaluated are the methods of Cann (3), Laval-Jeantet (4), Goodsitt's calibration approach (5), Goodsitt's basic approach (5) and Nickoloff's method (6). It was concluded that the methods of Goodsitt and Nickoloff give the best results for estimation of bone mineral and fat content within the trabecular region of the vertebral body. The method of Cann gives bone mineral content estimates that are more accurate than the estimates obtained with the single-energy method, but is inferior to the methods of Goodsitt and of Nickoloff. The method of Cann does not give a fat content estimate. It was shown that the method of Laval-Jeantet will not give optimal results due to the use of a double intercept in its algorithm (1).

Estimates obtained with the calibration method of Goodsitt will show a variance due to the choice of both the tissue mimicking materials in the reference device and to the calibration technique (namely, peripheral versus central calibration). Estimates obtained with the method of Nickoloff, which is essentially the same as Goodsitt's basic approach, will vary due to accuracy of the determination of the effective energy and due to the choice of the material-dependent coefficients used in the algorithm (1,2).

The question as to what the influence of these disturbing factors will be in vivo, remains to be solved. Therefore, the findings of previous chapters will be translated to a (semi)clinical environment. For this purpose, a patient simulation study was performed. The vertebral body and different tissue-equivalent materials are described in terms of their X-ray attenuation characteristics. Changes in composition of the vertebral body are simulated and the influence of different calibration materials and effective energy differences are evaluated.

5.2 THE PATIENT SIMULATION STUDY

The simulation study can be divided into four parts:

1)   Description of the human anatomy in terms of X-ray attenuation

characteristics.

2)   Description of the human anatomy and its changes due to aging and pathologic conditions.

3)   Description of materials used for calibration purposes in terms of X-ray attenuation characteristics.

4)   Possibility to simulate influences inherent to the use of a CT scanner.

5.2.1. Composition of the vertebral body

For the patient simulation studies, it is necessary to describe the anatomic constituents of the trabecular region of the vertebral body in terms of their attenuation characteristics. The vertebral body consists of bone mineral (calcium hydroxyapatite) within a collagen matrix, adipose tissue (or yellow marrow) and hematopoietic tissue (or red marrow). The composition of the vertebral body changes with aging and disease; e.g. in aging, trabecular bone volume decreases, while the volume fraction of adipose tissue increases and the volume fraction of hematopoietic tissue decreases (7-12).

If the elemental composition and the mass density for the distinct constituents are known, the linear attenuation coefficient for the constituents can be calculated (see appendix A, for more details). The compositions and mass densities can be found in the literature:

Bone mineral

Bone mineral consists primarily of calcium hydroxyapatite, $(Ca_{10}(PO_4)_6(OH)_2)$ distributed in a collagen matrix. The mass density of bone mineral is estimated at 3.06 g/cm^3. This description of bone mineral was utilized by Nickoloff et al (6) for their calculations of the material specific coefficients used in their postprocessing dual-energy method. It was also used by Mazess (7), in a theoretical analysis of the accuracy error due to the fat content when using single-energy quantitative CT for bone mineral content determination. A similar analysis was performed by Crawley et al (13). More detailed reports on the mass density of bone mineral are the studies of Gong et al (14,15), Mueller et al (16) and Galante et al (17).

Collagen

The mass density of collagen is quoted as 1.38 g/cm^3 (7). Its elemental composition can be given as 54% C, 23% O, 16% N and 7% H (percentage by weight). This is the elemental composition for protein in general, as

recommended by the ICRP (International Commission on Radiological Protection) in the report of the task group on reference man, in which a reference individual for estimation of radiation dose is described (18).

Water

Water (H_2O) has a mass density of 1.00 g/cm^3.

Trabecular bone substance

Normal mineralized trabecular bone substance can be defined as a collagen matrix, with 58% of weight calcium hydroxyapatite, 32% collagen, and 10% water and a mass density of 1.92 g/cm^3 (7,10,16). This is comparable to the description of normal cortical bone (18-20).

The marrow space

The marrow space within the trabecular region of the vertebral body is filled with hematopoietic tissue and adipose cells.

Hematopoietic tissue

Nickoloff and coworkers (6), described a non-adipose tissue compartment within the marrow space, which comprehended red marrow and water, with a mass density of 1.02 g/cm^3. This figure was derived from Mazess (7). Mazess assumed that red marrow contains 30% lipid. However, according to the studies of Woodard and White (19-20), red marrow contains 40% lipid and has a mass density of 1.03 g/cm^3. This is also according to the ICRP recommendations (18).

Adipose tissue

Different descriptions and names are given to the adipose compartment within the marrow space. According to Mazess (7), who called it yellow marrow, it has a mass density of 0.93 g/cm^3 and contains 80% lipid. Nickoloff et al (6) used a mass density of 0.92 g/cm^3 for this compartment that was called adipose tissue. According to Woodard and White (19-20), yellow marrow contains 80% lipid, but has a mass density of 0.98 g/cm^3. This is also the ICRP recommendation (18). In addition, Woodard and White (20) have described three different types of adipose tissue, with mass densities varying between 0.93 g/cm^3 and 0.97 g/cm^3 and percentages by mass of lipid between 87.3% and 61.4%.

5.2.2 Model for the trabecular region and computation of CT data

Description of the trabecular region

For our simulation study, the trabecular region is divided into three different compartments, that can be discerned histological. An osseous compartment filled

with the collagen matrix and mineral deposits, and the marrow space which itself can be divided into two distinct compartments, namely blood without fat, with a mass density of 1.06 g/cm³ (20) and adipose tissue with the highest lipid content and a mass density of 0.93 g/cm³ (20).

For normal trabecular bone substance, we used the description according to Woodard and White (20) with a mass density of 1.92 g/cm³. A summary of the elemental compositions and the mass densities of the various compartments used

TABLE 5.1. Tissue description of the components of the vertebral body.

Element	Trabecular Bone:	Blood:	Adipose Tissue:
H	3.4	10.2	11.6
C	15.5	11.0	68.1
N	4.2	3.3	0.2
O	43.5	74.5	19.8
P	10.3	0.1	----
Ca	22.5	----	----
Na	0.1	0.1	0.1
K	----	0.2	----
S	0.3	0.2	0.1
Mg	0.2	----	----
Cl	----	0.3	0.1
Fe	----	0.1	----
Mass density (g/cm³)	1.92	1.06	0.93

Elemental composition in percentage by weight and mass density in g/cm³. (Derived from ref. 20)

for the calculations of the linear attenuation coefficients is given in Table 5.1.

The calculated linear attenuation coefficients for the various constituents of the trabecular region of the vertebral body are shown in Table 5.2 for an energy range of 40 - 80 keV.

Computation of CT data.

In computed tomography the CT number (CT) is related to the linear attenuation coefficient by:

$$CT\{E\} = 1000 \; (\mu\{E\}-\mu_w\{E\}) \; / \; \mu_w\{E\} \qquad [1]$$

TABLE 5.2. Linear attenuation coefficients (μ in cm⁻¹) for the constituents of the vertebral body.

Energy (keV)	Trabecular Bone:	Blood:	Adipose Tissue:
40	1.274	0.267	0.220
50	0.814	0.227	0.197
60	0.605	0.207	0.183
70	0.495	0.195	0.175
80	0.429	0.185	0.168

where, μ_w is the linear attenuation coefficient of water at energy E. Using Equation 1, CT numbers were generated for the different constituents of the vertebral body.

The CT number of the trabecular region of the vertebral body itself (CT_v) was generated using the equation:

$$CT_v\{E\} = CT_{bs}\{E\}V_{bs} + CT_{bl}\{E\}V_{bl} + CT_{at}\{E\}V_{at} \qquad [2]$$

where, V_i is the fraction of volume of the constituents within the trabecular region of the vertebral body; the subscripts v, bs, bl and at, indicate the trabecular region of the vertebral body, bone substance, blood and adipose tissue, respectively.

Using Equation 2, CT numbers for imaginary vertebral bodies with varying compositions can be generated. A derivation of Equation 2 can be found in chapter 3.

Description of changes in the vertebral morphometry due to aging.

In order to simulate a wide range of different compositions of vertebral bodies, the composition of the trabecular region of the vertebral body was changed according to changes that occur in aging. CT numbers were calculated for different compositions: trabecular bone volume decreases in steps of 1% (11.1 mg/cm³ calcium hydroxyapatite), changing from 20% (222.5 mg/cm³) to 5% (55.6 mg/cm³); blood volume was decreased in steps of 1%, changing from 60 - 45%; adipose tissue volume was increased in steps of 2%, changing from 20 - 50% (Figure 5.1). The changes in vertebral body composition are similar to those found in histological studies of the vertebral body by Dunnill et al (8), and by Burkhardt et al (9).

CT data were generated for SEQCT and DEQCT at 50 and 70 keV. These energies were chosen because they approximate the effective energies at tube potentials of 70 and 120 kVp, respectively. For postprocessing DEQCT the following methods were used to generate bone mineral and, if possible, fat
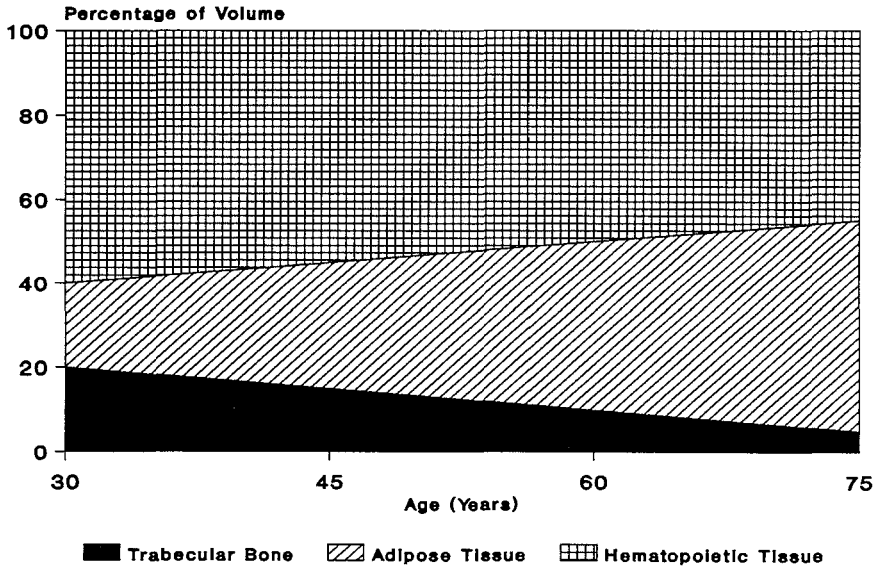

Figure 5.1. Changes in vertebral body composition due to aging.

content estimates: Cann's method, Goodsitt's calibration approach and Nickoloff's method (see chapter 3 for a detailed description of the various DEQCT methods). Goodsitt's basic approach would give the same results as Nickoloff's approach (1) and is therefore not used in this chapter.

5.2.3 Reference devices and material dependent coefficients

The influence of the choice of calibration materials on SEQCT, Cann's method and Goodsitt's calibration approach was evaluated by simulating different reference devices:

1) A reference device consisting of materials that are "identical" to those used for description of the trabecular region of the vertebral body.

2) The "identical" bone equivalent, but the fat equivalent changed to the CIRS (Computerized Imaging Reference Systems, Norfolk, Va) fat

equivalent.

3) K_2HPO_4 in water as bone equivalent and "identical" adipose tissue as fat equivalent.

4) K_2HPO_4 in water as bone equivalent and the CIRS fat equivalent.

K_2HPO_4 was chosen because, up to now, it is the most widely used bone equivalent material for calibration purposes. The CIRS fat equivalent was chosen, because it was used as calibration material by Mayo-Smith et al (21) in their DEQCT studies of the intravertebral fat content of patients with Cushing's disease and anorexia nervosa.

In Nickoloff's method, energy dependent material specific coefficients are used (1). These coefficients were calculated using the tissue descriptions in Table 5.1. creating "identical" coefficients. In order to simulate the influence of the coefficients on bone mineral and fat content estimation, the tissue descriptions for calculating the coefficients were changed from those used for description of the vertebral body; "non-identical" coefficients. Blood was changed to the red marrow specification (mass density 1.03 g/cm^3) (20) and the adipose tissue description was changed to the alternative adipose tissue descriptions (mass densities 0.95, 0.97 and 0.98 g/cm^3) (20). The linear attenuation coefficients for the various tissue descriptions are given in Table 5.3.

5.2.4 Non-uniform effective energies

In order to simulate a difference in effective energy between the place of the vertebral body and the place of the reference device, as can occur in clinical practice, CT numbers of the trabecular region were calculated for 55 and 75 keV

TABLE 5.3. Linear attenuation coefficients (μ in cm^{-1}) for the constituents used for calculating the material specific coefficients for the method of Nickoloff et al. All tissue descriptions according to reference 20.

Energy in keV	Red Marrow	Adipose 1	Adipose 2	Yellow Marrow
40	0.264	0.237	0.229	0.234
50	0.227	0.209	0.203	0.208
60	0.208	0.193	0.188	0.194
70	0.196	0.183	0.179	0.184
80	0.187	0.176	0.172	0.177
mass density in g/cm^3:	1.03	0.97	0.95	0.98

also, assuming an elevation of 5 keV at the place of the vertebral body, due to spectral beam hardening. The elevation of 5 keV was chosen according to our experiences in the phantom studies (chapter 4).

5.3 RESULTS

5.3.1 Differences between methods under "ideal" conditions

Figure 5.2 shows the results for bone mineral estimates obtained with SEQCT and the various DEQCT methods under "ideal" circumstances, namely an "identical" reference device and uniform effective energies. On the horizontal axis the age is given. This, in fact, represents the compositions of the vertebral body as given in Figure 5.1. On the vertical axis the difference between the bone
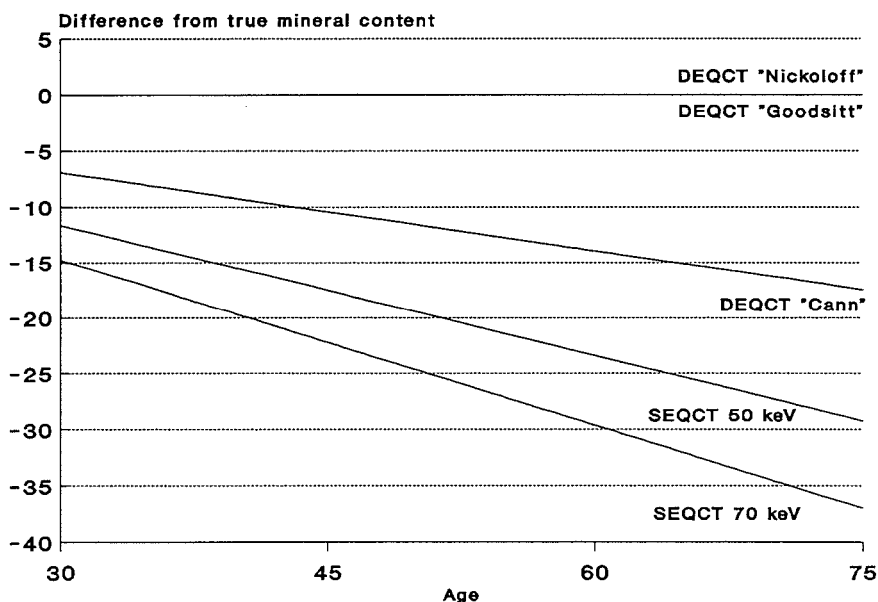
Figure 5.2. SEQCT and DEQCT results under "ideal" conditions. Difference from true bone mineral content in mg/cm³.

mineral estimate and the true bone mineral content is given in mg/cm³.

It is seen, that the DEQCT methods of Nickoloff and Goodsitt give excellent results. The DEQCT method of Cann gives better bone mineral estimates

compared with SEQCT. There is an underestimation of true bone mineral content that increases with increasing adipose tissue volume and decreasing trabecular bone volume, from 7 to 17 mg/cm^3 (as a percentage of true bone mineral content, from 3 to 31%).

SEQCT underestimates the bone mineral content, following the same trend. Underestimation is larger at a higher effective energy: at 50 keV underestimation increases from 12 to 29 mg/cm^3 (5 to 53%), at 70 keV underestimation increases from 15 to 37 mg/cm^3 (7 to 67%).

5.3.2 Influences of reference devices and material dependent coefficients

In figure 5.3 the results are shown for SEQCT at 50 keV, if the bone mimicking material in the reference device is changed to K$_2$HPO$_4$. The true bone mineral content is underestimated from 3 to 28 mg/cm^3 (2% to 50%). The underestimation is less than with the "identical" reference device, but is more
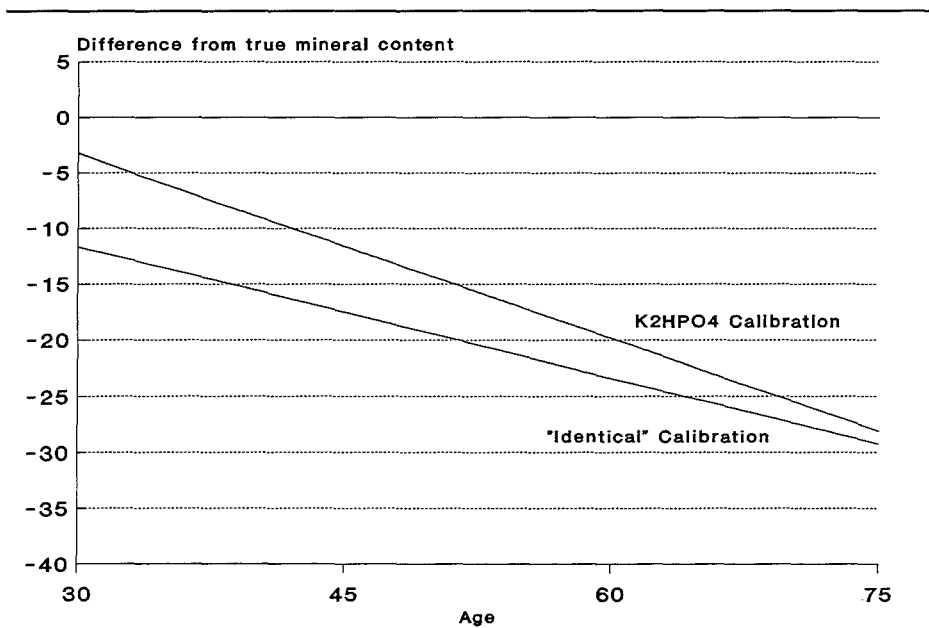

Difference from true mineral content

Figure 5.3. SEQCT 50 keV results for "identical" and K$_2$HPO$_4$ calibration. Difference from true mineral content in mg/cm^3.

sensitive to increasing adipose tissue volume (steeper slope).

60

Figure 5.4 shows the results for Cann's method with the two bone mimicking materials. With K_2HPO_4 the true bone mineral content is underestimated from 5
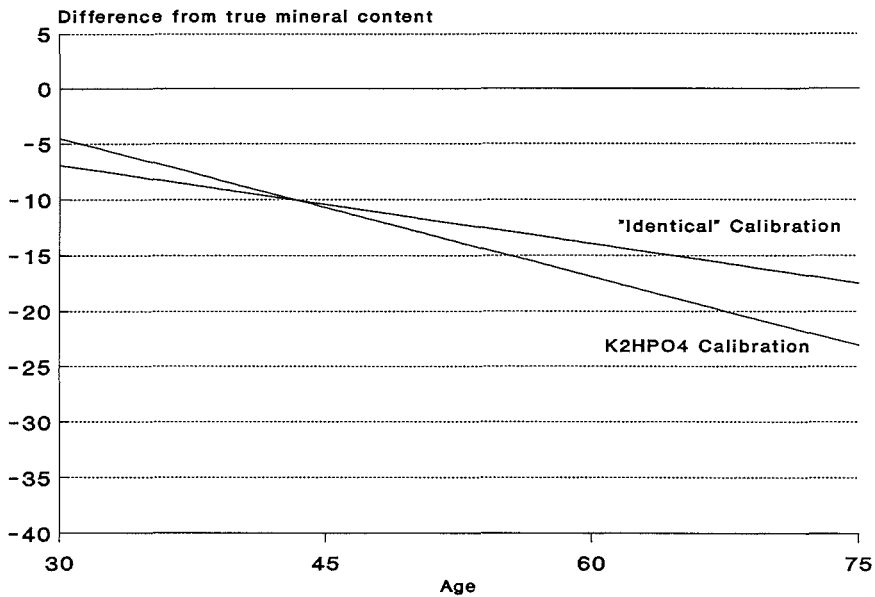

Figure 5.4. DEQCT results for the method of Cann et al. "Identical" versus K_2HPO_4 calibration. Difference from true mineral content in mg/cm^3.

to 23 mg/cm^3 (2 to 42%).

In Figure 5.5.A the results are shown for Goodsitt's method obtained with four different reference devices. The bone mineral content can be estimated accurately if the "identical" reference device is used. It is seen that if only the fat equivalent is changed (cal 2) the bone mineral content is underestimated from 3 mg/cm^3 (1%) to 7 mg/cm^3 (13%). If only the bone equivalent is changed (to K_2HPO_4; cal 3), the bone mineral content is underestimated from 7 mg/cm^3 (3%) to 10 mg/cm^3 (18%). If both tissue mimicking materials are changed (cal 4), the bone mineral content is underestimated from 6 mg/cm^3 (3%) to 16 mg/cm^3 (30%). The corresponding fat content estimates are given in Figure 5.5.B, the same horizontal axis is used as for the graphic presentation of the bone mineral estimates. On the vertical axis the absolute difference (in percentage volume of fat) between the fat content estimates and the true fat content is given. The
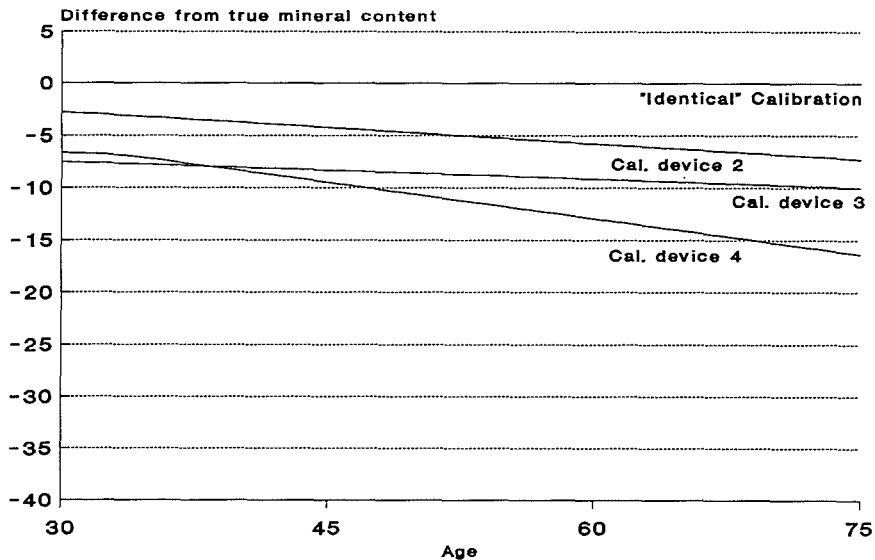
Figure 5.5.A. DEQCT bone mineral results for the method of Goodsitt et al. "identical" versus "non-identical" calibration. Difference from true mineral content in mg/cm³.

intravertebral fat content can be estimated accurately if the "identical" reference device is used. By changing the fat equivalent (cal 2) the true fat content is underestimated ranging from 7 to 17% (percentage of fat by volume). By changing the bone equivalent (cal 3) the fat content is underestimated ranging from 27 to 20%. By changing both equivalent materials (cal 4) the fat content is underestimated ranging from 24 to 32%.

In Figure 5.6.A the results are shown for bone mineral content estimation with the method of Nickoloff. Results for the "identical" tissue description and results obtained if the tissue descriptions used for determination of the energy dependent material specific coefficients are different from the tissue description of the constituents of the vertebral body, are shown. If the tissue description for fat is different, bone mineral content is overestimated. Overestimation of bone mineral content increases as the true bone mineral content decreases. The largest error occurs if the fat description is changed to the yellow marrow description.

The fat content estimates for the same simulation set-up are shown in Figure 5.6.B. If the adipose tissue description is changed, the fat content is overestimated. Overestimation increases with decreasing trabecular bone volume.
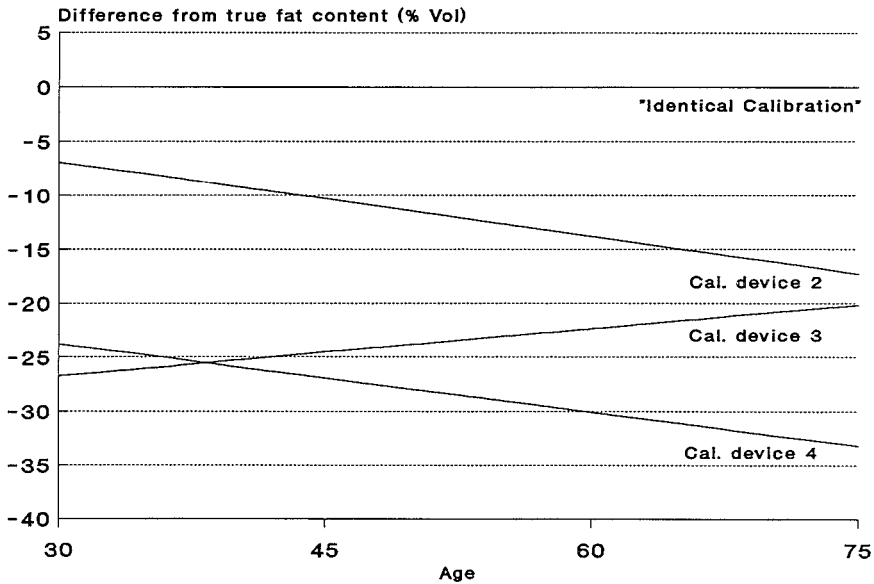
62

Figure 5.5.B. DEQCT fat content results for the method of Goodsitt et al. "Identical" versus "non-identical" calibration.
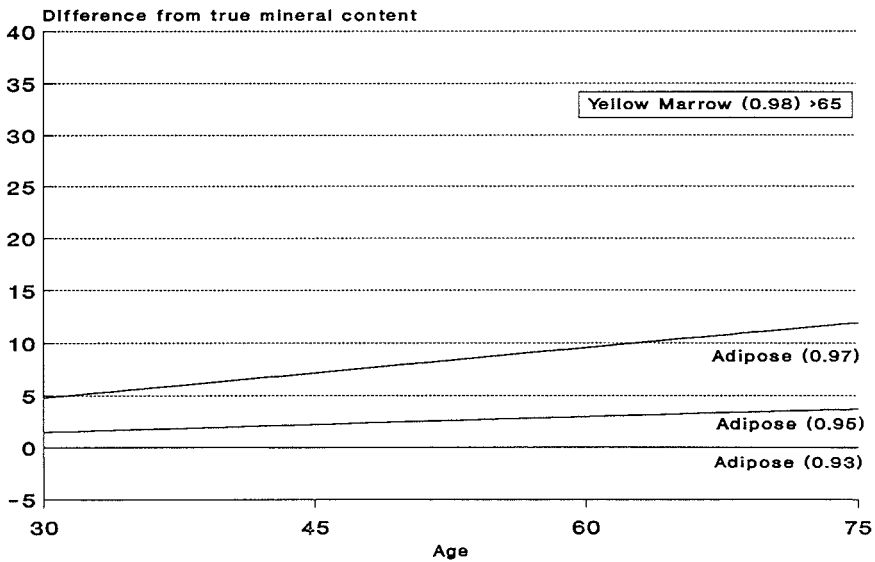

Figure 5.6.A. DEQCT bone mineral results for the method of Nickoloff et al. Adipose tissue description is changed for the calculation of the material dependent coefficient.

However, the overestimation given as percentage of the true fat content is fixed: 140% for adipose 2, 231% for adipose 1 and 1046% for the yellow marrow description.
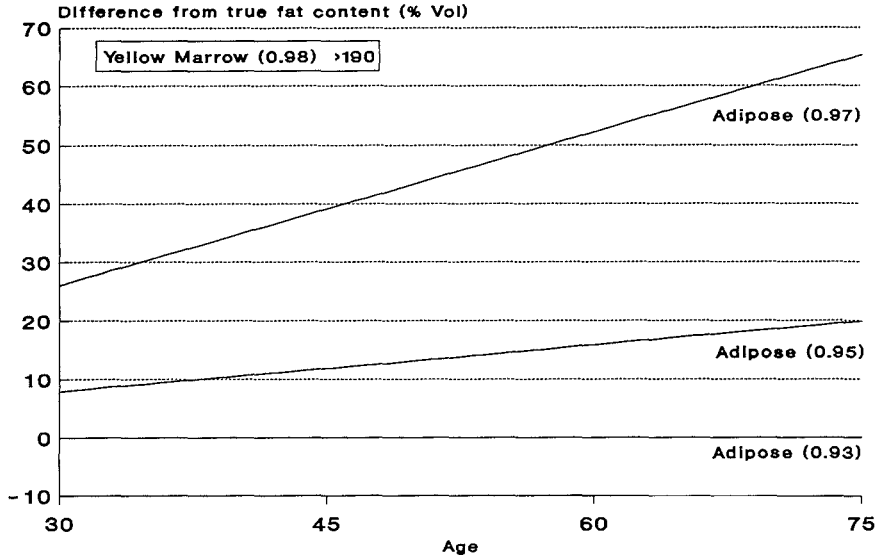

Figure 5.6.B. DEQCT fat content results for the method of Nickoloff et al. Adipose tissue description is changed for the calculation of the material dependent coefficient.

In Figures 5.6.C and 5.6.D the results are shown if the adipose tissue description and/or the hematopoietic tissue description is changed. In all cases the bone mineral content is overestimated. If only the hematopoietic tissue description is changed the bone mineral content is overestimated from 9 - 7 mg/cm^3 (4 - 12%). The difference between the bone mineral estimates and the true bone mineral content is nearly fixed. This is true also, if the adipose tissue description is altered to the descriptions with mass densities of 0.95 or 0.97 g/cm^3. With the yellow marrow description the difference increases with decreasing trabecular bone volume, although the overestimation is less compared with Figure 5.6.A. The fat content is overestimated in all cases (Figure 5.6.D). Overestimation decreases with the adipose (0.93 g/cm^3) description, and increases with all other adipose tissue descriptions.

64

Difference form true mineral content

(chart with axes: y-axis from -5 to 40, x-axis "Age" from 30 to 75)

Yellow Marrow (0.98)

Adipose (0.97)
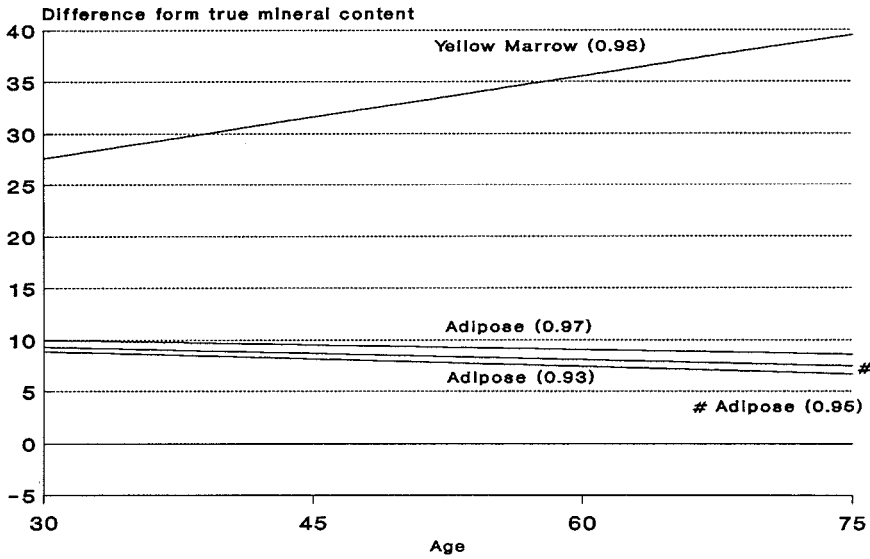
Adipose (0.93)

Adipose (0.95)

Figure 5.6.C. DEQCT bone mineral results for the method of Nickoloff et al. Adipose and soft tissue descriptions are changed for calculation of the material dependent coefficients.

5.3.4 Influences of non-uniform effective energies

Figure 5.7 shows the results for the bone mineral estimates obtained with the DEQCT and SEQCT methods, if the effective energies for the vertebral body are 5 keV higher than for the "identical" reference device. For all methods the bone mineral content is underestimated, ranging from 79 - 12 mg/cm^3 (36 - 22%) for the DEQCT methods of Nickoloff and of Goodsitt; from 57 - 25 mg/cm^3 (26 - 45%) for Cann's method; from 42 - 34 mg/cm^3 (19 - 61%) for SEQCT at 50 keV; and from 32 - 39 mg/cm^3 (14 - 71%) for SEQCT at 70 keV.
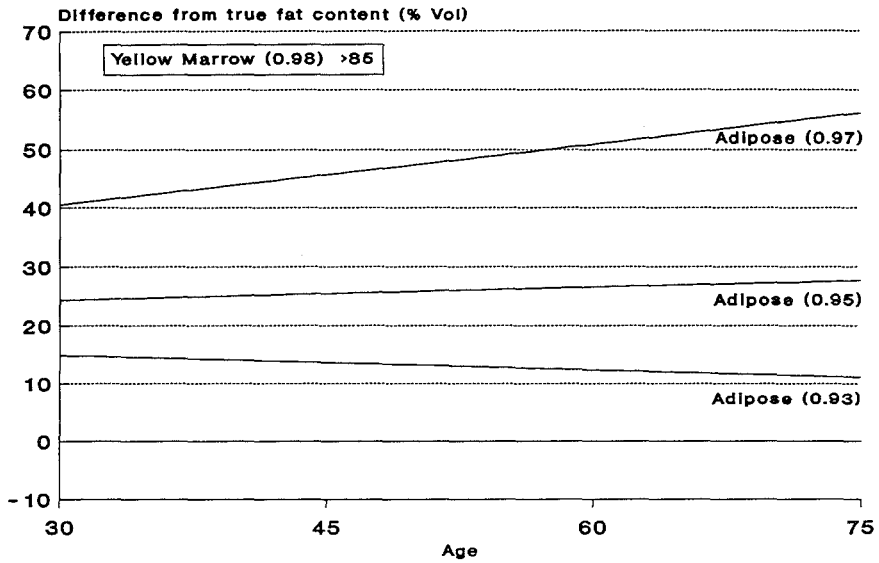
Figure 5.6.D. DEQCT fat content results for the method of Nickoloff et al. Adipose and soft tissue descriptions are changed for calculation of the material dependent coefficients.
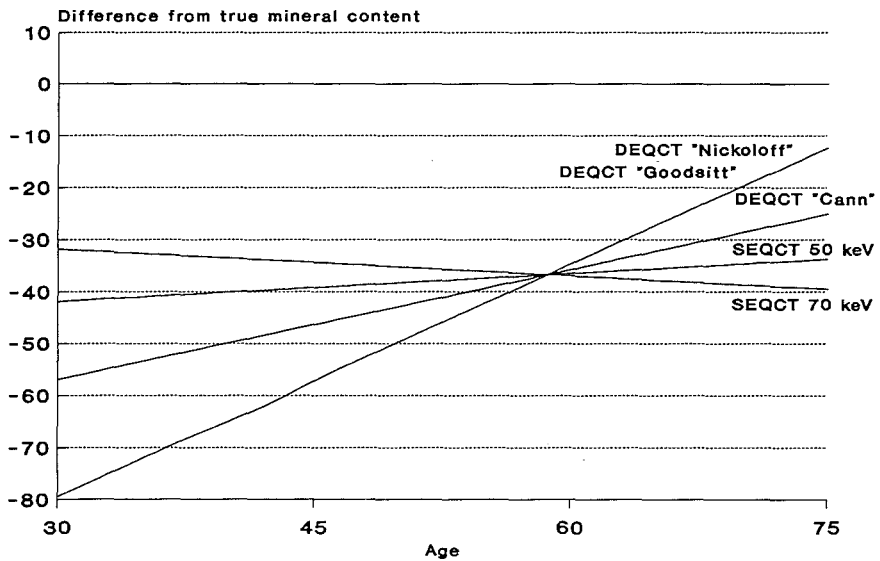

Figure 5.7. SEQCT and DEQCT results. A 5 keV difference in effective energy exists between the simulated vertebral body and the simulated "identical" reference device.

5.4 DISCUSSION

The findings shown in Figures 5.2, 5.5, 5.6.A and 5.6.B demonstrate that in an ideal situation, i.e. reference materials identical to the anatomic tissues, uniform effective energies and absence of scanner dependent error sources, like field inhomogeneity, the postprocessing dual-energy algorithms of Goodsitt and of Nickoloff are capable of an accurate estimation of bone mineral content and fat content in the trabecular region of the vertebral body. This was already predicted in our theoretical evaluation of the various postprocessing algorithms (chapter 3, (1)) and illustrated in the phantom studies (chapter 4, (2)).

If the bone-mimicking material in the reference device is changed to K_2HPO_4 the estimates obtained with SEQCT improve. This seems to be a contradiction. However, it is due to a fortunate coincidence that the attenuation characteristics of K_2HPO_4 partially compensate the fat error. The same observation was made by Crawley et al (12).

The estimates obtained with Goodsitt's calibration approach vary considerably with the tissue mimicking materials used in the reference device (Figures 5.5.A and B). This is especially true for the fat content estimates. This was also illustrated in the phantom studies (2). In this simulation set-up, changes from the "ideal" situation result in underestimation of bone mineral and fat content. Underestimation increases with an increasing true fat content. However, in all instances, it is less than the underestimation of bone mineral content seen with single-energy QCT (Figure 5.3).

The bone mineral and fat content, as calculated with the method of Nickoloff et al., are overestimated, if the tissue description of the hematopoietic or the adipose tissue is altered. However, the bone mineral estimates are better than with single-energy QCT at 50 keV, except when the yellow marrow description is used for the adipose tissue description. The fat content estimates vary considerably.

If a difference of 5 keV in effective energy is simulated (that can occur in practice) between the central site of the vertebral body and the peripheral site of the reference device, bone mineral and fat content are underestimated for the DEQCT methods of Goodsitt and Nickoloff. The underestimation decreases with increasing fat content. The accuracy is influenced negatively by this effective energy difference.

Values that are outside the physiological range are obtained easily due to

improper calibration materials or effective energy differences. This is especially true for the fat content estimates. In a patient study published by Rosenthal et al. (22), this observation was also described. The fat content of several radiated and non-radiated vertebral bodies was measured with DEQCT (Goodsitt's calibration approach). Fat fractions calculated were > 100% in two of the three radiated vertebral bodies.

Goodsitt et al (5) also observed this phenomenon while evaluating the "basic approach" (see chapter 3) in a phantom study. They proposed an additional constraint to the algorithm, namely that each volume fraction component must be positive. Nickoloff and Feldman (6) suggested a graphical solution to this problem. For various adipose tissue volumes between 20% and 80%, the values for the trabecular bone volume that would yield the CT numbers measured in the trabecular part of the vertebral body at both scanning energies are determined and graphed. The point of intersection should give the correct value for the trabecular bone volume and the adipose tissue volume. If, however, the curves do not intersect, the point of closest approach is selected. Although not stated in the original paper (6), this means that calculated values for the adipose tissue volume will be cut off at 20% or at 80%. For example, in our simulation study for Nickoloff's method with 5 keV energy elevation, this would mean that the fat content estimates would be cut off at 20% fat by volume for a true fat content ranging from 20 - 44%. This will obscure differences. The "uncorrected" estimates range from -64 to 16% for the same true fat content range. In that case, differences in fat content will be exaggerated. Therefore, the limitation of estimates to the expected physiological range can obscure information.

In summary: in this chapter the DEQCT methods that appeared to be the most valuable in the theoretical analysis (chapter 3) and in the phantom studies (chapter 4), are evaluated in a patient simulation set-up. For Goodsitt's calibration approach it is shown, that especially for fat content determination, it is important to use reference materials that closely mimick the anatomic constituents of the vertebral body. Materials mimicking trabecular bone substance (including the collagen matrix), intravertebral hematopoietic tissue, and intravertebral adipose tissue should be used. Development of these materials has been announced (23).

An accurate description of the anatomic constituents is also necessary for Nickoloff's method, so that the material specific coefficients can be calculated. A

more accurate description of the elemental composition and mass density of the various constituents of the vertebral body would improve the accuracy of bone mineral and fat content estimation with this method.

However, apart from this problem, accuracy will be greatly impaired by the effective energy differences at both scanning energies, between the site of the vertebral body and the site of the reference device. In practice, this problem will be the major problem in performing postprocessing DEQCT.

APPENDIX A

Calculation of linear attenuation coefficients.
In the domain of diagnostic energies, the linear attenuation coefficient μ of an element of atomic number, Z, at energy E is given by:

$$\mu = r\ N_a\ \sigma(Z,E)\ /\ A \qquad\qquad\qquad [Ap.1],$$

where r is the mass density; N_a is Avogadro's number; σ (Z,E) is the total atomic cross section of the X-ray interaction process (coherent scattering, incoherent scattering and photo-electric effect); A is the atomic mass.

The linear attenuation coefficient for a mixture or compound can be computed from:

$$\mu = r\ \sum_k \Omega_k\ (N_a\ /\ A_k\ )\ \sigma_k\ (Z,E) \qquad\qquad [Ap.2],$$

where, Ω_k is the mass fraction of the kth atomic constituent.

The different interaction cross sections are computed according to the method of Hawkes and Jackson (24).

5.5 REFERENCES

1.   van Kuijk C, Grashuis JL, Steenbeek JCM, Schütte HE, Trouerbach WTh. Evaluation of postprocessing dual-energy methods in quantitative computed tomography. Part 1: Theoretical considerations. Invest Radiol 1990;25:876-881.

2.   van Kuijk C, Grashuis JL, Steenbeek JCM, Schütte HE, Trouerbach WTh. Evaluation of postprocessing dual-energy methods in quantitative computed tomography. Part 2: Practical Aspects. Invest Radiol 1990;25:882-889.

3.   Cann CE, Gamsu G, Birnberg FA, Webb WR. Quantification of calcium in solitary pulmonary nodules using single and dual-energy CT. Radiology 1982;145:493-496.

4.   Laval-Jeantet AM, Cann CE, Roger B, Dallant P. A post-processing dual-energy technique for vertebral CT densitometry. J Comput Assist Tomogr 1984;8:1164-1167.

5.   Goodsitt MM, Rosenthal DI, Reinius WR, Coumas J. Two post-processing CT techniques for determining the composition of trabecular bone. Invest Radiol 1987;22:209-215.

6.   Nickoloff EL, Feldman F, Atherton JV. Bone mineral assessment: new dual-energy approach. Radiology 1988;168:223-228.

7.   Mazess RB. Errors in measuring trabecular bone by computed tomography due to marrow and bone composition. Calc Tissue Int 1983;35:148-152.

8.   Dunnill MS, Anderson JA, Whitehead R. Quantitative histological studies on age changes in bone. J Path Bact 1967;94:275-291.

9.   Burkhardt R, Kettner G, Böhm W, Schmidmeier M, Schlag R, Frisch B, Mallmann B, Eisenmenger W, Gilg TH. Changes in trabecular bone, hematopoiesis and bone marrow vessels in aplastic anemia, primary osteoporosis and old age: a comparative histomorphometric study. Bone 1987;8:157-164.

10.   Arnold JS, Bartley MH, Tont SA, Jenkins DP. Skeletal changes in aging and disease. Clin Orthop Rel Res 1966;49:17-38.

11.   Tanaka Y, Inoue T. Fatty marrow in the vertebrae. A parameter for hematopoietic activity in the aged. J Geront 1976;31:527-532.

12.   Mosekilde L. Sex differences in age-related loss of vertebral trabecular bone mass and structure: Biomechanical consequences. Bone 1989;10:425-432.

13.   Crawley EO, Evans WD, Owen GM. A theoretical analysis of single-energy CT bone-mineral measurements. Phys Med Biol 1988;33:1113-1127.

14.   Gong JK, Arnold JS, Cohn SH. The density of organic and volatile and non-volatile inorganic components of bone. Anat Rec 1964;149:319-324.

15.   Gong JK, Arnold JS, Cohn SH. Composition of trabecular and cortical bone. Anat Rec 1964;149:325-332.

16.   Mueller KH, Trias A, Ray RD. Bone density and composition. J Bone J Surg 1966;48-A:140-148.

17. Galante J, Rostoker W, Ray RD. Physical properties of trabecular bone. Calc Tiss. Res 1970;5:236-246.

18. ICRP (Snyder WS, Cook MJ, Nasset ES, Karhausen LR, Parry Howells G, Tipton IH). Report on the task group of reference man. ICRP report 23. 1975 Pergamon Oxford.

19. Woodard HQ, White DR. Bone models for use in radiotherapy dosimetry. Brit J Radiol 1982;55:277-282.

20. Woodard HQ, White DR. The composition of body tissues. Brit J Radiol 1986;59:1209-1219.

21. Mayo-Smith W, Rosenthal DI, Goodsitt MM, Klibanski A. Intravertebral fat measurements with quantitative CT in patients with Cushing disease and anorexia nervosa. Radiology 1989;170:835-838.

22. Rosenthal DI, Hayes CW, Rosen B, Mayo-Smith W, Goodsitt MM. Fatty replacement of spinal bone marrow due to radiation: Demonstration by dual-energy quantitative CT and MR imaging. J Comput Assist Tomogr 1989;13:463-465.

23. Goodsitt MM, Johnson RH. New quantitative CT calibration phantom for estimating the fat and mineral content of vertebrae. Presented as work in progress at the 75th scientific assembly and annual meeting of the Radiological Society of North America [RSNA], Chicago 1989. Presentation Nr 1324.

24. Hawkes DJ, Jackson DF. An accurate parametrisation of the x-ray attenuation coefficient. Phys Med Biol 1980;25:1167-1171.

CHAPTER 6

PATIENT SIMULATION STUDIES:
MINERALIZATION AND BONE MARROW CHANGES

6.1 INTRODUCTION

In the previous chapter, the influence of mismatching reference materials and of effective energy differences was discussed for SEQCT and postprocessing DEQCT in relation to changes in composition of the vertebral body that can be expected to occur in aging. A linear decrease in trabecular bone volume and hematopoietic tissue volume and a compensatory increase in adipose tissue volume was assumed. Furthermore, it was assumed that mineralization of the trabecular bone substance does not change.

In this chapter, we will consider the influence of changes in bone mineralization on QCT data, assuming that the volumes of trabecular bone, of hematopoietic tissue and adipose tissue do not change. This influence should be investigated because accuracy of postprocessing DEQCT methods could be impaired by changes in bone mineralization, since in these methods it is assumed implicitly that mineralization of the trabecular bone substance does not change. The influence of altered mineralization on QCT data is evaluated using the patient simulation set-up for SEQCT and the postprocessing DEQCT methods of Cann et al., Nickoloff et al. and of Goodsitt et al.

Another problem, that will be discussed in this chapter, is the influence on QCT data of bone marrow changes without an accompanying change in bone mineral content of the vertebral body. This is of importance because SEQCT is used in monitoring bone density changes in a variety of disorders and treatments (1-6). SEQCT is preferred for longitudinal studies because of its better precision compared with DEQCT. However, interpretation of longitudinal changes in SEQCT data is difficult, because the bone equivalent value is influenced by true bone mineral content changes and/or by bone marrow changes. The latter is of importance in osteoporosis treatment research. One has to be aware that actual bone loss or bone gain can be obscured by bone marrow changes and that bone marrow change itself can simulate changes in bone mineral content. The accuracy problem in SEQCT due to intravertebral fat content is reported extensively (7-15). However, the clinical implications for monitoring treatment

regimens or the natural course of diseases has received only little attention in the literature (15).

In order to evaluate the influence of bone marrow changes on QCT data, an additional study was performed, again using the simulation set-up. Changes in bone marrow composition were simulated by altering the volumes of the marrow constituents without changing the trabecular bone volume. Mineralization of the trabecular bone substance was kept constant.

6.2 METHODS

Simulation of bone mineralization changes

In the patient simulation study, as described in chapter 5, it is assumed that the trabecular bone substance has a fixed mineralization (58% of weight calcium hydroxyapatite, 32% collagen and 10% water). To simulate mineralization changes, the trabecular bone substance is decomposed into its basic constituents. Equation 2 of chapter 5 is altered to:

$$CT_v\{E\} = CT_{bm}\{E\}V_{bm} + CT_c\{E\}V_c + CT_w\{E\}V_w + CT_{bl}\{E\}V_{bl} + CT_{at}\{E\}V_{at}$$

In contrast to Equation 2 of chapter 5, the volume fractions of bone mineral (V_{bm}) and collagen (V_c) and water (within the trabecular bone substance) (V_w) are treated separately, in order to simulate changes in bone mineralization.

The linear attenuation coefficients for bone mineral (calcium hydroxyapatite; mass density 3.06 g/cm^3) are 1.791 cm^{-1} at 50 keV and 0.959 cm^{-1} at 70 keV; for collagen (mass density 1.38 g/cm^3) 0.282 cm^{-1} at 50 keV and 0.250 at 70 keV (compare with Table 5.2).

A decrease in mineralization is simulated by decreasing the percentage of weight of bone mineral and increasing the percentage of weight of water (Table 6.1). The mass density of trabecular bone substance decreases from 1.918 g/cm^3 to 1.718 g/cm^3. These data are according to the findings of Müeller et al (16) and the suggestions of Weissberger et al (17) and those of Mazess (7).

The composition of the vertebral body changes in aging, as discussed in chapter 5. Therefore, the influence of altered mineralization was performed for different compositions of the trabecular region of the vertebral body more or less corresponding to age differences as follows:

TABLE 6.1. Simulation of diminished mineralization of trabecular bone substance.

	Percentage of weight		Density in g/cm³
Mineral:	Collagen:	Water:	Bone substance:
58%	32%	10%	1.918
57%	32%	11%	1.893
56%	32%	12%	1.870
55%	32%	13%	1.846
54%	32%	14%	1.824
53%	32%	15%	1.802
52%	32%	16%	1.780
51%	32%	17%	1.759
50%	32%	18%	1.738
49%	32%	19%	1.718

A: 20% trabecular bone volume, 60% hematopoietic tissue volume and 20% adipose tissue volume; for an individual of young age (30 years).

B: 15% trabecular bone volume, 55% hematopoietic tissue volume and 30% adipose tissue volume; for a middle-aged person (45 years).

C: 10% trabecular bone volume, 50% hematopoietic tissue volume and 40% adipose tissue volume; for an individual of advancing age (60 years).

Simulation of bone marrow changes

Equation 2 of chapter 5 was used to simulate bone marrow changes. Trabecular bone volume was kept constant at 20%, 15%, and 10%, under the assumption that mineralization does not change. The remaining marrow volume was considered to be filled with hematopoietic tissue only. Subsequently, the hematopoietic tissue was replaced by adipose tissue in steps of 5% of volume, until the marrow space was filled completely with adipose tissue.

Calculation of CT data

CT numbers were generated at 50 and 70 keV. Bone mineral and, if possible, fat content estimates were calculated for the dual-energy method of Cann et al (18), the calibration method of Goodsitt et al (19), and the dual-energy method of Nickoloff et al (20), and for SEQCT at 50 keV.

For SEQCT and the postprocessing DEQCT methods of Cann and Goodsitt et al an "identical" calibration device was simulated. For the method of Nickoloff et al "identical" materials specific coefficients were simulated.

In chapter 5, it was shown that differences in effective energy between the reference device and the vertebral body have a large influence on the accuracy of QCT data (Figure 5.7). Therefore, in addition to the simulation of uniform effective energies, the influence of bone marrow changes was evaluated at an effective energy difference between vertebra and reference device of 5 keV.
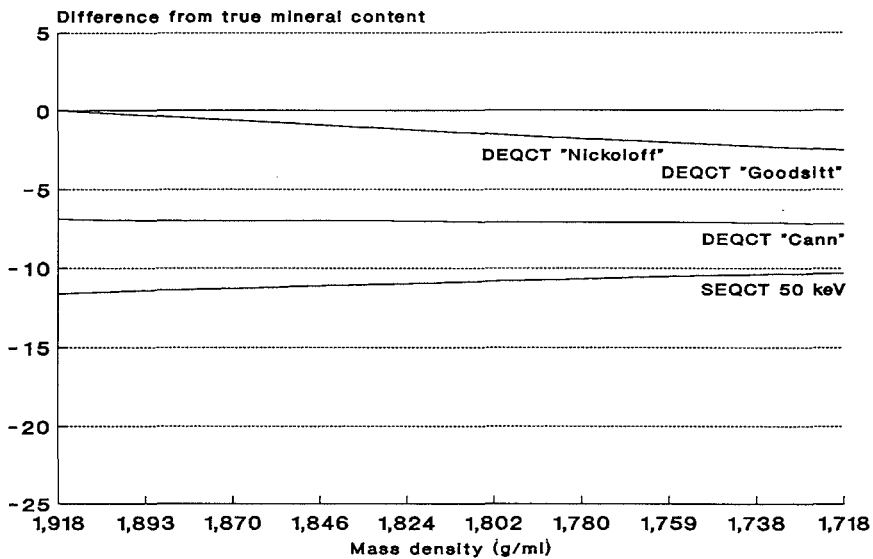
6.3 RESULTS

Mineralization changes.

Figure 6.1.A. SEQCT and DEQCT bone mineral results at a trabecular bone volume of 20%. Simulation of changes in mineralization of the trabecular bone substance. Difference from true mineral content in mg/cm³.

The results for bone mineral content determination with SEQCT at 50 keV and for DEQCT, are given in Figure 6.1.A for 20% trabecular bone volume and in Figure 6.1.B for 10% trabecular bone volume.

At 20% trabecular bone volume the bone mineral content is underestimated by SEQCT with approximately ± 11 mg/cm³ (in percentage of true bone mineral content ranging from 5 - 6%), if the mass density of trabecular bone substance ranges from 1.918 - 1.718 g/cm³. At 15% trabecular bone volume, the underestimation is ± 17 mg/cm³; in percentage ranging from 10 - 13%). At 10%
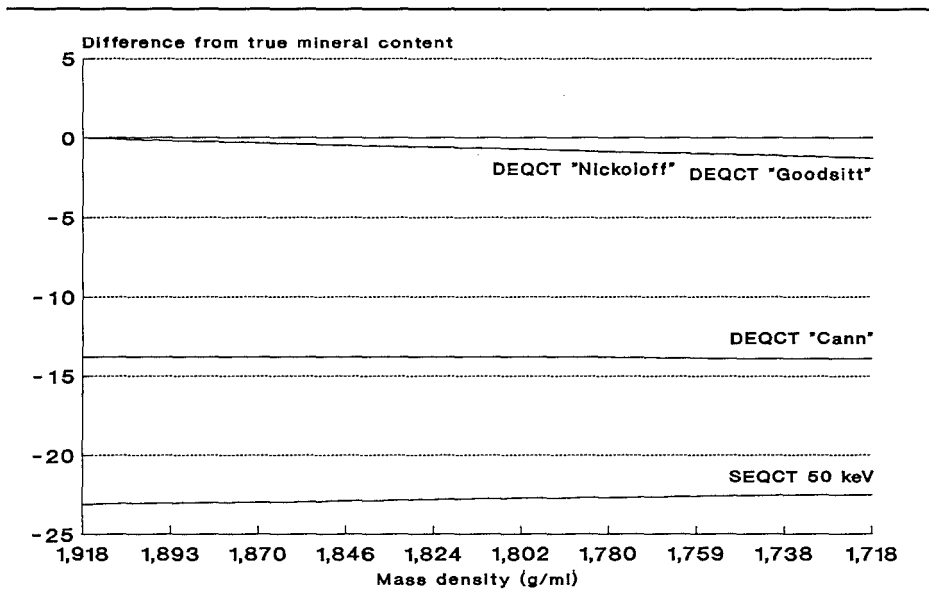
75

Figure 6.1.B. SEQCT and DEQCT bone mineral results at 10% trabecular bone volume. Simulation of changes in mineralization of trabecular bone substance. Difference from true mineral content in mg/cm³.

trabecular bone volume, the corresponding figures are $\pm$ 23 mg/cm^3; in percentage ranging from 21 - 27% underestimation. Underestimation of bone mineral content with SEQCT reported as an absolute difference is approximately constant for a given trabecular bone volume. Underestimation in percentage of true bone mineral content increases with decreasing trabecular bone volume and with decreasing mass density of the trabecular bone substance.

For the DEQCT method of Cann et al, bone mineral content is underestimated with 7 mg/cm^3 at 20% trabecular bone volume (3 - 4%); with 10 mg/cm^3 at 15% trabecular bone volume (6 - 8%); and with 14 mg/cm^3 at 10% trabecular bone volume (12 - 16%). Underestimation of bone mineral content with the DEQCT method of Cann et al reported as an absolute difference is approximately constant for a given trabecular bone volume. The underestimation in percentage of true bone mineral content shows the same trend as the SEQCT results. Underestimation is less than with SEQCT at 50 keV.

Bone mineral estimates are the same for the dual-energy methods of Nickoloff et al and Goodsitt et al. This is due to the fact that the same tissue descriptions are used for the calibration input for the method of Goodsitt et al as for the

calculation of the material dependent coefficients for the method of Nickoloff et al. Bone mineral content is underestimated slightly with decreasing mineralization. The maximum underestimation is 2.5 mg/cm³ (2%) at 20% trabecular bone volume and at a density of 1.718 g/cm³. The influence on fat content
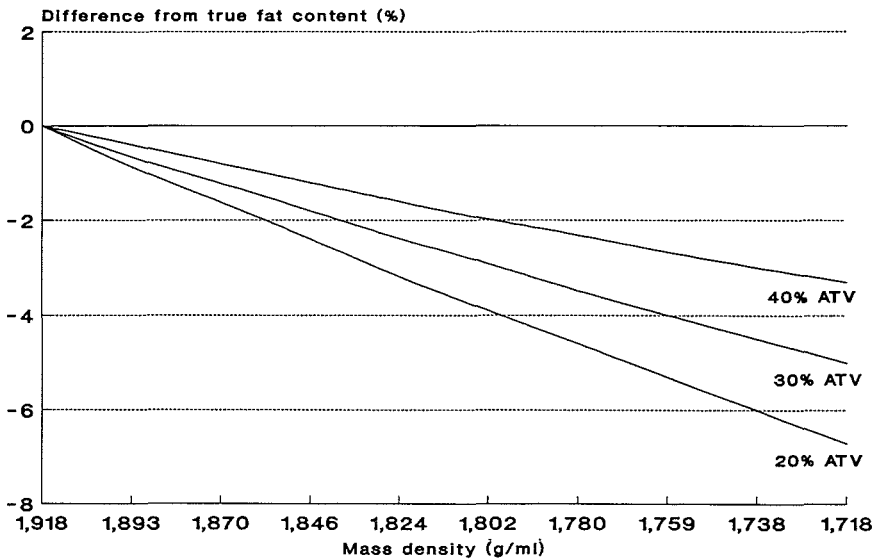

Figure 6.1.C. DEQCT (Method of Goodsitt and of Nickoloff) fat content results. Simulation of changes in mineralization of trabecular bone substance. Difference from true fat content in percentage of volume.

determination is more pronounced, as can be seen in Figure 6.1.C. Underestimation increases with decreasing mineralization and with decreasing true fat content. The maximum underestimation is 7% (percentage fat by volume) at 20% adipose tissue volume (ATV) and a mass density of 1.718 g/cm³ (as percentage of true fat content this is 33%).

Bone Marrow Changes

Results of bone mineral content determination with SEQCT and DEQCT if the marrow composition is changed are given in Figure 6.2.A for 20% trabecular bone volume and in Figure 6.2.B for 10% trabecular bone volume. On the horizontal axis the percentage volume of fat is given. On the vertical axis the bone mineral estimates are given as percentage of true bone mineral content.

As expected, the DEQCT methods of Goodsitt et al and Nickoloff et al give an
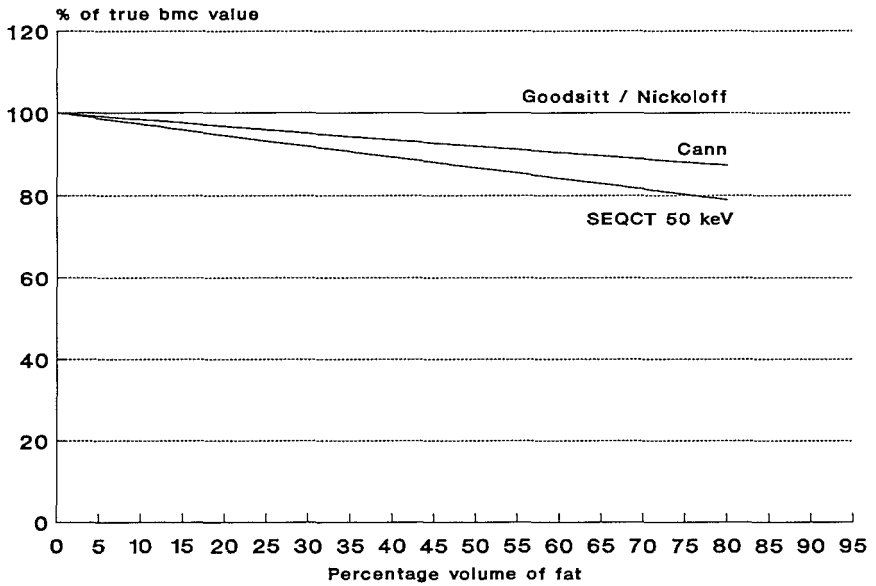
Figure 6.2.A. SEQCT and DEQCT bone mineral results at 20% trabecular bone volume. Simulation of bone marrow changes.
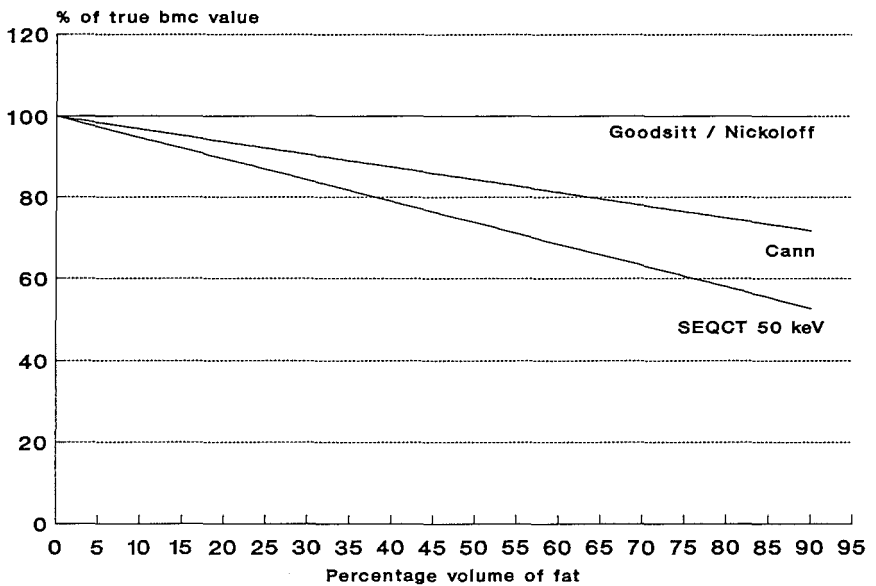

Figure 6.2.B. SEQCT and DEQCT bone mineral results at 10% trabecular bone volume. Simulation of bone marrow changes.

accurate estimation of bone mineral content. The DEQCT method of Cann reduces the fat-induced error with a factor of two. The SEQCT data are influenced by a change in marrow composition. There is increasing underestimation of true bone mineral content with increasing adipose tissue volume and with decreasing trabecular bone volume. With the "identical" calibration set-up, underestimation is 2.9 mg/cm^3 if 5% of volume is converted from hematopoietic to adipose tissue. For the DEQCT method of Cann, underestimation is 1.7 mg/cm^3 if 5% of volume is converted.

In Figure 6.2.C results are shown for bone mineral content estimation if bone marrow changes at a trabecular bone volume of 10% are simulated when there are effective energy differences. The influence on the accuracy of bone mineral content determination, defined as a deviation from true bone mineral content, is illustrated clearly. An effective energy difference impairs the accuracy, as already shown in Figure 5.7. A change of 5% in marrow volume is detected by SEQCT at 50 keV as a change of 2.7 mg/cm^3 in bone mineral content. The DEQCT method of Cann detects it as a change of 1.4 mg/cm^3 in bone mineral content,
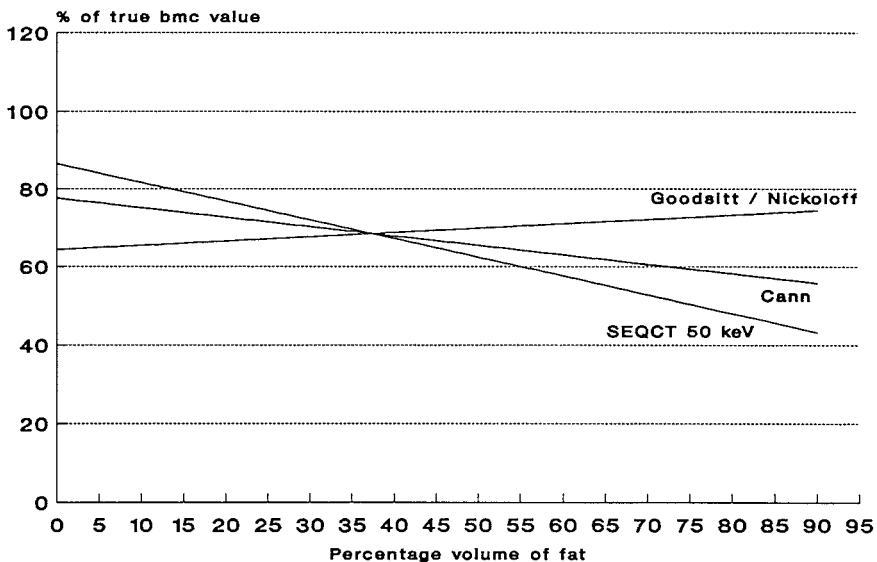

Figure 6.2.C. SEQCT and DEQCT bone mineral results at 10% trabecular bone volume. Simulation of bone marrow changes and 5 keV difference in effective energy.

while the DEQCT methods of Goodsitt and Nickoloff detect it as a change of 0.6 mg/cm³. An increase of fat volume is reflected by an increase in the bone equivalent value by the methods of Goodsitt and Nickoloff and by a decrease by SEQCT and the DEQCT method of Cann. An increase of 5% fat by volume is detected by the dual-energy methods as an increase of 6% fat by volume.

6.4 DISCUSSION

In this chapter, the influence of bone mineralization and bone marrow changes on QCT data is evaluated, using a patient simulation set-up.

Diminished bone mineralization, as in osteomalacia, will impair the accuracy of bone mineral measurements with the DEQCT methods of Goodsitt et al and Nickoloff et al only slightly. This accuracy error is small compared with the accuracy errors that arise from non-ideal calibration procedures or tissue descriptions, or from effective energy differences.

Simulation of bone marrow changes was performed to evaluate its influence on SEQCT data in longitudinal studies with the purpose of monitoring bone mineral content changes. A 5% change in bone marrow composition gives a change of 2.9 mg/cm³ (2.7 mg/cm³ with 5 keV difference) in the bone equivalent value. At 70 keV, the change will be even larger, namely 3.7 mg/cm³ (data not shown). At a low initial bone mineral content of 100 mg/cm³ (± 9% trabecular bone volume), this change would give a 3% change in the bone equivalent value. A greater change in bone marrow composition of 10% would give a 6% change in the bone equivalent value. At a very low initial bone mineral content of 60 mg/cm³ (± 5% trabecular bone volume), a change of 5% in bone marrow composition gives a 5% change in bone equivalent value. Evaluation with SEQCT of treatment regimens known to affect fat metabolism and body composition, like anabolic steroids (21), could be hampered by this phenomenon. The expected error exceeds the precision error of SEQCT. Postprocessing DEQCT (the methods of Goodsitt and Nickoloff) could be a (partial) solution to this problem, because the bone equivalent value is not influenced by bone marrow alterations in the "ideal" situation and only slightly when effective energy differences are taken into account. In addition, changes in bone marrow composition can be monitored. In order to give a more definite judgement, the precision of postprocessing DEQCT will be discussed in the next chapter.

6.5 REFERENCES

1.   Ettinger B, Genant HK, Cann CE. Postmenopausal bone loss is prevented by treatment with low-dosage estrogen with calcium. Ann Intern Med 1987;106:40-45.

2.   Reid IR, King AR, Alexander CJ, Ibbertson HK. Prevention of steroid-induced osteoporosis with (3-amino-1-hydroxypropylidene)-1,1-bisphosphonate (APD). Lancet 1988;578:143-146.

3.   Hesch RD, Busch U, Prokop M, Delling G, Rittinghaus EF. Increase of vertebral density by combination therapy with pulsatile 1-38hPTH and sequential addition of calcitonin nasal spray in osteoporotic patients. Calcif Tissue Int 1989;44:176-180.

4.   Genant HK, Block JE, Steiger P, Glüer CC, Ettinger B, Harris ST. Appropriate use of bone densitometry. Radiology 1989;170:817-822.

5.   Finkelstein JS, Klibanski A, Neer RM, Doppelt SH, Rosenthal DI, Segre GV, Crowley Jr WF. Increases in bone density during treatment of men with idiopathic hypogonadotropic hypogonadism. J Clin Endoc Metab 1989;69:776-783.

6.   Grecu EO, Weinshelbaum A, Simmens R. Effective therapy of glucocorticoid-induced osteoporosis with medroxyprogesterone acetate. Calcif Tissue Int 1990;46:293-299.

7.   Mazess RB. Errors in measuring trabecular bone by computed tomography due to marrow and bone composition. Calcif Tissue Int 1983;35:148-152

8.   Mazess RB, Vetter J. The influence of marrow on measurement of trabecular bone using computed tomography. Bone 1985;6:349-351.

9.   Rohloff R, Hitzler H, Arndt W, Frey KW. Experimentelle Untersuchungen zur Genauigkeit der Mineralsalzgehaltsbestimmung spongiöser Knochen mit Hilfe der quantitativen CT (Einenergiemessung). Fortschr Röntgenstr 1985;143:692-697.

10. Laval-Jeantet AM, Roger B, Bouysse S, Bergot C, Mazess RB. Influence of vertebral fat content on quantitative CT density. Radiology 1986;159:463-466.

11. Burgess AE, Colborne B, Zoffmann E. Vertebral trabecular bone: comparison of single and dual-energy CT measurements with chemical analysis. J Comput Assist Tomogr 1987;11:506-515.

12. Webber CE. The effect of fat on bone mineral measurements in normal subjects with recommended values of bone, muscle and fat attenuation coefficients. Clin Phys Physiol Meas 1987;8:143-158.

13. Crawley EO, Evans WD, Owen GM. A theoretical analysis of the accuracy of single-energy CT bone-mineral measurements. Phys Med Biol 1988;33:1113-1127.

14. Glüer CC, Reiser U, Davis CA, Rutt BK, Genant HK. Vertebral mineral determination by quantitative computed tomography (QCT): accuracy of single and dual-energy measurements. J Comput Assist Tomogr 1988;12:242-258.

15. Glüer CC, Genant HK. The impact of marrow fat on accuracy of quantitative CT. J Comput Assist Tomogr 1989;13:1025-1035.

16.   Müeller KH, Trias A, Ray RD. Bone density and composition. J Bone Joint Surg 1966;48A:140-148.

17.   Weissberger MA, Zamenhof RG, Aronow S, Neer RM. Computed tomography scanning for the measurement of bone mineral in the human spine. J Comput Assist Tomogr 1978;2:253-262.

18.   Cann CE, Gamsu G, Birnberg FA, Webb WR. Quantification of calcium in solitary pulmonary nodules using single and dual-energy CT. Radiology 1982;145:493-496.

19.   Goodsitt MM, Rosenthal DI, Reinius WR, Coumas J. Two postprocessing CT techniques for determining the composition of trabecular bone. Invest Radiol 1987;22:209-215.

20.   Nickoloff EL, Feldman F, Atherton JV. Bone mineral assessment: new dual-energy approach. Radiology 1988;168:223-228.

21.   Hassager C, Podenphant J, Johansen JS, Jensen J, Christiansen C. Changes in soft tissue body composition and plasma lipid metabolism during nandrolone decanoate therapy in postmenopausal osteoporotic women. Metabolism 1989;38:238-242.

CHAPTER 7

PRECISION OF POSTPROCESSING DUAL-ENERGY QUANTITATIVE CT METHODS

7.1 INTRODUCTION

In the previous chapters, accuracy errors were the main topic of interest in the evaluation study of postprocessing DEQCT methods. It was shown that the postprocessing dual-energy methods of Goodsitt et al and Nickoloff et al can improve the accuracy of bone mineral measurements compared with single-energy and the DEQCT method of Cann et al. Furthermore, these methods allow an estimate of bone marrow composition. In chapter 6 it was shown that the interpretation of SEQCT data in longitudinal studies is hampered by the uncertainty introduced by (unknown) changes in marrow composition. However in clinical practice SEQCT is preferred for longitudinal studies, because of its better precision (1-3).

Precision is influenced by a number of factors: 1) CT scanner variability; 2) operator variability; and 3) patient variability (1,4-13).

1) CT scanner variability refers to instabilities of the apparatus. Detector instabilities or variability in the spectral quality of the X-ray tube due to tube aging or tube replacement cause CT number variability. Field non-uniformities also cause CT number variability. Changes in table height (vertical displacement of the object) or lateral displacement of the object within the scan field can cause CT number changes. Therefore, absolute CT numbers can not be used in longitudinal studies. Reference devices were introduced in QCT offering a partial solution to this problem (4). Further, a strict scanning protocol (fixed object position, fixed table height, fixed scanning and reconstruction parameters) and the use of quality assurance programs will minimize this error. The current stability for CT scanners is reported to be better than 1 HU (Hounsfield Unit) (10).

2) Operator variability refers to the ability of the operator to relocalize the mid-vertebral slice. Positioning of the mid-vertebral slice in vivo can be done by using a volumetric multi-slice and reformatting technique. A number of contiguous slices are made through the lumbar spine. Then a new image representing a predefined mid-vertebral volume is synthesized using specific software (4).

However, in routine practice it is customary to select the mid-vertebral slice on a lateral computed image of the lumbar spine. This slice selection procedure is influenced by the experience and skill of the operator. Kalender et al (13) showed that differences of 1-2 mm in mid-vertebral slice selection were common. This leads to an error of 1-2% in the bone mineral equivalent value. Therefore, an automated slice selection program was developed by Kalender et al (13), that reduces the operator variability. It should be noted, however, that operator interaction is still needed in 10% of the cases (13). If operator interaction is required for the region of interest (ROI) selection for bone mineral measurements, it can be an additional source for variability. Louis et al (6) showed the mean absolute value of intrasubject variation to be 2.6 mg/cm^3 for SEQCT and 4.1 mg/cm for preprocessing DEQCT with manual selection of the ROI and without repositioning the patient. With repositioning of the patient (and consequently adding a positioning error) the variability increased to 3.8 mg/cm^3 for SEQCT and to 6.0 mg/cm^3 for preprocessing DEQCT. Automated ROI definition with the possibility of operator interaction reduced the variability to 0.4 mg/cm^3 for SEQCT and 0.5 mg/cm^3 for preprocessing DEQCT without patient repositioning and to 2.7 mg/cm^3 for SEQCT and 2.8 mg/cm^3 for preprocessing DEQCT with patient repositioning.

3) Patient variability refers to the variability in CT number due to changes in the patient's size or composition, e.g. the presence of bowel gas.

The reproducibility for SEQCT studies is reported (as coefficient of variation) to be better than 1% in "dedicated" research centers and 2-4% in routine practice. The precision for postprocessing DEQCT is generally believed to be worse because of the propagation of errors associated with combining data from two separate scans. Exact figures for the precision of postprocessing DEQCT methods have not been reported recently.

7.2 METHODS AND MATERIALS

An embalmed specimen of a human lumbar spine was used. In order to render the specimen airfree, it was held under water for 24 hours in a vacuum tank. Then, the specimen was fixed rigidly within a circular water tank, and placed in the CT scanner. Scanning was done with the Philips Tomoscan 350. CT slices of 6 mm thickness were made at 120 kVp (120 mAs) and at 70 kVp (480 mAs). A
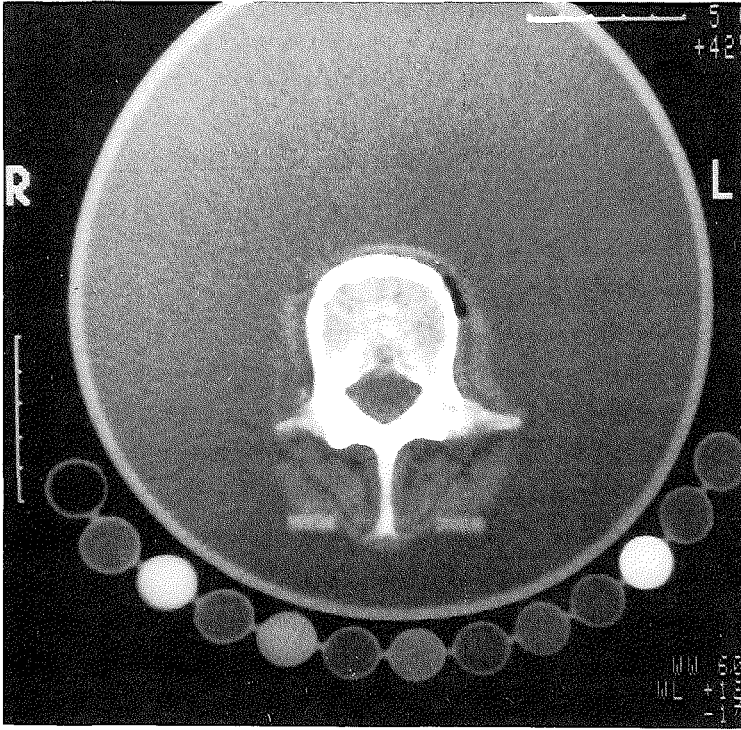
Figure 7.1. CT image of cadaver specimen of lumbar spine in water tank.

reference device consisting of circular tubes with different solutions of K_2HPO_4 in water (0, 50, 100, 200, 400 mg/cm^3) and liquid paraffin was scanned simultaneously with the water tank. A CT image of the experimental set-up is shown in Figure 7.1.

A circular region of interest (ROI) was used within the trabecular region of the vertebral body. Localization of the ROI on the other kVp image was done on exactly the same position.

Experiment 1: Scanner variability.

A mid-vertebral slice was defined through the third lumbar vertebra on the lateral image. Scans were made alternately at 120 kVp and 70 kVp; this was repeated five times. The same was done for the third and fourth lumbar vertebra.

Experiment 2: Slice selection variability.

A mid-vertebral slice was defined through the second lumbar vertebra on the lateral image. Scans were made alternately at 120 and 70 kVp. Then, the table

was moved 0.5 mm automatically and the scans were repeated. A maximum deviation from the center of 2 mm (up or down) was allowed.

For both experiments, QCT results were calculated for the single-energy method at 120 and 70 kVp. Postprocessing DEQCT results were calculated according to the methods of Cann et al, Goodsitt et al (calibration method; K_2HPO_4 solutions and liquid paraffin as fat equivalent), and Nickoloff et al. The water-offset value for the method of Nickoloff et al, was assessed by defining three circular ROI's within the water tank; left, above and right of the vertebral body.

Experiment 3: Simulation study.

Apart from the in vitro study, that could be limited in value by the small number of observations, precision figures for scanner variability were determined with the patient simulation set-up (see chapters 5 and 6). The composition of the vertebral body was fixed and the CT numbers at 50 and 70 keV were calculated. Normal distributions with means equal to the input CT numbers and a standard deviation of 1, assuming a CT number reproducibility of ± 1 HU for the CT scanner, were generated using a random number generation procedure (Statgraphics, Version 4.0, University edition; Statistical Graphics Corporation; Rockville, Maryland). 250 data points were generated for each CT number, separately.

QCT data were calculated using random pairs of CT numbers, assuming an "ideal calibration" set-up. Calculations were performed at three different compositions of the vertebral body to evaluate a dependency on tissue composition: A. 20% trabecular bone volume, 20% adipose tissue volume and 60% hematopoietic tissue volume: B. 15% trabecular bone volume, 30% adipose tissue volume and 55% hematopoietic tissue volume: C. 10% trabecular bone volume, 40% adipose tissue volume and 50% hematopoietic tissue volume.

In this chapter, the precision is defined as standard deviation of the mean for all experiments.

7.3 RESULTS

Experiment 1: Scanner variability.

QCT data for the various methods are given in Table 7.1. Data are given as the mean with standard deviation of five measurements. In addition the bone mineral equivalent values are averaged for the three lumbar vertebrae. The precision of

TABLE 7.1. Scanner variability (Philips Tomoscan 350).

Vertebra	L2	L3	L4	Average L2-L4
70 kVp Beq	88.7 (± 0.4)	95.2 (± 0.4)	98.3 (± 0.5)	94.1 (± 0.2)
120 kVp Beq	93.4 (± 0.4)	99.7 (± 0.5)	102.2 (± 0.2)	98.4 (± 0.3)
Cann Beq	78.5 (± 1.9)	85.4 (± 2.1)	89.6 (± 1.3)	84.5 (± 0.9)
Goodsitt Beq	66.7 (± 3.4)	74.3 (± 3.9)	79.8 (± 2.1)	73.6 (± 1.9)
Goodsitt Fat	-22.4 (± 3.3)	-21.4 (± 3.7)	-18.8 (± 1.6)	-20.9 (± 1.8)
Nickoloff Beq	84.9 (± 2.0)	90.6 (± 4.0)	94.4 (± 2.9)	90.0 (± 2.1)
Nickoloff Fat	-5.5 (± 2.9)	-4.9 (± 6.0)	-3.5 (± 4.2)	-4.6 (± 3.2)

Bone equivalent values (Beq) in mg/cm^3 (mean and standard deviation).
Fat content values in percentage fat by volume.

bone mineral measurements, given as the largest standard deviation of the measurements of the individual vertebral bodies, are 0.5 mg/cm^3 for SEQCT at 70 kVp; 0.5 mg/cm^3 at 120 kVp; 2.1 mg/cm^3 for the method of Cann et al; 3.9 mg/cm^3 for the calibration method of Goodsitt et al; and 4.0 mg/cm^3 for the method of Nickoloff et al. For bone equivalent values, determined by averaging the values of the three consecutive vertebral bodies, the precision figures are 0.2 mg/cm^3 for SEQCT at 70 kVp; 0.3 mg/cm^3 at 120 kVp; 0.9 mg/cm^3 for the method of Cann et al; 1.9 mg/cm^3 for the calibration method of Goodsitt et al; and 2.1 mg/cm^3 for the method of Nickoloff et al. The precision of fat content estimates, given as the largest standard deviation of the measurements of the individual vertebral bodies, are 3.7% (percentage volume of fat) for the calibration method of Goodsitt et al; and 6.0% for the method of Nickoloff et al. For the fat content values, determined by averaging the values of the three consecutive vertebral bodies, the precision figures are 1.8% for the calibration method of Goodsitt et al; and 3.2% for the method of Nickoloff et al.

Experiment 2: Slice selection variability.

The results are given in Table 7.2. The standard deviation for bone mineral estimates obtained with a maximum deviation of 1 mm (n = 5), is 1.5 and 1.4 mg/cm^3 for the SEQCT measurements at 70 and 120 kVp, respectively. The standard deviation for bone mineral measurements obtained with postprocessing DEQCT methods is larger; 2.0 mg/cm^3 for the method of Cann et al, 2.8 mg/cm^3

TABLE 7.2. Results of Experiment 2: Slice selection variability.									
Slice position	-2.0	-1.5	-1.0	-0.5	0.0	0.5	1.0	1.5	2.0
SE 70 kVp	88.1	87.4	90.9	90.7	93.9	93.2	93.6	93.5	91.4
SE 120 kVp	93.2	93.6	96.0	95.8	98.8	98.1	98.2	98.1	96.9
Cann	76.9	73.8	79.7	79.6	83.2	82.5	83.8	83.6	79.6
Goodsitt Beq	63.5	56.7	68.6	66.3	71.1	71.5	73.6	70.7	66.8
Goodsitt Fat	-25.5	-31.4	-23.2	-25.1	-23.6	-22.6	-20.7	-23.3	-25.4
Nickoloff Beq	78.8	78.5	85.2	87.2	91.4	92.8	93.6	90.9	84.4
Nickoloff Fat	-12.0	-13.4	-6.9	-4.4	-2.3	0.1	0.8	-2.4	-9.1

Slice position in mm. Bone equivalent value (Beq) in mg/cm^3. Fat content in percentage fat by volume.

for the calibration method of Goodsitt et al, and 3.7 mg/cm^3 for the method of Nickoloff et al. For fat content estimates the standard deviation is 1.6% for the calibration method of Goodsitt et al, and 3.2% for the method of Nickoloff et al. The standard deviation for bone mineral estimates obtained with a maximum deviation of 2 mm (n = 9), is 2.4 mg/cm^3 for SEQCT at 70 kVp, 2.0 mg/cm^3 at 120 kVp, 3.4 mg/cm^3 for the method of Cann, 5.2 mg/cm^3 for the method of Goodsitt and 5.7 mg/cm^3 for the method of Nickoloff. The standard deviation for fat content estimates is 3.0% for the method of Goodsitt and 5.1% for the method of Nickoloff.

Experiment 3: Patient simulation results.

The precision is the same for all vertebral body compositions; for SEQCT at 50 keV it is 0.4 mg/cm^3, at 70 keV 0.7 mg/cm^3. For the DEQCT method of Cann the standard deviation is 1.5 mg/cm^3 and for the DEQCT methods of Goodsitt and of Nickoloff 3.3 mg/cm^3. The standard deviation for the fat content estimate is 5% fat by volume.

7.4 DISCUSSION

The experiments presented in this chapter were designed to assess the precision of the postprocessing DEQCT methods. Variability of the CT number on the Philips Tomoscan 350 with the scanning parameters as reported in the materials and methods section, was assessed using an embalmed specimen of the lumbar spine. Averaging the bone mineral content results for three consecutive vertebral

bodies, as is usual in QCT, gives precision figures (given as standard deviation of the mean of five measurements) of less than 0.5 mg/cm^3 for SEQCT, less than 1.0 mg/cm^3 for Cann's DEQCT method, and less than 2.5 mg/cm^3 for the other DEQCT methods. The largest standard deviation for the fat content estimation was found to be 3.2% volume of fat for Nickoloff's method.

The influence of slice selection is shown clearly in Table 7.2, and it emphasizes the importance of the slice selection procedure. The estimates vary due to the inhomogeneity of the vertebral body. Therefore, an automated slice selection procedure is mandatory.

The precision figures predicted with the patient simulation set-up are close to those found in the in vitro study for assessing the CT scanner variability.

Variability due to the positioning of the ROI was not assessed, because it is possible to automatize this procedure completely, which eliminates this variability (13,14).

In clinical practice, the precision of QCT measurements will be less. Patient movement during scanning will cause positioning errors. Long-term scanner variability will be impaired by changes in scanner hardware and software. In the latter case, strict quality assurance protocols and regular system calibration procedures are necessary to monitor stability of CT systems used for QCT.

Furthermore, in patients with a low trabecular bone volume in the vertebral body, an improper relocalization of the mid-vertebral slice decreases precision due to increased inhomogeneity of the vertebral body. In a SEQCT study performed on the same CT scanner in 1987, the reported coefficient of variation, as obtained by scanning 10 osteoporotic patients twice with repositioning of the patient, was reported to be 2.7% (15). The scanning parameters were 120 kVp, 120 mAs, with an additional Copper filter and 6 mm slice thickness. Recent SEQCT precision estimates reported for other CT systems are given for comparison: Siemens DRH CT scanner, 0.4% coefficient of variation for short-term scanner stability and 1.6% for short-term variability including repositioning of a anthropomorphic phantom (11); General Electric GE9800 CT scanner, 1.5% for in vivo short-term variability including repositioning (12). The simulation study showed that the precision figures for scanner instability is independent of the vertebral body composition. However, if the precision was given as coefficient of variation (100*SD/mean), the precision would be dependent on vertebral composition. Therefore, comparison of precision figures given as coefficient of

variation can be misleading.

If we consider the precision figures from the patient simulation study, as the best that can be expected from current CT scanner designs, and combine the data with the bone marrow change simulation study (as presented in chapter 6) SEQCT at low kilovolt peak values has a precision of $\pm$ 0.4 mg/cm^3 and additional an uncertainty of 2.9 mg/cm^3 per 5% of marrow volume, due to conversion of marrow constituents, in interpretation of data. DEQCT with Nickoloff's method or Goodsitt's method has a precision of $\pm$ 3.3 mg/cm^3, without uncertainty in interpretation of data. These theoretical data suggest that postprocessing DEQCT, in spite of a decreased precision, could be used in monitoring changes in bone mineral content in the trabecular region of the vertebral body, if changes in the marrow composition are suspected. However, this is only true if precision levels are reached that are comparable with those presented in this chapter. This is only possible with strict scanning and measurement procedures and automatization of as many steps as possible within the QCT protocol (e.g. mid-vertebral slice selection and ROI positioning in vertebral body and reference device).

Apart from the precision figures, the estimates themselves should be discussed. The 120 kVp SEQCT bone mineral content estimates are higher than the 70 kVp SEQCT estimates, while the estimates obtained with Cann's method are lower than with both SEQCT settings. This is the opposite of what one would expect, for the intravertebral adipose tissue should render the 120 kVp data lower than the 70 kVp data. Further, the estimates with Cann's method would be influenced less by the intravertebral adipose tissue and give higher estimates than those obtained with SEQCT.

Different explanations for this phenomenon should be considered. The estimates are biased by the difference in effective energy at the place of the vertebral body and the place of the reference device. Adressing this problem, reported in chapter 5 and the results shown in Figure 5.7, suggest that this explanation is correct. In this simulation, it was shown that high energy SEQCT estimates can be larger than low energy SEQCT estimates, and that Cann's method can give estimates below SEQCT estimates.

The estimates could be biased by the embalming process of the vertebral body, the intravertebral fat could have been washed out and could have changed the attenuation characteristics of the marrow component of the trabecular region of

the vertebral body. The fat content results obtained with Goodsitt's method and Nickoloff's method seem to confirm this. The estimated fat content is negative for the methods of Goodsitt and of Nickoloff. However, the fat content estimates obtained with Goodsitt's method are biased by the choice of non-ideal calibration materials (K_2HPO_4 and paraffin). The fat estimates with the DEQCT method of Nickoloff could be biased by the choice of the tissue description used for calculating the material dependent coefficients. The bone mineral content estimates with the method of Cann are lower than the SEQCT estimates. This can not be explained fully by a disappearance of the intravertebral adipose tissue alone. For, in that case, the bone mineral estimates with Cann's method would be close to the SEQCT estimates. Therefore, the bias due to the effective energy differences seems to be the most important.

7.5 REFERENCES

1. Felsenberg D, Kalender WA, Banzer D, Schmilinsky G, Heyse M, Fischer E, Schneider U. Quantitative computertomographische Knochenmineralgehaltsbestimmung. Fortschr Röntgenstr 1988;148:431-436.

2. Felsenberg D. Quantitative Knochenmineralgehaltsbestimmung mit der Zwei-Spektren-Computertomographie. Radiologe 1988;28:166-172.

3. Glüer CC, Genant HK. Impact of marrow fat on accuracy of quantitative CT. J Comput Assist Tomogr 1989;13:1023-1035.

4. Cann CE, Genant HK. Precise measurement of vertebral mineral content using computed tomography. J Comput Assist Tomogr 1980;4:493-500.

5. Breatnach E, Robinson PJ. Repositioning errors in measurement of vertebral attenuation by computed tomography. Brit J Radiol;1983:299-305.

6. Rosenthal DI, Ganott MA, Wyshak G, Slovik DM, Doppelt SH, Neer RM. Quantitative computed tomography for spinal density measurement. Factors affecting precision. Invest Radiol 1985;20:306-310.

7. Kalender WA, Klotz E, Suess C. Vertebral bone mineral analysis: an integrated approach with CT. Radiology 1987;164:419-423.

8. Hangartner TN, Battista JJ, Overton TR. Performance evaluation of density measurements of axial and peripheral bone with x-ray and gamma-ray computed tomography. Phys Med Biol 1987;32:1393-1406.

9. Louis O, Luypaert R, Kalender W, Osteaux M. Reproducibility of CT bone densitometry: Operator versus automated ROI definition. Eur J Radiol 1988;8:82-84.

10. Cann CE. Quantitative CT for determination of bone mineral density: a review. Radiology 1988;166:509-522.

11. Sandor T, Weismann B, Brown E. Effect of intervertebral changes of the spinal trabecular and cortical mineral content on the precision requirements in longitudinal single and dual-energy computed tomography examinations. Med Phys 1989;16:218-224.

12. Steiger P, Block JE, Steiger S, Heuck AF, Friedlander A, Ettinger B, Harris ST, Glüer CC, Genant HK. Spinal bone mineral density measured with quantitative CT: effect of region of interest, vertebral level, and technique. Radiology 1990;175:537-543.

13. Kalender WA, Brestowsky H, Felsenberg D. Bone mineral measurement: automated determination of mid-vertebral CT section. Radiology 1988;168:219-221.

14. Grashuis JL, de Baat L, van Veen LCP, Zwamborn AW, Trouerbach WTh. Semi-automatic contour detection in CT-scans of the lumbar spine. (Abstract). Calcif Tissue Int 1989;44:147.

15. van Berkum FNR, Birkenhäger JC, van Veen LCP, Zeelenberg J, Birkenhäger-Frenkel DH, Trouerbach WT, Stijnen T, Pols HAP. Noninvasive axial and peripheral assessment of bone mineral content: a comparison between osteoporotic women and normal subjects. J Bone Min Res 1989;4:679-685.

CHAPTER 8

PATIENT CASE STUDIES

8.1 INTRODUCTION

In chapter 3, five different postprocessing methods for dual-energy quantitative computed tomography were evaluated theoretically and it was shown that the methods of Goodsitt and Nickoloff could exactly estimate the bone mineral content and could also provide an exact fat content estimate. However, as indicated in previous chapters of this thesis, problems may rise when DEQCT is used in clinical practice.

In the phantom studies, described in chapter 4, two major problems were encountered:

1) The difference in effective energy between the location of the region of interest and the location of the reference device. In QCT of the vertebral body, the accuracy of bone mineral and fat content estimations is influenced by the differences in effective energies between the centrally located vertebral body and the peripherally located reference device.

2) The tissue equivalence of calibration materials within the reference device for the method of Goodsitt or the exact description of the anatomical tissues for calculation of the material specific coefficients for the method of Nickoloff. If the X-ray attenuation characteristics of the materials used for reference or if the description of the anatomical tissues are not matched perfectly to those of the anatomic constituents of the vertebral body, the accuracy of bone mineral and fat content estimation is deteriorated.

In chapter 5, these problems were transferred to a simulated clinical environment. It was predicted that in clinical practice the accuracy of DEQCT is influenced negatively by these problems. Further, it was shown that bone mineral and fat content estimates outside the physiological range are obtained easily.

Improvement of accuracy, defined as deviation of the estimate from the true bone mineral content, is advocated as a reason to perform DEQCT instead of SEQCT. The results presented in this thesis have shown that in a controlled environment this concept is true. However, if realistic clinical conditions are encountered, accuracy is impaired by the problems discussed above.

For the clinical use of DEQCT, two questions remain to be discussed:

1) Can DEQCT be of value in the interpretation of longitudinal data? and

2) Can DEQCT give useful information about the intravertebral fat content?

Concerning the first question, the answer can be found in chapters 6 and 7. The study presented in chapter 6, in which bone marrow changes were simulated without a change in bone mineral content, showed that DEQCT could be of value in the proper interpretation of longitudinal changes.

Concerning the second question, the answer could also be extracted from the phantom and simulation studies. Although the accuracy of fat content determination in terms of deviation from the true fat content is low, differences between patient groups can probably be detected.

The answers to the questions are drawn from the phantom and simulation studies and should be verified in clinical practice.

Therefore, an in vivo study is presented in this chapter: SEQCT and postprocessing DEQCT were performed in six patients and the results are discussed.

8.2 PATIENTS, METHODS AND MATERIALS

Two studies were performed.

Study 1:

The aim of this study was to verify the results as presented in the simulation study for the method of Nickoloff, when different tissue descriptions were used for calculation of the material specific coefficients (Figures 5.6.A through D). In the simulation study (chapter 5) it was shown that when the tissue descriptions were changed for calculation of the material specific coefficients, bone mineral and fat content estimates were higher than obtained with the descriptions used to model the vertebral body. Especially, if the yellow marrow description was used to define the adipose tissue compartment within the bone marrow, the estimates were elevated extensively. The in vivo experiment should demonstrate similar findings.

Patients:

Two patients, referred to the department of radiology for QCT, were selected randomly.

Patient 1: a 53-year-old healthy postmenopausal female referred to the

department for screening.

Patient 2: a 26-year-old male with juvenile osteoporosis referred for monitoring of his bone mineral status.

Methods and materials:

CT scanning was performed with a Philips Tomoscan 350. The scanner was calibrated before scanning the patient according to the instructions of the manufacturer. Axial CT slices were made of the fourth lumbar vertebra. Mid-vertebral slices with a width of 6 mm were made at a tube potential of 120 kVp, with a tube current of 200 mA and an exposure time of 0.6 seconds (Computed Tomographic Dose Index: 14 mGy) and at a tube potential of 70 kVp with a tube current of 400 mA and an exposure time of 1.2 seconds (Computed Tomographic Dose Index: 11 mGy). The images were reconstructed at a field of view of 240 mm. The patients were scanned in a supine position, the legs elevated to decrease the lordotic curvature of the spine. A reference device containing solutions of K_2HPO_4 in water (0, 50, 100, 200, 400 mg/cm^3) was placed on the scan table under the lumbar region of the spine. As fat equivalent the subcutaneous fat tissue of the patients was used. An example of a reconstructed image is shown in Figure 8.1.

A circular ROI was used to determine the mean CT number of the trabecular region of the vertebral body and of the materials in the reference device. An irregular hand-drawn ROI was used to determine the mean CT number of an area containing subcutaneous fat.

Different material dependent coefficients were used for the algorithm of the method of Nickoloff. Fat description and soft-tissue description were varied in the same way as described in chapter 5. For soft-tissue equivalent, either "blood" with a mass density of 1.06 g/cm^3 or "red marrow" with a mass density of 1.03 g/cm^3 was used. For fat equivalent, the descriptions were "adipose" with a mass density of 0.97 g/cm^3; "adipose" with a mass density of 0.95 g/cm^3; "adipose" with a mass density of 0.93 g/cm^3 and "yellow marrow" with a mass density of 0.98 g/cm^3. All descriptions are according to the data presented by Woodard and White (1).

Study 2:

There were two objectives in this study. Firstly, to demonstrate the influences of two different calibration techniques in vivo; namely, a central non-simultaneous
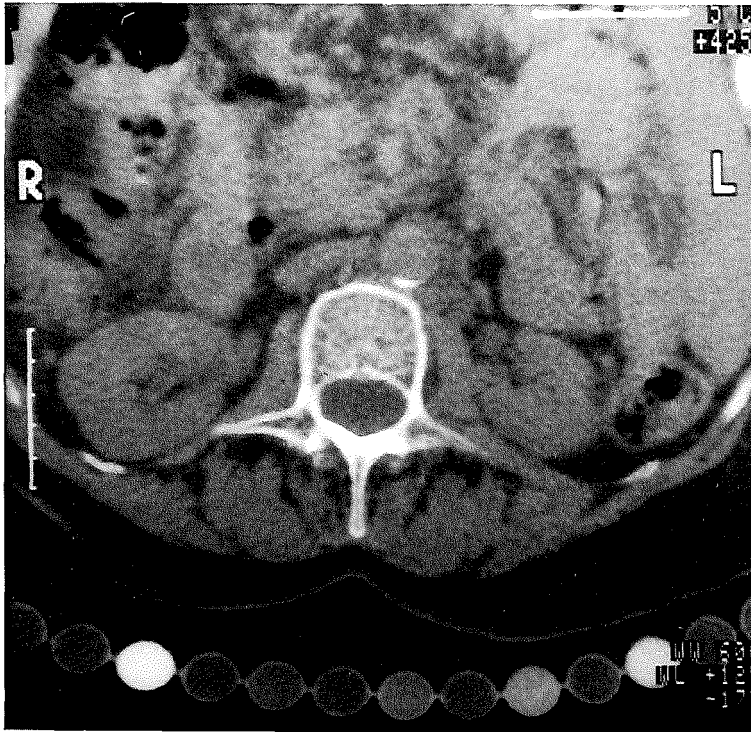
Figure 8.1. CT image of patient case study.

calibration technique and a peripheral simultaneous calibration technique. Secondly, to evaluate the interpretation of bone mineral content estimates and especially the fat content estimates as obtained with SEQCT and postprocessing DEQCT in four patients with a variety of metabolic bone disorders, from which it was expected that the intravertebral fat content would differ significantly.

Patients:

Patient A: a 35-year-old male with idiopathic osteopenia.

Patient B: a 62-year-old female with senile osteoporosis.

Patient C: a 63-year-old female with polycythemia and accompanying osteoporosis.

Patient D: a 58-year-old female with Cushing's disease.

All patients were referred to the department of diagnostic radiology for QCT.

The patients were chosen deliberately. It was expected that patient B would have a higher fat content than patient A, who was younger and had no obvious

signs of adiposity. Patient C was expected to have a low fat content due to the abundance of hematopoïetic tissue compared with patient B. Both patients were of the same age and were diagnosed to have osteoporosis. Patient D was expected to have a high fat content due to the increased adiposity in Cushing's syndrome.

Methods and Materials:

CT scanning was performed as described in study 1.

For patient A, a ROI was defined within the perirenal fat tissue to determine the mean CT number for fat reference, because there was not enough subcutaneous fat tissue present in this case.

Two different calibration techniques were used. A simultaneous peripheral calibration technique with the reference device as described for study 1, and a non-simultaneous central calibration technique using the CIRS anthropomorphic phantom with trabecular inserts, containing 0, 50, 100, and 200 mg/cm^3 dipotassium hydrogenphosphate in water. More details about the CIRS phantom and the inserts are in chapter 4.

The bone mineral equivalent value and, if possible, the fat equivalent value was estimated using SEQCT and postprocessing DEQCT according to the methods of Cann, Goodsitt (calibration approach) and Nickoloff. For the method of Nickoloff, the "blood" description and the "adipose 0.93 g/cm^3" description was used as input for the material dependent coefficients.

8.3 RESULTS

The results for experiment 1 are given in Table 8.1. If the "blood" description is used, bone mineral estimates are the lowest for "adipose 0.93" and the highest for "yellow marrow". The same observations can be made, if the "red marrow" description is used. Moreover, the findings are similar for the fat content estimates. These findings are exactly the same as predicted in the patient simulation studies shown in Figures 5.4 A through D (chapter 5).

The results for study 2 are given as the mean of the equivalent values of the two vertebrae scanned and are presented in Figure 8.2 for the simultaneous peripheral calibration set-up (A. bone mineral estimates and B. fat content estimates), and in Figure 8.3 for the non-simultaneous central calibration set-up.

TABLE 8.1. Results of experiment 1. Bone mineral and fat content estimates with the method of Nickoloff if the material specific coefficients are changed

Patient 1:
Soft Tissue Equivalent: Blood (1.06)   Red Marrow (1.03)

Fat-Description:

Adipose 1	152.0	mg/cm^3	141.3	mg/cm^3
(0.97)	153	%	124	%
Adipose 2	140.8	mg/cm^3	140.0	mg/cm^3
(0.95)	93	%	92	%
Adipose 3	135.9	mg/cm^3	139.1	mg/cm^3
(0.93)	66	%	72	%
Yellow Marrow	347.9	mg/cm^3	177.9	mg/cm^3
(0.98)	749	%	220	%

Patient 2:
Soft Tissue Equivalent: Blood (1.06)   Red Marrow (1.03)

Fat-Description:

Adipose 1	172.1	mg/cm^3	132.9	mg/cm^3
(0.97)	329	%	222	%
Adipose 2	147.9	mg/cm^3	130.5	mg/cm^3
(0.95)	199	%	163	%
Adipose 3	137.3	mg/cm^3	129.0	mg/cm^3
(0.93)	142	%	128	%
Yellow Marrow	653.8	mg/cm^3	198.4	mg/cm^3
(0.98)	1616	%	393	%

Bone mineral content estimates in mg/cm^3 calcium hydroxyapatite and fat content estimates in percentage fat by volume.
All tissue descriptions according to Woodard and White (1).
Between brackets () = mass density in g/cm^3.

For all patients the bone mineral estimates are low compared with reference values (2-4), indicating a low bone mineral content (osteopenia) for all patients. The estimates are lower at 120 kVp. With the postprocessing DEQCT method of
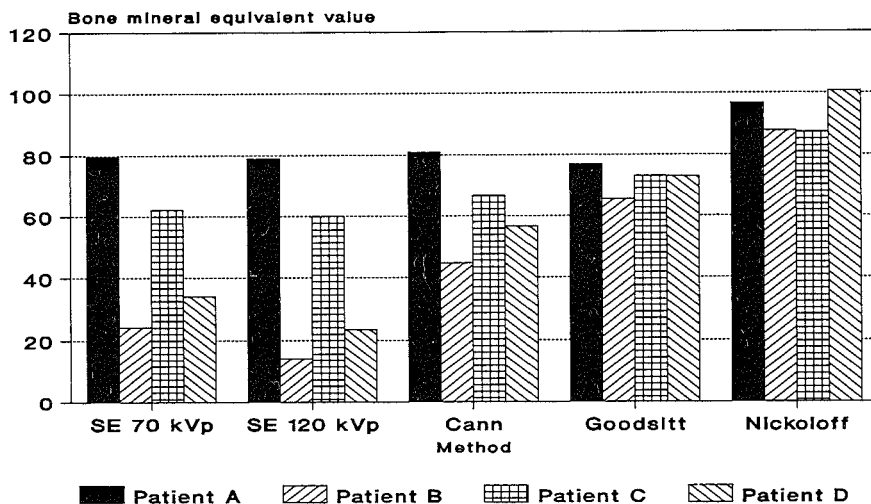
Figure 8.2.A. Patient results for bone mineral content assessment with the simultaneous peripheral calibration technique.
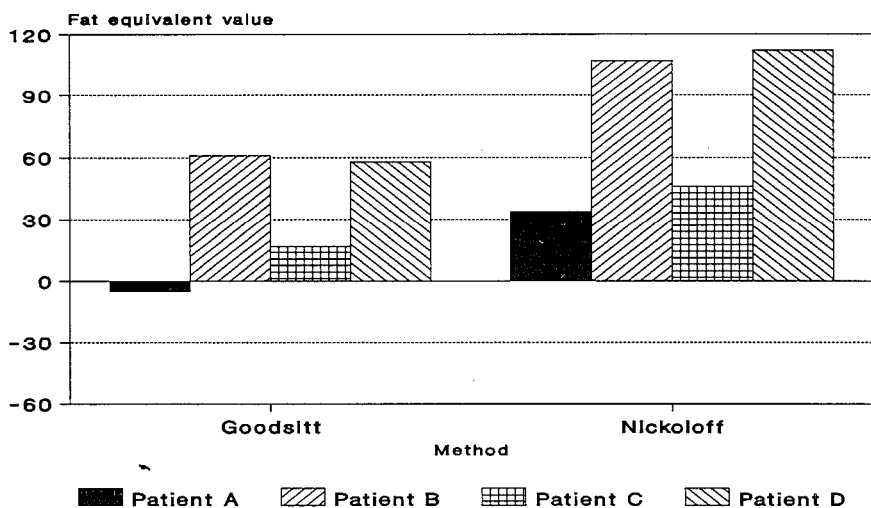

Figure 8.2.B. Patient results for fat content assessment with the simultaneous peripheral calibration technique.

Cann the bone mineral estimates are higher than with SEQCT, but the increase in the estimates compared with SEQCT is patient dependent. The increase is small for patients A and C, but large for patient B and D. With the postprocessing DEQCT method of Goodsitt the bone mineral estimates are higher compared with

the method of Cann, except for patient A. The differences in bone mineral estimates between patients as observed with SEQCT and the DEQCT method of Cann are diminished. With the postprocessing DEQCT method of Nickoloff the bone mineral estimates are the highest. Differences between patients are small.

The fat content estimates show striking differences between patients. Patient A (juvenile osteopenia) and patient C (polycythemia and osteoporosis) have low fat content estimates compared with patient B (senile osteoporosis) and patient D (Cushing's syndrome).
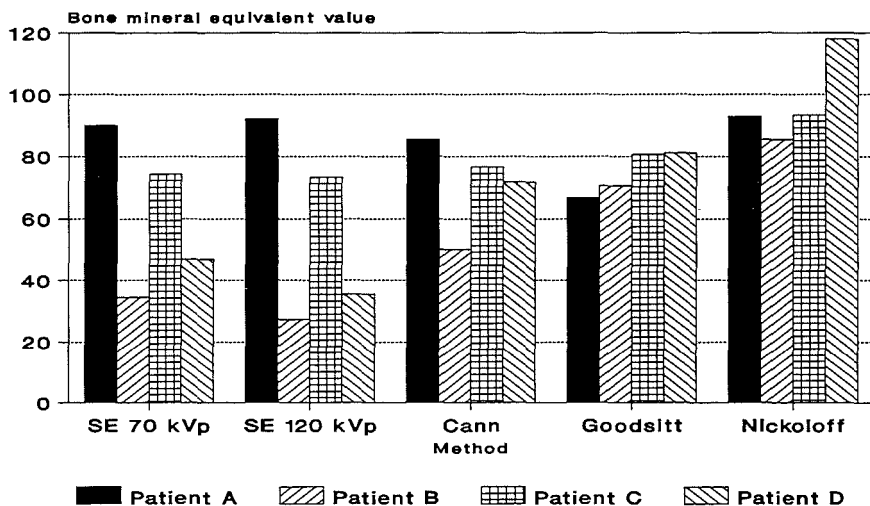

Figure 8.3.A. Patient results for bone mineral assessment with non-simultaneous central calibration.

The estimates are lower at 120 kVp for patients B, C and D, but higher for patient A. With the postprocessing DEQCT method of Cann the bone mineral estimates are higher than with SEQCT for patients B, C and D, but lower for patient A. With the postprocessing DEQCT method of Goodsitt the bone mineral estimates are higher compared with the method of Cann, except for patient A. With the postprocessing DEQCT method of Nickoloff the bone mineral estimates are the highest.

Again, the fat content estimates show striking differences between patients. Comparison of results obtained with the peripheral calibration technique with those obtained with the central technique shows that differences between patients show the same trend for SEQCT and for the postprocessing DEQCT
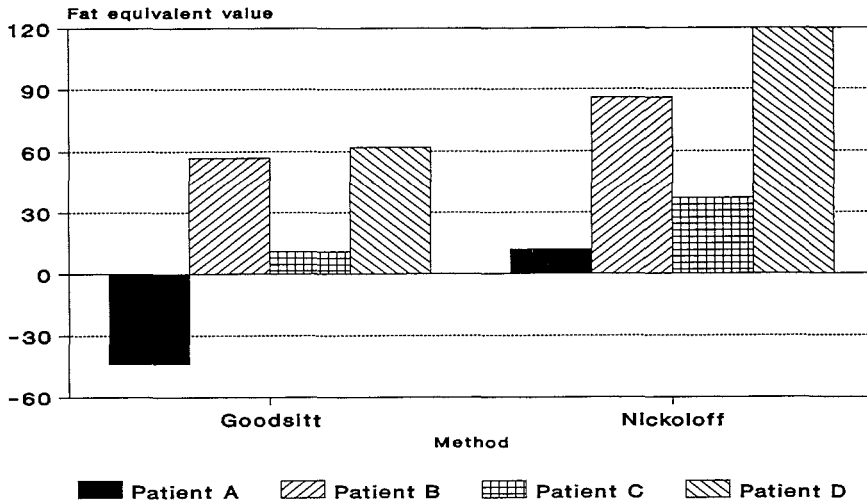
100

Figure 8.3.B. Patient results for fat content assessment with the non-simultaneous central calibration technique.

method of Cann. However, differences between patients are not the same for the other postprocessing DEQCT methods. For the method of Goodsitt the bone mineral estimates, obtained with the peripheral technique, are the highest for patient A followed by patients C and D and the lowest for patient B. The estimates obtained with the central technique are the highest for patient D, followed by patients C and B and the lowest for patient A. For the method of Nickoloff, the ranking order is D, A, B, C for the peripheral technique and D, C, A, B, for the central technique. The differences between the bone mineral estimates are larger for the central calibration technique.

The ranking order of the fat content estimates did not change between the different calibration techniques for the method of Nickoloff. The ranking order for the fat content estimates obtained with the method of Goodsitt with the simultaneous calibration technique is B, D, C, A and with the non-simultaneous technique D, B, C, A. However, the fat content estimates obtained with the method of Goodsitt for patients B and D are almost the same.

8.4 DISCUSSION

The aim of the study presented in this chapter was to verify the simulation studies and to demonstrate the use of DEQCT in clinical practice.

Study 1 confirms the trends seen in the patient simulation studies for the method of Nickoloff, if different tissue descriptions for calculating the material dependent coefficients are used.

The results from study 2 show that the differences in bone mineral estimates between patients with SEQCT are enlarged artificially due to the influence of fat content. Patients with the same true bone mineral content, but with a difference in intravertebral fat content, will show a difference in the bone mineral estimate obtained with SEQCT. This was already shown in chapter 6. Results with the methods of Goodsitt and Nickoloff presented in this chapter show a smaller difference in bone mineral estimates between the patients, but a large difference in fat content. Patient C with polycythemia and osteoporosis has a much lower fat content than Patient B with senile osteoporosis. This is reflected by a great difference in bone mineral estimates as obtained with SEQCT. The difference is smaller between the estimates obtained with the DEQCT method of Cann. The method of Cann reduces the fat-induced error by a factor of two, as was shown in the phantom studies (chapter 4) and simulation studies (chapters 5 and 6). This is reflected in the patient results by a diminishing of the differences between the bone mineral estimates of different patients. With the methods of Goodsitt and Nickoloff the difference is smaller again, suggesting that the patients do not differ much in bone mineral content.

The fat content estimates differ substantially. The patient with polycythemia shows low fat content estimates. This suggests an increase in intravertebral hematopoietic tissue, as could be expected with the disease. The patient with senile osteoporosis shows a fat content estimate similar to the patient with Cushing's disease. Because age matched controls were not included in this study, it is not possible to state if the estimates are higher than can be expected for age. It is clear that further patient studies are required to analyze differences in intravertebral fat content in metabolic bone diseases.

The influence of another calibration technique in the reference device is demonstrated clearly in study two. The order for the bone mineral estimates changes for the DEQCT methods of Goodsitt and of Nickoloff. This means, that differences observed between patient groups can differ depending on the

calibration set-up.

The results obtained by the simultaneous peripheral calibration technique are biased by two factors: 1) non-ideal reference materials for those methods using calibration materials or non-ideal material specific coefficients for the method of Nickoloff and 2) effective energy differences. The results obtained by the non-simultaneous central calibration technique are biased by non-ideal reference materials or non-ideal material specific coefficients. By using a central technique, effective energy differences between the centrally located vertebral body and a peripherally placed reference device are partially corrected.

However, an accurate estimation of the effective energy at the place of the vertebral body is possible only if the central calibration device (in this case the CIRS phantom with inserts) has exactly the same X-ray attenuation and beam hardening characteristics as a real patient. Furthermore, it should have the same size as the patient. In practice, patients can differ in size considerably, e.g. a patient with Cushing's syndrome is larger because of an increased adiposity associated with the disease. Therefore, it is mandatory to match the size of the anthropomorphic phantom as close as possible to the size of the patient.

In summary; study 1 confirms the trend in bone mineral and fat content estimates obtained with the method of Nickoloff, as shown in the patient simulation set-up in chapter 5. In study 2 striking differences in fat content estimates were found between the patients presented in this chapter. Differences in bone mineral content estimates between patients as obtained with SEQCT are exaggerated due to the influence of intravertebral fat.

8.5 REFERENCES

1. Woodard HQ, White DR. The composition of body tissues. Br J Radiol 1986;59:1209-1219.

2. Montag M, Dören M, Meyer-Galander HM, Montag Th, Peters PE. Computertomographisch bestimmter Mineralgehalt in der LWS-Spongiosa. Normwerte für gesunde perimenopausausale Frauen und Vergleich dieser Werte mit der Wirbelsäulenbelastung. Radiologe 1988;28:161-165.

3. Compston JE, Evans WD, Crawley EO, Evans C. Bone mineral content in normal UK subjects. Br J Radiol 1988;61:631-636.

4. Kalender WA, Felsenberg D, Louis O, Lopez P, Klotz E, Osteaux M, Fraga J. Reference values for trabecular and cortical vertebral bone density in single and dual-energy quantitative computed tomography. Eur J Radiol 1989;9:75-80.

CHAPTER 9
CONCLUSIONS.

Computed tomography scanners are designed for imaging the human body. The images obtained show the human anatomy in section and provide depth information to the radiologist. Using three-dimensional reconstruction algorithms, it is even possible to provide images to a clinician that gives a view which corresponds to the perception of human anatomy as presented in medical school. While CT scanners are primarily dedicated to diagnostic imaging, they can be used to provide quantitative information on human body composition and physiology. This feature of CT scanning, called quantitative CT, has been used primarily for estimation of bone mineral content within the skeleton. The bone mineral content analysis within the vertebral body of the lumbar spine with single-energy QCT (SEQCT) has become a well-established method for monitoring changes due to aging, disease and therapeutic interventions.

In SEQCT, the trabecular region of the vertebral body is in fact described as a two-compartment model, namely bone mineral within a watery environment. In reality, the trabecular region of the vertebral body is a multi-component entity consisting of bone mineral deposited in a collagen matrix that forms a complex three-dimensional structure. This structure is surrounded by hematopoietic and adipose tissue. All the components have different X-ray characteristics, which is neglected in part when SEQCT is performed. Therefore, the accuracy of SEQCT measurements for estimation of bone mineral content within the spine is limited and interpretation of changes in the bone mineral equivalent value is difficult. A decrease in the bone mineral equivalent value can be ascribed to a real change in bone mineral content, but also to a change in bone marrow composition, namely a conversion of red marrow to yellow marrow. Several investigators have therefore proposed dual-energy QCT (DEQCT) to solve this problem. By adding an extra measurement at a different energy, the trabecular region can now be described to consist of three compartments. Since intravertebral fat tissue is the most disturbing factor in SEQCT, due to its specific X-ray attenuation characteristics, it is treated as a separate compartment using DEQCT, ruling out its negative influence on the accuracy of bone mineral measurements. Moreover, its content can now be measured, which could be a valuable goal in itself. The amount of fat tissue within the trabecular region may be a predictor of the

metabolic capability in this region.

Several methods for postprocessing DEQCT have been proposed in the past. Postprocessing DEQCT is relatively easy to perform; in fact, it is two times SEQCT.

It was the aim of the studies presented in this thesis to evaluate the various postprocessing DEQCT methods.

Ideally, the questions that should be answered by the evaluation are:

1. What are the differences and similarities between the various postprocessing DEQCT methods?
2. Are some methods better than others?
3. Do they really improve the accuracy of bone mineral measurements compared with SEQCT?
4. Can these methods give a reliable estimate of intravertebral fat content?
5. What are the practical problems when these methods are used in clinical practice?
6. Is there a place for DEQCT in clinical practice at this moment?
7. What areas of future research could improve the performance of postprocessing DEQCT methods?

Five different postprocessing DEQCT methods were evaluated, each named after the author who published the method. The evaluation was made in several steps:

1. A theoretical analysis of the algorithms used in the different methods (chapter 3).
2. An analysis of the methods by applying the dual-energy methods in a phantom study on a standard CT scanner (chapter 4).
3. An analysis of the problems encountered in the phantom study, by transferring these to a patient simulation set-up. This set-up allows the modelling of a range of physiologic and pathologic conditions within the trabecular region of the vertebral body, as well as the modelling (separately or combined) of error sources inherent to the method or to the use of a CT scanner (chapters 5 and 6).
4. An analysis of the precision of the postprocessing methods by an in vitro study, using a human cadaver specimen of the lumbar spine (chapter 7).
5. Initial experiences in clinical use, presented by patient case studies, demonstrate the practical consequences of DEQCT (chapter 8).

Theoretical evaluation of the five DEQCT methods show that only two of these methods will produce optimal results, namely the basic approach of Goodsitt et al and the method of Nickoloff et al. The calibration approach of Goodsitt et al will produce optimal results only if calibration materials are available that exactly mimick the anatomic constituents of the vertebral body. The method of Cann et al will not produce optimal results; furthermore, it does not provide a fat content estimate. The method of Laval-Jeantet does not give optimal results, due to a methodological error in the algorithm.

These conclusions were confirmed by the phantom studies.

At this point, the methods that give optimal results focus on two different approaches:

A.   The "calibration" approach. The trabecular region of the vertebral body is described as a three-compartment model and the contents of these compartments is mimicked by reference materials. Then simultaneous calibration can be performed, by placing the reference materials near the patient within the scan field. This is called simultaneous peripheral calibration. Or the calibration can be performed non-simultaneously using an anthropomorphic phantom allowing to scan reference materials at a location in the scan field were the vertebral body would be normally. This is called non-simultaneous central calibration.

B.   The "effective energy" approach. In this approach the three-compartment model is not mimicked by reference materials. It is assumed that the compartments can be identified by "material dependent coefficients" that can be calculated if the effective energy, defined as the equivalent monochromatic energy of the polychromatic X-ray spectrum, is known or can be estimated. In practice, the effective energy is estimated using a reference device.

In theory both approaches can exactly estimate the bone mineral content. In practice, however, accuracy is impaired by the choice of tissue equivalent materials for calibration purposes (or for calculation of material dependent coefficients); by effective energy differences between the place of the region of interest and the place of the reference device; or inaccuracies in the energy estimation.

The results presented in this thesis show that a proper tissue equivalence is mandatory. To ensure this, several conditions should be fulfilled. An exact

knowledge of the attenuation characteristics of the biological materials within the region of interest is mandatory. The elemental compositions and the mass densities of the various anatomical tissues within the region of interest should be known. In the case of vertebral bone mineral estimation with postprocessing DEQCT, the description for the fat tissue compartment within the vertebral body is especially important. Different compositions for fat tissue are given in the literature and it is not yet clear, which is the best for intravertebral fat tissue. More research is necessary to obtain an accurate description of the intravertebral fat tissue to facilitate choice of the right fat-equivalent material. Another condition that should be fulfilled is proper parametrization of the attenuation characteristics of biological and tissue equivalent materials to ensure an accurate matching.

The second problem encountered, the effective energy difference, is caused by beam hardening of the polychromatic X-ray beam towards the center of the object of interest. Beam hardening correction schemes are implemented on a CT scanner that correct this problem, but never completely. They are usually optimized for circular phantoms filled with water which are placed within the center of the scan field. However, the human body is not circular and the human body does not consist of 100% water. The beam hardening problem in quantitative CT should be investigated more fundamentally. Second-order beam hardening corrections or empirical beam hardening correction schemes should be evaluated more extensively for their use in QCT.

The problem due to the effective energy differences could be avoided partially by performing a central calibration technique. The phantom used for that purpose should be anthropomorphic in configuration and should have exactly the same X-ray beam hardening characteristics as the patients that will be assessed. Furthermore, it must be possible to change its size to match it as closely as possible to the size of the patient. Another disadvantage of a central calibration technique is that it is performed non-simultaneously. It can not correct for short-term CT scanner fluctuations. However, the variability of the CT scanner performance is minimal in modern scanner designs.

The results presented in the previous chapters, show that postprocessing DEQCT may be valuable in clinical practice. Postprocessing DEQCT must be used in longitudinal studies on bone mineral content changes, if significant changes in the bone marrow composition are anticipated. Furthermore, postprocessing

DEQCT can be used for evaluation of fat content differences between groups of patients. These are the main applications of postprocessing DEQCT in clinical practice up to now, provided that some basic requirements are fulfilled, namely:

A.   A strict quality assurance protocol on the CT scanner used.

B.   Automation of as many steps as possible in the scanning and analysis protocol.

C.   A strict scanning protocol.

Summary.

CT scanners can be used to provide quantitative information on body composition. Its main application is for bone mineral content estimation within the lumbar vertebral body. This is usually done with a single-energy technique. The estimates obtained with this technique are influenced by the intravertebral fat content, which varies interindividually and with disease. Dual-energy techniques have been proposed to solve the fat-error, but their exact value is unknown. The aim of the studies presented in this thesis, is to evaluate different postprocessing dual-energy methods for quantitative computed tomography for bone mineral and fat content analysis within the trabecular region of the vertebral body. Comparison of these methods by transforming them to a standard set of equations, reveals that only two out of five methods would give optimal results (chapter 3). This is confirmed in phantom studies (chapter 4). In the phantom studies, two major problems for performing postprocessing DEQCT are encountered: 1) the accuracy of the tissue equivalence of reference materials or accuracy of tissue description and 2) the effective energy difference between the site of the vertebral body and the reference device. Using a patient simulation model, the influence of these disturbing factors on the accuracy of bone mineral and fat content estimation is evaluated for different clinical conditions (chapters 5 and 6). The precision of the bone mineral and fat content determination with postprocessing DEQCT is evaluated in chapter 7. In addition to an in vitro experiment, the precision is estimated using the patient simulation model. The results from chapters 5 through 7, show that postprocessing DEQCT can be of value in clinical practice. Postprocessing DEQCT should be used in longitudinal studies on bone mineral content changes, if significant changes in the bone marrow composition are anticipated. Furthermore, postprocessing DEQCT can be used for evaluation of fat content differences between groups of patients. Striking differences in the fat content estimates are seen in a number of patients with different metabolic disorders (chapter 8). It is concluded that the theoretical superb accuracy of bone mineral measurements obtained with postprocessing DEQCT, can be eliminated by practical problems such as improper tissue equivalence of the reference materials and energy differences between the region of interest and the reference device. More research is necessary to obtain an exact knowledge of the elemental compositions and mass densities of the various

anatomical structures within the vertebral body, especially intravertebral fat tissue. Beam hardening corrections, implemented in the CT scanner, should be evaluated for their effect on QCT.

Samenvatting (Summary in Dutch).

CT scanners kunnen naast het afbeelden van de menselijke anatomie worden gebruikt om kwantitatieve informatie te verkrijgen over de compositie van weefsels. Het belangrijkste toepassingsgebied is tot op heden het bepalen van het botmineraalgehalte in het wervellichaam. In deze studie wordt de waarde van verschillende methoden om kwantitatieve computer tomografie (CT) met twee energieën te verrichten, met als doel het bepalen van het botmineraalgehalte en het vetgehalte in het wervellichaam, onderzocht. Deze methoden worden verondersteld een betere schatting te geven van het botmineraalgehalte dan de kwantitatieve computer tomografische techniek die gebruik maakt van één energie.

De verschillende methoden werden allereerst vergeleken door ze terug te brengen tot een en dezelfde mathematische formule. Daarmee werd aangetoond dat slechts twee methoden optimale resultaten zullen geven (hoofdstuk 3). Dit zijn de methode gepubliceerd door Goodsitt et al, die gebruik maakt van referentie materialen en de methode gepubliceerd door Nickoloff et al, die gebruik maakt van materiaal specifieke coëfficiënten en van een schatting van de effectieve energieën van de gebruikte röntgenspectra.

Met behulp van een fantoomstudie werd de theoretische voorspelling uit hoofdstuk 3 bevestigd (hoofdstuk 4). Uit de fantoomstudie bleek dat er twee grote problemen zijn by de praktische uitvoering van deze vorm van kwantitatieve CT. Wil men de werkelijke waarden van het botmineraalgehalte en van het intravertebrale vetgehalte zo dicht mogelijk benaderen, dan dienen de referentie materialen een hoge mate van weefselequivalentie te bezitten of de te berekenen materiaal specifieke coëfficiënten moeten zo goed mogelijk de waarden van de te meten anatomische structuren benaderen. Voorts moet er rekening mee worden gehouden dat door stralenopharding van het röntgenspectrum, er verschillen zijn in effectieve energieën op verschillende plaatsen in het scanveld, wanneer zich in het scanveld een object bevindt.

Deze invloeden werden verder bestudeerd in een patiënt simulatie studie (hoofdstukken 5 en 6). Uitgaande van de elementaire compositie en de massadichtheid van de verschillende anatomische weefsels werd de inhoud van het wervellichaam gemodelleerd. Tevens werden verschillen in de compositie van het wervellichaam gemodelleerd voor fysiologische (veroudering) en pathologische

111

(verstoorde botmineralisatie, aandoeningen van het beenmerg) processen. In dezelfde proefopstelling konden ook het gebruik van verschillende referentiematerialen en verschillen in effectieve energie binnen het scanveld worden gesimuleerd. Hieruit bleek dat, hoewel de methoden in theorie in staat zijn het botmineraalgehalte en het vetgehalte nauwkeurig te bepalen, de nauwkeurigheid aanzienlijk wordt verslechterd door de eerder genoemde factoren. Tevens bleek dat de kwantitatieve CT methode met één energie moeilijk interpreteerbare botmineraal-equivalente waarden levert in follow-up studies. De methode die van één energie gebruik maakt wordt nadelig beïnvloed door veranderingen die in het beenmerg optreden. De methode die gebruik maakt van twee energieën heeft hier nagenoeg geen last van.

Hoewel de reproduceerbaarheid van de bepalingen slechter is met de tweeenergieën techniek ten opzichte van de techniek die gebruik maakt van één energie, zoals werd aangetoond in hoofdstuk 7 in een kadaver studie en een simulatie studie, wordt de interpretatie van de bepalingen makkelijker in een longitudinaal onderzoek wanneer men de twee-energieën methode gebruikt. Deze techniek moet dan ook worden gebruikt als men vermoed dat er veranderingen in het beenmerg zouden kunnen optreden tijdens het vervolgen van een pathofysiologische proces of van een therapeutische interventie.

Voorts kan met de twee-energieën techniek een uitspraak worden gedaan over verschillen in vetgehalte tussen groepen van patiënten met een verschillend ziektebeeld.

Een en ander werd nog eens geïllustreerd in hoofdstuk 8, waar enige patiënten met een laag botmineraalgehalte en waarvan kon worden verwacht dat ze zouden verschillen in vetgehalte, werden gedemonstreerd. Er werden met behulp van de twee-energieën techniek inderdaad grote verschillen gevonden in het gemeten vetgehalte.

Om echter de voordelen van de twee-energieën techniek volledig te kunnen uitbuiten, zal nog nader onderzoek moeten worden verricht.

Om weefselequivalente materialen beter te definiëren, of beter materiaal specifieke coëfficiënten te kunnen berekenen, zal een gedetailleerd onderzoek moeten worden verricht naar de elementaire compositie en de massadichtheden van de verschillende weefsels in het wervellichaam. Voorts zal moeten worden onderzocht op welke manier de verstorende effecten van de opharding van het röntgenspectrum het best kunnen worden gecorrigeerd wanneer men een CT

scanner wil gebruiken voor kwantitatieve doeleinden, naast het routine gebruik voor het genereren van voor diagnostiek geschikte afbeeldingen van de humane anatomie.

Dankwoord.

Dank ben ik verschuldigd aan Prof.Dr. H.E. Schütte, hoofd van de afdeling radiodiagnostiek, mijn promotor, die mij alle vrijheid heeft gegeven om dit proefschrift te schrijven. Tevens, dank ik Dr. W.Th. Trouerbach, belast met de leiding van de afdeling experimentele radiodiagnostiek, die mij, gedurende de bijna drie jaar die ik op de experimentele afdeling doorbracht, altijd aanmoedigde en tot prestaties aanspoorde.

De hulp van Dr.Ir J.L Grashuis, van de afdeling medische informatica van de Erasmus Universiteit, en de hulp van Drs. J.C.M. Steenbeek, werkzaam bij Philips Medical Systems, bij het schrijven van dit proefschrift is zeer belangrijk voor mij geweest. Vanaf het begin van het onderzoek waren we een uitstekend team.

Zij, die dagelijks met mij op de experimentele afdeling doorbrachten: A.W. Zwamborn, Mw W.J. van Leeuwen en L. de Baat, dank ik voor de goede sfeer en hun advies en hulp in vele zaken. T. Rijsdijk wordt bedankt voor het fotowerk.

Dit proefschrift was nooit geschreven zonder de steun van mijn vrouw, Elly, die de manische en de depressieve periodes die een promovendus doormaakt, altijd wist op te vangen.

Het onderzoek gepresenteerd in dit proefschrift werd mede mogelijk gemaakt door een subsidie van het ministerie van economische zaken; stimulerings programma medische technologie, projectnummer MTR 89001. Het project werd mede mogelijk gemaakt door Philips Nederland B.V. en Philips Medical Systems B.V.

CURRICULUM VITAE

De schrijver van dit proefschrift werd geboren op 1 april 1962 te Dordrecht. Na het behalen van het VWO diploma aan het Johan de Witt Gymnasium te Dordrecht (ß-richting) in 1980, werd door hem de studie scheikunde aangevangen aan de Rijksuniversiteit te Leiden. In 1981 begon hij aan de studie geneeskunde aan dezelfde universiteit. Het doctoraalexamen werd in 1986 behaald. In 1988 werd het artsexamen afgelegd. In zijn studententijd was hij met name actief in verschillende facultaire bestuursorganen.

Sinds 1988 is de schrijver verbonden aan de afdeling radiodiagnostiek (Hoofd: Prof.Dr. H.E. Schütte) van het Academisch Ziekenhuis "Dijkzigt" Rotterdam en van de Erasmus Universiteit te Rotterdam. Hij is betrokken bij fundamenteel en toegepast klinisch onderzoek op het gebied van kwantitatieve röntgentechnieken. Op 1 januari 1991 is hij gestart met de opleiding in het specialisme radiodiagnostiek.

De schrijver is gehuwd en heeft een dochter.

Dordrecht, Januari 1991.